ISTANBUL TECHNICAL UNIVERSITY ★ GRADUATE SCHOOL OF SCIENCE ENGINEERING AND TECHNOLOGY

INVESTIGATION OF CNT SMART PAINT FOR STRUCTURAL HEALTH MONITORING IN ADVANCED AND NANO-ENHANCED CARBON FIBER COMPOSITES

M.Sc. THESIS

Yağmur ATEŞCAN

Department of Aeronautics and Astronautics Engineering

Aeronautics and Astronautics Engineering Programme

DECEMBER 2015

ISTANBUL TECHNICAL UNIVERSITY ★ GRADUATE SCHOOL OF SCIENCE ENGINEERING AND TECHNOLOGY

INVESTIGATION OF CNT SMART PAINT FOR STRUCTURAL HEALTH MONITORING IN ADVANCED AND NANO-ENHANCED CARBON FIBER COMPOSITES

M.Sc. THESIS

Yağmur ATEŞCAN
511131141

Department of Aeronautics and Astronautics Engineering

Aeronautics and Astronautics Engineering Programme

Thesis Advisor: Asst. Prof. Dr. Hülya CEBECİ

DECEMBER 2015

İSTANBUL TEKNİK ÜNİVERSİTESİ ★ FEN BİLİMLERİ ENSTİTÜSÜ

GELİŞMİŞ VE NANO TAKVİYELİ KOMPOZİT MALZEMELER İÇİN KARBON NANOTÜP İÇERİKLİ AKILLI BOYANIN YAPISAL SAĞLIK İZLEME İÇİN GELİŞTİRİLMESİ

YÜKSEK LİSANS TEZİ

Yağmur ATEŞCAN
511131141

Uçak ve Uzay Mühendisliği Anabilim Dalı

Uçak ve Uzay Mühendisliği

Tez Danışmanı: Yrd. Doç. Dr. Hülya CEBECİ

ARALIK 2015

Yağmur Ateşcan, a **M.Sc.** student of ITU **Graduate School of Science Engineering and Technology** student ID **511131141**, successfully defended the **thesis** entitled "**INVESTIGATION OF CNT SMART PAINT FOR STRUCTURAL HEALTH MONITORING IN ADVANCED AND NANO-ENHANCED CARBON FIBER COMPOSITES**", which she prepared after fulfilling the requirements specified in the associated legislations, before the jury whose signatures are below.

Thesis Advisor :	**Asst. Prof. Dr. Hülya CEBECİ** Istanbul Technical University	.....
Jury Members :	**Assoc. Prof. Dr. Aytaç ARIKOĞLU** Istanbul Technical University	.....
	Asst. Prof. Dr. Nuri SOLAK Istanbul Technical University	.....

Date of Submission : **27 November 2015**
Date of Defense : **25 December 2015**

To my Family,

FOREWORD

Firstly, I would like to show my special gratitude and appreciation to my supervisor, Assist. Prof. Dr. Hülya Cebeci, for contributing valuable and inspiring advices, and feedback on my works during the thesis. Moreover, I would like to thank Assist. Prof. Dr. Elif Özden-Yenigün, Assoc. Prof. Dr. Demirkan Çöker and their students for helping me on fabricaton and testing of my specimens. Furthermore, I would like to thank Müslüm Çakır for helps to perform mechanical tests. Lastly, I would like to thank to Aeronautical Materials and Novel Manufacturing Technologies Research Group members for always motivating and supporting me during my thesis studies.

December 2015

Yağmur Ateşcan
(Research Assistant)

TABLE OF CONTENTS

Page

ABBREVIATIONS

A-CNT : Aligned Carbon Nanotube
AFM : Atomic Force Microscope
CFp-RC : Carbon Fiber Prepreg Reinforced Composites
CFRP : Carbon Fiber Reinforced Polymer
CNF : Carbon Nanofiber
CNT : Carbon Nanotube
CNT-PNCs : Carbon Nanotube – Polymer Nanocomposites
CVD : Chemical Vapor Deposition
DMM : Digital Multimeters
E-Beam : Electron Beam
ECN : Electrospun Carbon Nanofiber
EMI : Electromagnetic Interference
FRPC : Fiber Reinforced Polymer Composite
GFRP : Glass Fiber Reinforced Polymer
GNP : Graphene Nanoplate
HRTEM : High Resolution Transmission Electron Microscopy
ILSS : Interlaminar Shear Strength
MWCNT : Multiwall Carbon Nanotube
PE-CVD : Plasma Enhanced Chemical Vapor Deposition
PVB : Polyvinyl Butyral
SBS : Short Beam Shear
SEM : Scanning Electron Microscopy
SHM : Structural Health Monitoring
SWCNT : Single Wall Carbon Nanotube
TEM : Transmission Electron Microscopy
TGA : Thermal Gravimetric Analysis
th-CVD : Thermal Chemical Vapor Deposition
VA-CNT : Vertically Aligned CNT
VARTM : Vacuum Assisted Resin Transfer Molding

LIST OF TABLES

Page

LIST OF FIGURES

Page

INVESTIGATION OF CNT SMART PAINT FOR STRUCTURAL HEALTH MONITORING IN ADVANCED AND NANO-ENHANCED CARBON FIBER COMPOSITES

SUMMARY

Fiber reinforced polymer composites are widely used in aerospace, automotive, civil and marine applications, through their excellent mechanical properties, and low density. With improving technology, the demand for lighter, stronger and reliable materials increases day by day. To satisfy these demands, deeply researches are being carried out on advanced and nano-enhanced composite structures. Since the composites are laminated structures, most of the damage types generate under the surface of structures and that is why composites are more vulnerable to failure during operation. Therefore, structural health monitoring (SHM) is an essential application to provide reliability and cost saving for aerospace operations. There are many SHM methods like strain gauges, fiber optic sensors and lamb waves; however, because of their multifunctionality, such as high mechanical properties, electrical and thermal conductivity, carbon nanotubes (CNTs) are novel applications for SHM methods. There are mainly two types for adding CNTs into the system, one of them is embedding CNTs within the composite and the other one is applying onto the surface of structure. In this study, both growth CNTs which are synthesized using thermal chemical vapor deposition (th-CVD) method and commercially provided CNTs from Sigma Aldrich are used for CNT based SHM application. CNT embedded polymer nanocomposites (CNT-PNCs) are applied onto the surface of carbon fiber reinforced polymer (CFRP) composites as a smart paint for strain sensing. In addition to SHM application, nano-enhanced cylindrical composite structures are fabricated and torsional tests are performed in this study to determine the failure mode of these structures before applying CNT based SHM method.

To synthesize CNTs, using th-CVD method Si substrate covered with Alumina oxide and Ferrous catalyst are used and C_2H_4/H_2 gases are deposited at atmospheric pressure with specified recipe. Growth and commercially provided CNTs are added into the epoxy resin and shear mixing and homogenization are applied for dispersion of CNTs. For CNT based SHM applications percolation threshold is a critical parameter to obtain an effective system. So, the first step of this study is determining percolation threshold for CNT-PNCs. 0.1, 0.25 and 0.5 wt% growth CNTs and 0.25, 0.5 and 1 wt% Sigma-CNTs are used to fabricate CNT-PNCs. 2-probe electrical conductivity measurement method is used to determine electrical conductivity of CNT-PNCs. According to electrical conductivity measurements, electrical conductivity of growth CNT-PNCs ($0.3x10^{-3}$-$5x10^{-1}$ S/m) are beyond the percolation threshold even at low CNTs loading, however Sigma CNT-PNCs have six order of magnitude lower electrical conductivity than growth CNT-PNCs. As a result, growth CNT-PNCs are applied onto the surface of CFRP composites, which are fabricated by vacuum infusion method, with specified dimensions as a smart paint for strain

sensing. Elastic mode, plastic mode and flextural tests are applied for CFRP composites and resistance change of CNT smart paint is measured simultaneously with keithly source meter. When is compaired with base specimen, which does not containe CNTs, CNT smart paint displays an important effect on resistance change. According to results, resistance change of 0.25 and 0.5 wt% CNT embedded smart paints show a decisive increament related to strain changes. While the resistance change is higher for 0.25 wt% CNT smart paint (120%) at elastic mode tension tests, 0.5 wt% CNT smart paint displays higher resistance change (300%) for plastic mode tension and flextural tests where the composite specimens are totally fractured. This would be the result of tunneling effect and for high strain conditions, tunneling effect lose its importance. Since the carbon fibers are conducting materials and they also carry electrons when the CNT smart paint is fractured, CFRP composite structure have to be eliminated from CNT smart paint application to determine real effectiveness of CNT smart paint as a strain sensor. That is why, at the last step of SHM application, insulator acrylic paint is applied between CNT smart paint and CFRP composites. Flextural test is performed on these specimens and a sudden and huge increment is obtained for resistance change of CNT smart paint.

Nano-enhancement is an ongoing research area for novel applications, so at the second part of this study, nano-enhanced cylindrical composite structures are fabricated to determine their failure modes, which is important for investigation of effectiveness of SHM systems on these structures. Electrospinning method is used to fabricate electrospun carbon nanofibers (ECNs) mats. Since CNT agglomeration is a critical problem for application of electrospinning and aspect ratio of CNTs is effective on agglomeration, Sigma-CNTs with 5 μm length are used to obtaine well dispersed CNTs in ECNs mats. To prepare polymer solutions, 10 wt% polyvinyl butyral (PVB) is added in methanol and Sigma CNTs are also added with different weight fractions (0.5, 1 and 2 wt%). Polymer solutions are magnetically stirred for 24 hours to provide homogenious dispersion of CNTs and electrospinning is directly applied on carbon fiber prepreg. For fabrication of carbon fiber prepreg reinforced composites (CFp-RC) 10 plies of carbon fiber prepreg are wrapped on a cylindrical Teflon mold continuously and a Teflon hose is used as an outer mold. The specimen fabrication of the CFp-RC cylinder with embedded ECNs mats includes three types of specimens, such as base specimen, middle interphase specimen and separate interphase specimen. Base specimens without ECNs mats are fabricated as reference materials. For middle interphase specimens the ECNs mats are applied to middle four surfaces and for separate interphase specimens ECNs mats are applied to separate four surfaces. Torsion tests are applied on composite specimens and shear stress vs. shear strain data are obtanined to determine effect of ECNs mats on interlaminar shear strength (ILSS) properties of composites. 0.5 and 1 wt% CNT ECNs mats specimens show higher shear stress results when compared with base specimens, however 2 wt% CNT ECNs mats specimens have lower shear strength results. The worse results of 2 wt% CNT-ENCs mats specimens might be attributed to CNTs agglomeration and decreased curing degree that causes decrease on mechanical properties of structures. Since cylindrical composites are hard to fabricate by hand, the mechanical test results are affected from fabrication conditions. To eliminate this problem, Mode-I Mode-II mixture test specimens are also fabricated in the second part of this study to determine effectiveness of ECNs mats on ILSS properties of laminated composites. To fabricate test specimens, 16 plies carbon fiber prepreg are used and only one layer of ECNs mat is used for each specimens. ECNs mat coated carbon fiber prepreg is placed to the middle surface of laminates. ECNs mat is

applied upto the crack initiation points and a release film is placed after the ECNs mats to obtaine delamination at the middle surface. Mode-I Mode-II mixture tests will be performed on these specimens and effect of ECNs mats on ILSS of composite structures will be determined. After the investigation of failure modes of nano-enhanced composites, CNT based SHM method will be applied to the nano-enhanced and complex shaped structures.

GELİŞMİŞ VE NANO TAKVİYELİ KOMPOZİT MALZEMELER İÇİN KARBON NANOTÜP İÇERİKLİ AKILLI BOYANIN YAPISAL SAĞLIK İZLEME İÇİN GELİŞTİRİLMESİ

ÖZET

Fiber takviyeli polimer matrisli kompozit malzemeler havacılık, otomotiv, denizcilik gibi pek çok alanda önemli ölçüde kullanılmaktadır. Gelişen teknolojiye bağlı olarak hafif, dayanıklı ve güvenilir malzemeler için olan talep her geçen gün artmaktadır. Bu talepleri karşılayabilmek ve yenilikçi uygulamalar gerçekleştirebilmek için gelişmiş ve nano takviyeli kompozit malzemeler üzerinde ciddi çalışmalar yapılmaktadır. Kompozit malzemeler yüksek mekanik özellikleri ve hafifliği, kimyasal ve çevre koşullarına gösterdiği direnç gibi üstün özelliklerine rağmen katmanlı yapıları nedeni ile hasar oluşumu ve hasarın ilerlemesi konusunda büyük sorunlar göstermektedir. Kompozit malzemelerde çatlak ilerlemesinin takip edilmesi oldukça zordur, ayrıca ara katmanlarda oluşan hasarlar gözle muayene gibi basit yöntemlerle tespit edilememekte ve bunlar için özel muayene yöntemlerinin kullanılması gerekmektedir. Havacılık sektöründe en çok karşılaşılan sorunlardan birisi parçaların yorulma nedeni ile hasara uğramasıdır. Kullanılan parçalar tekrarlanan yüke maruz kaldıklarında yorulmakta ve belli bir sınırın üzerinde yük uygulandığında ani ve kalıcı hasara uğramaktadırlar. Bu hasar planlanmmış bakım dönemlerinin arasında gerçekleştiğinde ciddi kazalara neden olabilmektedir. Bunun yanı sıra operasyon maliyetleri değerlendirildiğinde, büyük bir kısmını bakım ve onarım giderleri oluşturmaktadır. Herhangi bir hasar onarımının yapılmadığı kontrol amaçlı gerçekleştirilen bakımlar gereksiz yapılan masraf anlamına gelmektedir. Bütün bu durumlar dikkate alındığında hem güvenilir hem de tasarruflu operasyonların gerçekleştirilmesi için eş zamanlı yapısal sağlık izleme yöntemlerinin kullanılması ticari uygulamalar için büyük önem arz etmektedir.

Ticari olarak kullanılmakta olan gerinim ölçer ve fiber optik sensör uygulamaları ekonomik olmalarına rağmen geniş ölçekli yapılarda yeterli bilgiyi sağlamadıklarından verimli olarak kullanılamamaktadırlar. Bu nedenle, eş zamanlı yapısal sağlık izleme yöntemlerinin geliştirilmesi için çalışmalar gerçekleştirilmektedir. Bunların en dikkat çekeni, çok yönlü özellikleri ile pek çok kullanım alanı olan karbon nanotüplerin (KNT) yapısal sağlık inceleme metotlarında kullanılmasıdır. KNT'lerin sisteme eklenmesi için temel olarak iki yöntem bulunmaktadır. Bunlardan birisi KNT'lerin kompozit yapı içerisine entegre edilmesi, diğeri ise kompozitin yüzeyine uygulanmasıdır. Bu çalışma kapsamında hazırlanan KNT'li yapısal sağlık inceleme sistemi akıllı boya olarak kompozitin yüzeyine uygulanmış ve gerinim sensörü olarak kullanılmıştır.

Yapısal sağlık izleme sistemlerinin kullanılabilir hale gelmesi için önemli olan parametrelerden birisi sistemin mekanik değişimlere verdiği tepkinin doğru şekilde belirlenmesidir. Bu amaçla ilk etapta kompozit malzemelerin hasara uğrama şekli belirlenmelidir. Gelişmiş kompozit malzemeler yaygın olarak kullanıldığından bu

yapılar için bilgi edinmek mümkün iken, henüz gelişmekte olan bir alan olması nedeni ile nano-takviyeli kompozit malzemelerin hasar şekilleri tam olarak bilinmemektedir. Bu nedenle çalışmanın ikinci kısmında nano-takviye ile geliştirilmiş komplex şekilli kompozit malzemenin mekanik özellikleri belirlenecektir. Bu çalışmanın sonucunda ulaşılmak istenen hedef KNT'li yapısal sağlık izleme yönteminin hem gelişmiş hem de nano-takviyeli ve komplex şekilli kompozit yapılar için etkin bir şekilde kullanılmasıdır.

KNT'ler tek sıra karbon atomlarından oluşan bir grafen katmanının silindir şeklinde bükülerek birleşmesinden oluşan içi boş yapılardır. Bu yapıların çapları nanometre mertebesindeyken uzunlukları santimetre mertebesine kadar çıkabilmektedir. Bu durum yüksek uzunluk-çap oranı ve yüzey alanına sahip olmasını sağlamakta, ve bu gibi üstün özellikleri karbon nanotüpleri havacılık endüstrisi dahil bir çok alanda ileri teknoloji uygulamaları için kullanılmasını sağlamaktadır. KNT'ler temel olarak tek duvarlı ve çok duvarlı olmak üzere ikiye ayrılmaktadır. Tek duvarlı yapılarda bir tane grafen katmanı bulunurken çok duvarlı yapılarda iç içe geçmiş birden çok grafen katmanı bulunmaktadır. Genellikle çok duvarlı yapıların çapları 5nm ile 20 nm arasında değişim gösterirken tek duvarlı yapıya sahip KNT'lerin çapları 0.8 ile 2 nm arasındadır. Bu iki tip nanotüpün elektriksel ve mekanik özellikleri de farklılık göstermektedir.

KNT'ler kusursuz moleküler yapısı ve kuvvetli C-C bağlarından dolayı çok yüksek mekanik özelliklere sahiptir. Tek duvarlı bir nanotüp yaklaşık 1TPa'lık elastik modüle sahip iken çok duvarlı nanotüpler 1.8TPa elastik modüle sahip olabilmektedir. Bu değer yaklaşık olarak çeliğin 5 katına eşit olmaktadır. Nanotüplerin bu üstün özellikleri sayesinde, kompozit malzemelerin özelliklerini nanotüpler kullanarak geliştirmek, oldukça ilgi gören konular arasındaki yerini almıştır ve bu konuda yapılan çalışma sayısı her geçen gün artmaktadır. Bu tarz kompozitler nano-mühendislik kompozitleri veya nano-takviyeli gelişmiş kompozitler olarak adlandırılmaktadırlar.

Yüksek mekanik özelliklerinin yanı sıra KNT'ler yüksek elektriksel iletkenliğe de sahiptir. Teorik olarak elektriksel direnci 10^{-6} Ω.m gibi oldukça düşük bir değere sahiptir ve bakır ile karşılaştırıldığında yüksek elektrik iletkenliği göstermektedir. KNT'lerin elektriksel iletkenlik özellikleri kristal yapısına bağlı olarak değişmektedir. Fonksiyonlaştırmalar yapılarak elektriksel iletkenlik özelliklerinin daha da yüksektilmesi mümkündür.

KNT'lerin yapısal sağlık izleme sistemlerinde kullanılmasını sağlayan temel özellikleri elektriksel iletkenliklerinin ve piezo-rezistans (mekanik yükler altında elektriksel direncin değişmesi) özelliğinin yüksek olmasıdır. Havacılıkta kullanılan epoksi matrisler yalıtkan malzemelerdir ve fiber takviyeli epoksi kompozitlerin yapısına iletken dolgu malzemesi eklenerek elektriksel iletkenliklerinin yükseltilmesinde önemli olan parametre yalıtkan halden iletken hale geçtiği eşik (percolation threshold) değeridir. Bu değer kullanılan dolgu malzemesine, malzemenin geometrik özelliklerine, kompozit malzemenin içerisine entegre edilme şekline ve kullanılan matris çeşidine bağlı olarak farklılık göstermektedir. Literatürde KNT ile yapılan çalışmalar incelendiğinde bu eşiğin yaklaşık olarak ağırlıkça % 0.1 KNT değerine denk geldiği görülmektedir.

Bu çalışma kapsamında iki tip KNT kullanımıştır. Bunlardan ilki laboratuvar ortamında gerçekleştirilen termal kimyasal buhar biriktirme yöntemi ile sentezlenen KNT'ler, diğeri ise Sigma Aldrich firmasından ticari olarak satın alınan KNT'lerdir.

KNT sentezlemek için kullanılan farklı yöntemler vardır fakat hem ekonomik olması, hem de laboratuvar koşullarında üretime imkan sağlaması nedeni ile kimyasal buhar biriktirme yöntemi kullanılmıştır. Bu yöntem ayrıca farklı uzunluklarda yüksek saflıkta KNT sentezlenmesine imkan sağlamaktadır. Bu çalışmada, KNT'lerin epoksi içerisine dağıtılmasıyla hazırlanan polimer nanokompozitler kompozit yüzeyine akıllı boya olarak uygulanarak yapısal sağlık izleme sisteminde kullanılmıştır. Akıllı boya uygulamasına geçmeden önceki ilk adım hazırlanan KNT-polimer nanokompozitlerin elektirksel özelliklerinin incelenmesi ve iletkenlik eşiğinin belirlenmesidir. Hazırlanan KNT-polimer nanokompozitlerde kullanılan KNT'nin ağırlıkça oranı sentezlenen KNT'ler için % 0.1, 0.25 ve 0.5 olarak değişirken Sigma KNT için % 0.25, 0.5 ve 1 olarak değişmektedir. KNT-polimer nanokompozitlerin iletkenlik değerleri iki prob yöntemi kullanılarak ölçülmüştür. Bu yöntemde numunelere sabit bir voltaj uygulayarak direnç değerleri elde edilmiş ve farklı yüzdelerde KNT içeren polimer nanokompozitlerin iletkenlik özelliklerinin nasıl değiştiği incelenmiştir. Yapılan ölçümlerde Sigma KNT için elektirksel iletkenlik değerlerinin iletkenlik eşiğinin oldukça altında kaldığı görülmüş ve sentezlenen KNT'ler ile hazırlanan polimer nanokompozitler akıllı boya olarak uygulanmıştır.

Yapısal sağlık izleme testleri için karbon fiber takviyeli polimer kompozitler vakum infüzyon yöntemi ile üretilmiş ve gerekli boyutlarda kesilmiştir. Akıllı boya uygulaması bu kompozitlerin yüzeyine belirlenmiş boyutlar ile yapılmıştır. Bu çalışma kapsamında elastik ve plastik mode çekme testleri ve üç nokta eğme testleri gerçekleştirlmiştir. Mekanik testlerin gerçekleştirlmesi sırasında eş zamanlı olarak akıllı boya üzerine sabit bir voltaj uygulanmış ve gerinim değerlerinin değişime bağlı olarak elektriksel direncinde görülen değişimler takip edilmiştir. Elde edilen sonuçlar değerlendirilip KNT'siz baz numune ile karşılaştırıldığında KNT takviyeli akıllı boya uygulamasının gerinim değişimlerinin takip edilmesinde önemli bir farklılık yarattığı görülmüştür. Elde edilen direnç değişimleri KNT miktarına ve uygulanan mekanik yüke bağlı olarak değişiklik göstermektedir. Yapılan testlerde akıllı boyanın tamamen hasara uğraması durumunda elektrik akımının karbon fiber kompozit üzerinden akmaya devam etmesi akıllı boya uygulamasının gerinim sensörü olarak gösterdiği verimlilik durumunu etkilemektedir. Bu çalışmadaki amaç akıllı boyanın etkinliğini belirlemek olduğundan son yapılan testlerde akıllı boya ile karbon fiber kompozit arasına yalıtkan akrilik boya sürülmüştür. Bu uygulamada akıllı boyanın tamamen hasara uğraması durumunda elektriksel direnç değerinin ani olarak hızlı bir artış gösterdiği belirlenmiştir. Ayrıca bu uygulamada lamina hasarlanmasının direnç değerlerindeki ani artış noktaları ile net olarak takip edilebildiği görülmüştür. Bu çalışmanın bir sonraki adımı bu uygulamanın farklı yükleme koşulları altında test edilmesidir.

Bu tez çalışmasının ikinci aşamasında ise nano-takviyeli gelişmiş kompozitlerin üretimi ve testleri gerçekleştirlmiştir. Nano-takviyeli kompozitlerin üretimi için kullanılan farklı yöntemler bulunmaktadır. Bunlardan en yaygın olanı KNT'lerin polimer matris içerisine çeşitli yöntemler kullanılarak dağıtılmasıdır. Bu yöntemde karşılaşılan en büyük problem KNT'lerin topaklaşması ve homojen olarak yapı içerisine dağıtılamamasıdır. Bu problemi önlemek ve katmanlar arasında sürekli bir yapı oluşturabilmek için 'electrospinning' (polimer esaslı nanolif üretiminde kullanılan yöntem) yöntemi kullanılmıştır. Bu üretimlerde ağırlıkça % 0.5, 1 ve 2 oranlarında Sigma KNT kullanılmış ve solüsyonun hazırlanması için ağırlıkça %10 oranında polyvinyl butyral (PVB) eklenen methanol içerisine ilave edilerek 24 saat manyetik karıştırıcı ile karıştırılmıştır. Hazırlanan solüsyon ile karbon fiber prepreg

üzerinde nanolifler üretilmiştir. Bu çalışma kapsamında nanolif içermeyen, orta ara yüzeylerde ve aralıklı arayüzeylerde nanolif içeren olmak üzere üç farklı içi boş silindirik kompozit yapı üretilmiştir. Silindirik kompozitlerin üretilmesi için içte ve dışta teflon kalıplar kullanılmıştır.

Üretilen silindirik kompozitler üzerine burulma testi uygulanmıştır. Elde edilen sonuçlar nanolif içermeyen numunelerin sonuçları ile karşılaştırıldığında ağrlıkça % 0.5 ve 1 oranında KNT içeren nanolifli kompozitlerin daha yüksek kayma dayanımı gösterdikleri belirlenmiştir. Silindirik kompozitler prepreg katmanlarının elle sarılması ile üretildiğinden sarım koşulları mekanik özellikleri etkilemekte ve elde edilen sonuçların farklılaşmasına neden olmaktadır. Bu durumu engellemek ve yapı içerisine entegre edilen nanoliflerin mekanik özellikler üzerindeki etkinliğini tam olarak belirleyebilmek amacı ile Mode-I Mode-II test numuneleri üretilmiştir. Bu numuneler test edilerek nanoliflerin ara yüzey özelliklerine olan katkısı belirlenecektir.

Bu tez çalışmasının devamında ulaşılmak istenen hedef buradan elde edilen bilgiler kullanılarak KNT takviyeli yapısal sağlık izleme sisteminin nano-takviyeli ve kompleks şekilli kompozit yapılar üzerine uygulanması ve etkin bir şekilde eş zamanlı ölçümler için kullanılmasıdır.

1. INTRODUCTION

1.1 Advanced and Nano-enhanced Composites for Aerospace Applications

Fiber reinforced polymer composites (FRPC) have extensive application areas, such as aerospace, automotive, civil and marine structures, through their excellent mechanical properties, and low density. In addition, with improving technology the demand for lighter and stronger materials increases day by day. Even their superior in-plane tensile properties, composite materials have some weakness on compression and interlaminar properties [1]. Within these reasons, researchers try to also improve advanced composite materials using nanotechnology approaches especially for multifunctionality such as increased electrical conductivity in structural composites. To minimize the existing limitations of advanced fiber composites, as a nanotechnological approach carbon nanotube (CNT) reinforcement is utilized alongside advanced reinforcing fibers. These types of composites are called as nano-engineered and nano-enhanced composites [1]. To fabricate nano-enhanced composites, CNTs can be incorporated in a number of different ways within the commercial composite material forms, including within a fiber, as a thin coating on a fiber, as an inner layer, as a coating, as a part of the polymer resin by dispersion (Figure 1.1). CNTs significantly enhance the toughness and strength of the composite materials thoughy used in small quantities. In addition to this advantage, CNTs provide high electrical and thermal conductivity for insulator composite materials and therefore truly multifunctional for noval applications. In comparison, large-scale coating materials (foils, grids, honeycomb, etc.), which lead to weight increment and mechanical problems because of phase discontinuities, in nano-enhanced composites, properties are improved with small addition of CNTs, without significant changes in weight and fabrication methods [2].

Although advanced and nano-enhanced composites ensure mechanical improvement of composite structures, because of their architectural structure, composites are still exposed to failure such as delamination and fiber pull out. Since composite materials

are laminated structures, delamination and fiber rupture mostly occur under the surface of the structure and therefore cannot be detected by visual inspection. As reliability is a prerequisite for aerospace applications, structural health monitoring (SHM) is crucial for continued safe operation of composite structures. Necessity of SHM of existing structures ends up with a development of several techniques such as strain gauge, acoustic emission and lamb wave methods. However, with their superior properties, CNTs can be used as mechanical reinforcing and conductive material in aerospace composite structures for effective SHM. That is why, the focus of this study is using CNTs as multifunctional advanced materials to improve existing composite structures.

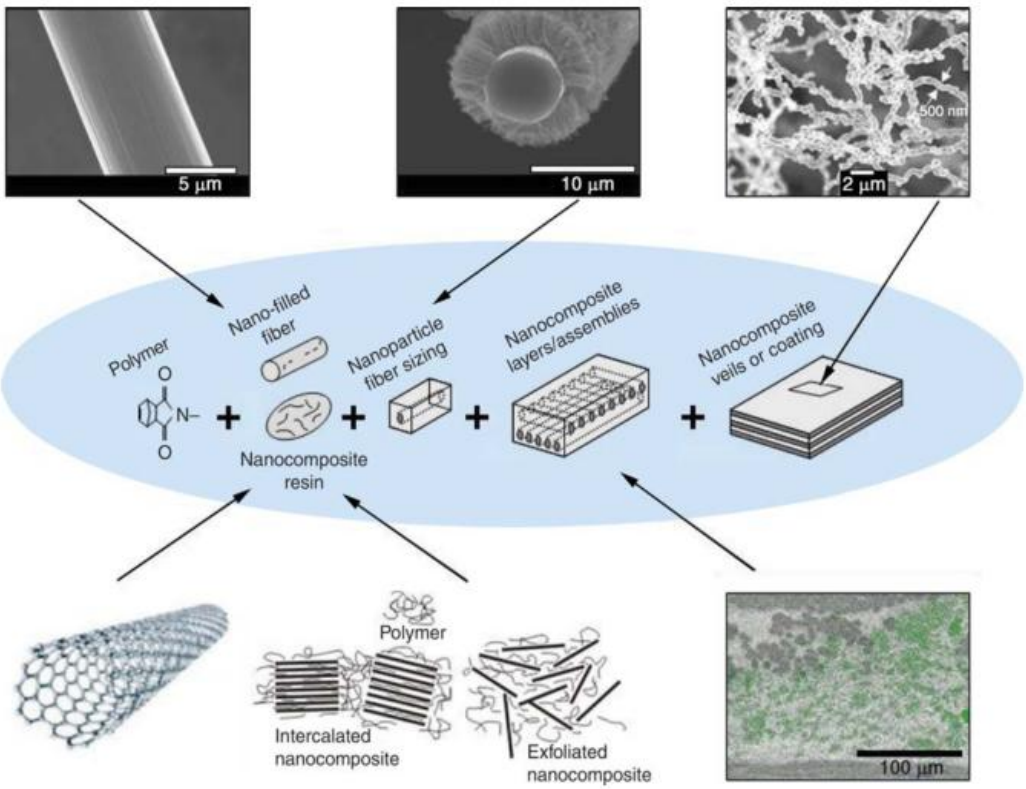

Figure 1.1 : The potential hierarchical integration of nanoparticles within a multiscale composite [2].

1.2 Motivation

With composite structures being increasingly incorporated into aerospace applications, in-situ SHM systems, which are used to detect and interpret changes in a structure during operation time, come into prominence in order to improve reliability and reduce life cycle costs [3]. Since, the inspection and repair of aerospace structures are time consuming and costly applications, SHM systems are

becaming key components of these structures. In addition, SHM systems have a specific importance for reliability of military appliations, since these structures sustain rapid load increment during sudden maneuvers.

Another necessity of using SHM systems for composites structures arises from heterogeneous structures of composites. Since the composites are laminated structures, most of the damage types generate under the surface of structures and that is why composites are more vulnerable to failure during operation.

Although there are many SHM methods that are commercially applied, using CNTs in SHM systems provides multifunctional enhancement of structures through their mechanical, electrical, thermal and piezoresistive properties. That is why; the aim of this study is the investigation of CNT-based SHM systems for composite structures.

First part of this study includes development of CNT-based SHM systems for damage sensing. Although there has been substantial research into CNTs as mechanical damage or strain sensors, the diversities of present investigation are;

- Applying CNT-based SHM system onto the surface of composite structure as a smart paint
- Using CNT-based SHM system both on advanced and nano-enhanced composites
- Investigating effectiviness of CNT-based SHM system on complex geometries

Since the essential contribution of CNTs on SHM systems comes from the piezoresistive property, a continuous current has to be applied on CNTs during operation to activate this property. At that point, adding CNT particles through dispersion into the composite structures and applying in-situ high current for the need of SHM detection can cause a temperature increase in the matrix because of Joule heating, which will cause the degradation of the composite material eventually. In addition, though there are many attempts to integrate CNTs into the advanced composites, new technologies must pass through several engineering and industrial criteria to be accepted for use. Therefore there is long time of integration of such a new application as a common technology. That is why; appliying CNT-based SHM systems onto the surface of a composite structure such as a strain gauge patch

(similar to a general strain sensor) is seen to be the most proper method to eliminate these problems.

In this study, to investigate CNT-based SHM systems, CNT embedded polymer nanocomposites (PNCs) (referred as CNT smart paint) are used as a strain sensor by applying onto the composite surface. To make a comparison between CNT types, both a commercial CNT from Sigma-Aldrich Co. and synthesized CNTs in laboratory of ITU-ARC are used to fabricate the CNT smart paint based on CNT-PNCs. High purity and quality vertically aligned CNTs are synthesized using thermal chemical vapor deposition (th-CVD) and to produce PNCs, CNTs are dispersed into the commercial epoxy system by two step approach. To determine the effect of CNT content, different weight fractions of CNTs are used in CNT-PNCs. 2-probe electrical conductivity measurements are performed for each type of CNT-PNCs to determine whether the CNT content reach to percolation threshold or not. PNC is applied onto the surface of carbon fiber reinforced polymer (CFRP) composite as a smart paint for damage detection. For in-situ SHM, while tension and flexural tests are performed, resistance change of smart paint is followed by a sourcemeter simultaneously (Figure 1.2).

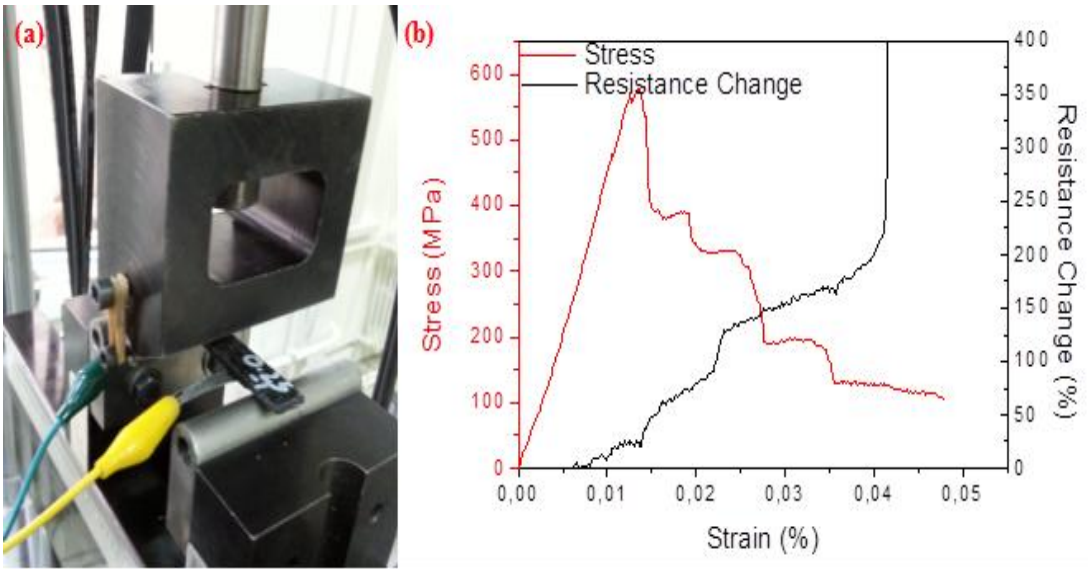

Figure 1.2 : (a) Flextural test setup, (b) Flextural test result of composite specimen and in-situ electrical resistance change of CNT smart paint.

The characteristics of damage in a particular structure play a key role in defining the architecture of the SHM system. Due to their improved properties, nano-enhanced composites display different failure modes than advanced composites are under same

loading conditions. In addition, geometric properties of structures also decisive for damage characterisitics. For these reasons, evaluation of CNT-based SHM systems for nano-enhanced and complex shaped structures has to be performed to completely determine damage sensing capabilities of CNT-based SHM systems.

Since, cylindrical structures are widely used in aerospace appliations, especially for engine shafts, hollow cylindrical structures are fabricated as a complex shaped structure for the second part of this study. Cylindrical structures mostly subject to torsional forces and due to their layered architecture of composites, interlaminar fracture occurs under loading. So, the first step of the second part for this thesis is to include improvement of interlaminar shear strength (ILSS) of conventional carbon fiber prepreg reinforced composites (CFp-RC). In this investigation, a commercial CNT (Sigma-Aldrich) with small length is used. Because of agglomeration problems of CNTs for high dispersion amounts, CNT embedded electrospun carbon nanofiber (ECN) mats are prepared through electrospinning to obtain a homogenious dispersion for CNTs. 0.5, 1 and 2 wt% CNTs are used in ECN mats and effect of CNT amount is determined. ECN mats are direcly fabricated on CFp-RC and, two different mat settings;

- Continuous (four mat layers are applied continuously between middle fiber layers)
- Separate (four mat layers are applied separately between fiber layers)

are used to determine effect of ECN mats on interlaminar shear properties of CFp-RC. Torsion tests are performed to evaluate the ILSS of ECN mat coated hollow cylindrical CFp-RC.

Because of the difficulties of cylindrical composite structure fabrication and effect of fabrication parameters on mechanical properties, the results of torsional tests are not be evaluated as required to determine effectiveness of ECN mats. So, flat specimens with same ECN mats for Mode-I Mode-II mixture fracture toughness test are also fabricated. In flat specimens, ECN mat is placed on the middle surface just after the crack initiation point.

As a future step of this study, SHM of nano-enhanced and curved composite structures will be performed to investigate applicability of CNT-based SHM systems on various composite structures.

2. LITERATURE RESEARCH

2.1 An Overview of Structural Health Monitoring for Composite Structures

Systems that capable of consistently monitoring status of structures in real time named as SHM systems. These systems are the combination of sub-systems such as diagnosis, prognosis, and life extension and predictive maintenance of structures. Diagnosis part of system consists of application in-situ monitoring methods such as strain gauge and fiber optic sensor applications or lamb waves and acoustic emission methods. Processing and interpretation of data that obtained from monitoring methods are achieved by prognosis sub-systems. To interpretate the data a preliminary study has to be performed to charactirize materials and sturctutes. A life extension and predictive maintenance part is also carried out as a last step of SHM applications [4].

For composite structures, SHM application is essential since damage such as delamination or fiber pullout often occurs under the surface of structure through their heterogenous architecture and damages that cannot be detected using traditional methods may cause catastropic failure.

There are many common SHM detection methods for composite structures such as strain gauge, fiber optic sensors and lamb wave. Strain gauges are flexible materials that can change shape through mechanical loads and deformation of strain gauge causes its electrical resistance to change. Strain is related to the resistance change by the quantity of gauge factor. Strain of the structure is calculated by multiplications of gauge factor and resistance change of strain gauge [5]. In fiber optic sensors there is a central silica core inscribed with Bragg gratings. Bragg gratings are refractive materials and the refractive index changes with strain. According to variation of refractive index the strain parameters of structures are determined [6]. In lamb wave method elastic waves propogate in solid structures, the reflection shape and frequency depending on material, thickness and boundary conditions. SHM techniques use lamb waves to reflect particular features such as fatigue cracks, voids,

and debonding in the sample, which requires intensive effort to reconstruct the detected signals reliably and efficiently [7]. Each of these methods has some strength and weak points. For instance, starin gauge is an easy and inexpensive method however; this method only gives local information. In a similar manner, lamb wave method is good at surface penetration but this system gives complex results to processing.

2.2 An Overview of Structural Health Monitoring with Novel Technologies Using CNTs

Besides traditional SHM techniques, using nanomaterials (such as graphene and CNTs) for SHM detection is a novel approach. CNTs are attractive materials because of their multifunctional properties and through their small sizes and low density they have various application fields. In aerospace applications, CNTs present a unique opportunity to improve both mechanical and electrical properties of structures without any weight penalty. CNTs are exceptionally stiff and strong, up to 1 TPa and 63 GPa respectively and also electrically conductive up to hundreds of Siemens per meter [8]. To make a comparison, CNTs are 100 times stronger than steel and can have metallic conduction 100 times more than copper over micron distances [9]. This multifunctionality of CNTs gives the opportunity to improve mechanical properties of composite structures and to use CNTs in SHM systems for simultaneously monitoring the strain conditions of structures during operation. Damage to or around CNTs typically increases their electrical resistance. Typical figures range from about 5% to 100% change in resistance correlated to around 1-3% strain, depending on how the CNTs are arranged, manufactured, which matrix system is used and how the samples are mechanically deformed [10]. CNTs can be integrated into the composite structure in various ways and can be used on the surface of the structure for SHM applications. One of the decisive parameter of CNTs usage in SHM system is percolation threshold, which is the distinctive point from insulator to conductor. As a conclusion, the percolating CNTs can be used in SHM systems to detect the geometrical condition of structures simultaneously during operation.

2.2.1 CNTs fundamentals and applications

CNTs are cylindrical graphene sheets that consist of bonded carbon atoms. Each CNT includes one or more graphene sheets and entitled according to the number of covered graphene sheet as single wall, double wall or multi wall CNTs. In spite of, very small diameter (less than 10 nm) carbon filaments which were observed in 1970's through synthesis of vapor grown carbon fibers prepared by the decomposition of benzene at 1100^{o}C in the presence of Fe catalyst particles, the first detailed systematic studies of carbon atom structures were reported by Iijima, when CNTs was observed by high resolution transmission electron microscopy (HRTEM), in 1991[11, 12]. As a result of their lightweightness with excellent mechanical, electrical and thermal properties, CNTs gain a strong place in every field of research and daily life, from small electronic devices to huge mechanical structures (see Figure 2.1) [13-17]. These broad application areas of CNTs attract the researchers and industries and lead to increase on number of publications and patents [13]. This increment provides an extension on application fields of CNTs and a cyclic improvement is achieved. Figure 2.2 shows the increment of fabrication capacity and number of publications and patents year-by-year basis.

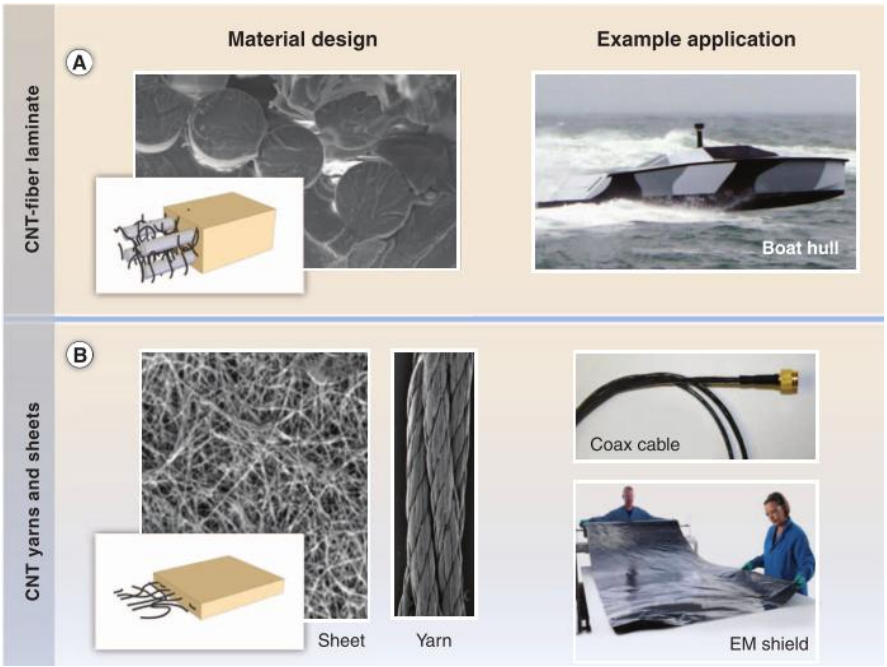

Figure 2.1 : Emerging CNT composites and macrostructures (a) micrograph showing the cross section of a carbon fiber laminate with CNTs dispersed in the epoxy resin and a lightweight CNT-fiber composite boat hull (b) CNT sheets and yarns used as lightweight data cables and electromagnetic shielding material [13].

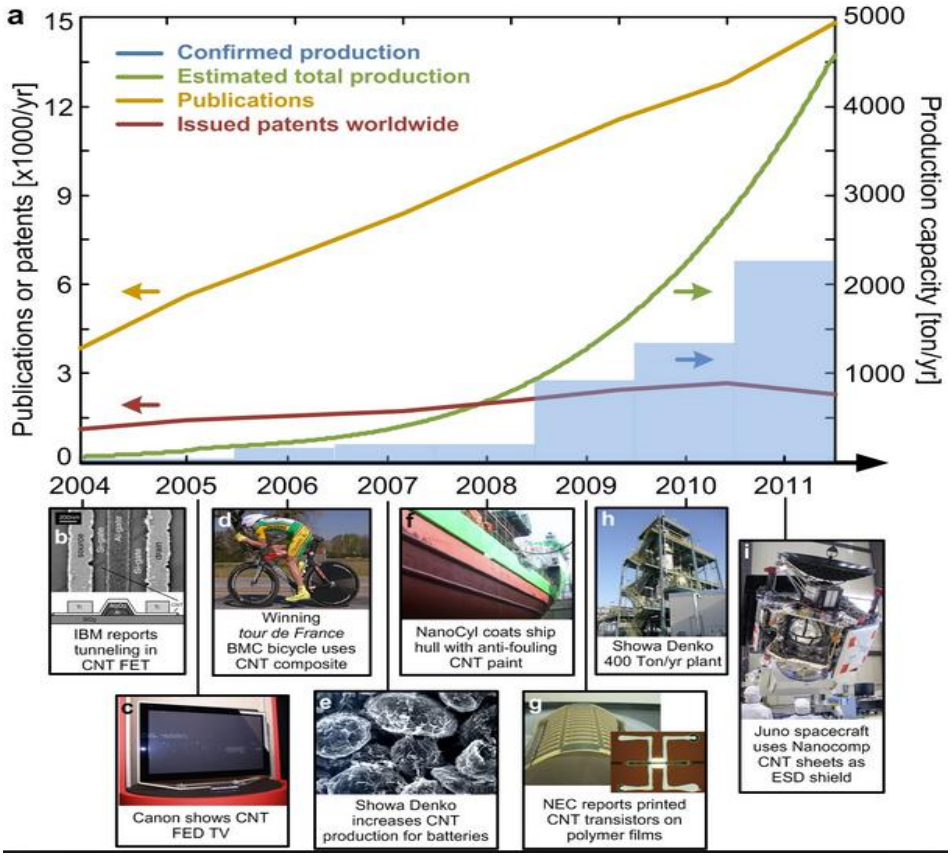

Figure 2.2 : (Top) Evolution of the production capacity of CNTs over the past years, along with numbers of yearly publications and patents. (Bottom) CNT application Milestone [13].

2.2.2 Chemical structure

CNTs considered as a new form of pure carbon. Carbon has four electrons in its outer valence shell; the ground state configuration is $2s^2 2p^2$. Diamond and graphite are considered as two natural crystalline forms of pure carbon. In graphite, sp^2 hybridization occurs, in which each atom is connected evenly to three carbons in the xy plane and a weak π bond is present in the z-axis. Graphene sheet is a 2-D hexagonal (honeycomb) lattice form of the sp^2 set [18]. Rolling sheets of graphene into cylinders form CNTs.

Nanotubes are nearly one-dimensional structures because of their high length to diameter ratio. The properties of nanotubes depend on atomic arrangement, the diameter and length of the tubes, and the morphology. CNTs have been classified according to the number of the walls as single wall (SW-) and multi wall (MW-) CNTs (Figure 2.3). A SWCNT is considered as a cylinder with only one wrapped graphene sheet and MWCNT consist more than one concentric wrapped graphene sheets [19, 20]. Diameters of SWCNT and MWCNT are typically from 0.8 to 2 nm

and from 5 to 20 nm, respectively and diameter of MWCNT can exceed 100 nm [13]. MWCNT has a range of interlayer spacing from 0.34 to 0.39 nm [21].

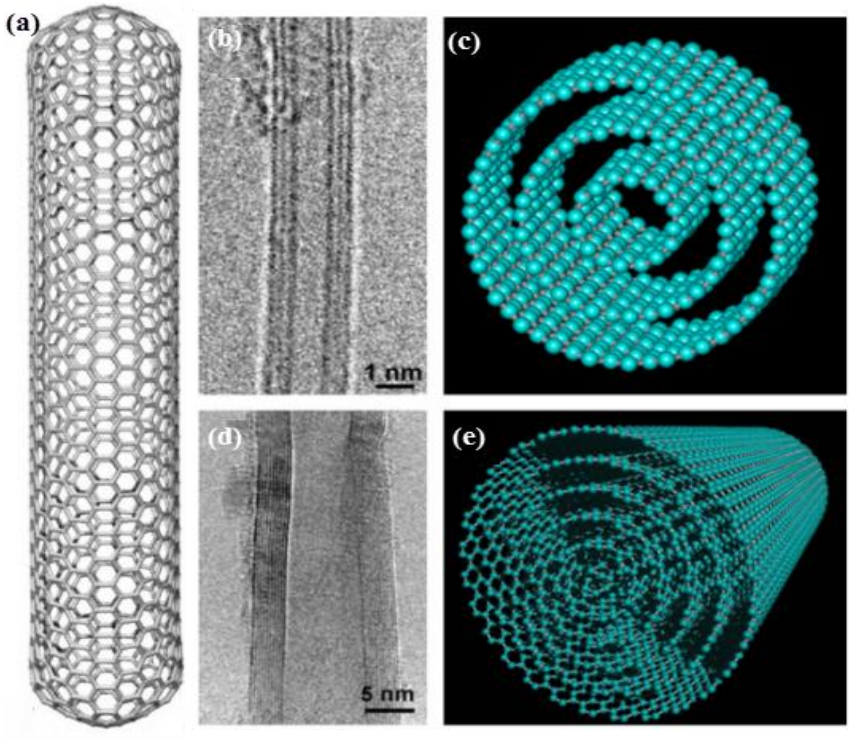

Figure 2.3 : Images of tubular carbon materials and molecular models representing their morphology. (a) Molecular model of a SWCNT [18]; (b) Triple-walled carbon nanotube and (c) molecular model of a triple-walled carbon nanotube; (d) HRTEM of a multi-walled carbon nanotube consisting of 10 nested tubules; (e) molecular model of a six-walled carbon nanotube [22].

The atomic structure of nanotubes is determined by the tube chirality, or helicity, that is defined by the chiral vector, $\mathbf{C_h}$, and the chiral angle, θ. The chiral vector, often known as the roll-up vector, can be described by the equation (2.1). In the equation, the integers (n, m) are the number of steps along the zigzag carbon bonds of the hexagonal lattice and $\mathbf{a_1}$ and $\mathbf{a_2}$ are unit vectors. The chiral angle determines the amount of twist in the tube [19]. All different tubes have chiral angle between zero to 30^o. Special tube types are the armchair tubes with $\theta=30^o$ and zigzag tubes with $\theta=0^o$. All other tubes are called chiral (Figure 2.4) [15].

$$\boldsymbol{C_h = n a_1 + m a_2} \tag{2.1}$$

The chirality of carbon nanotube is significant for the material properties. Especially, tube chirality has a strong impact on the electronic properties of carbon nanotubes.

Depending on the tube chirality, nanotubes can be either metallic or semiconducting. Mechanical properties were also affected from chirality. Although the chirality does not have a major effect on elastic stiffness, plays a key role in the nanotube plastic deformation. For instance, when an armchair nanotube is stressed in the axial direction, ductile fracture is observed [19].

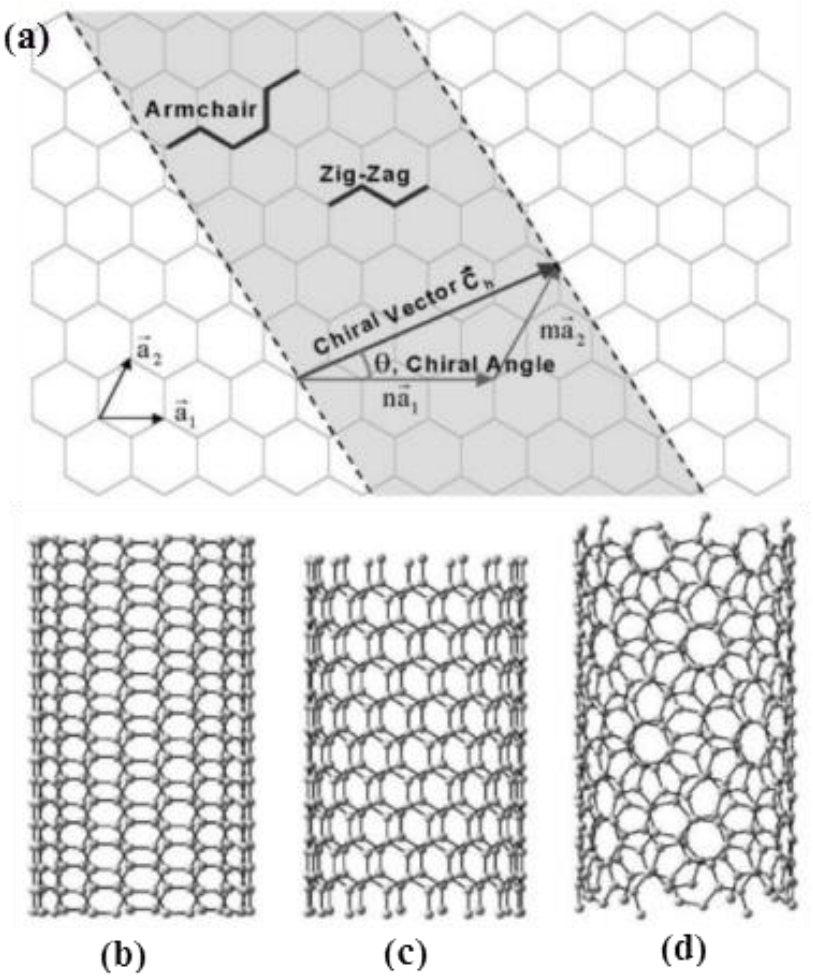

Figure 2.4 : (a) Schematic diagram showing how a hexagonal sheet of graphene is rolled to form a carbon nanotube [19] (b) armchair tube, (c) zigzag tube, (d) chiral tube [15].

2.2.3 CNTs synthesis

CNT structures (single- or multi-walled) can be synthesized by several techniques, which mainly involve gas phase processes. There are three techniques commonly used to grow CNTs:

- Arc discharge
- Laser ablation
- Chemical vapor deposition (CVD) [21].

The MWCNTs were first discovered in the soot of the arc-discharge method by Iijima [11]. Iijima and Ichihashi [23] first synthesized the SWCNTs by use of metal catalysts in the arc-discharge method in 1993. Catalytic growth of nanotubes by the CVD method was first used by Yacaman et al. [24]. The high temperature preparation techniques were first used to synthesize CNTs, but currently, these techniques have been substituted by low temperature CVD methods (<800°C), since the length, diameter, alignment, purity, density, and orientation of CNTs can be controlled by low temperature CVD methods [21]. In addition, CVD method is more appropriate to synthesize large-scale CNT for industrial applications [25]. Table 2.1 gives the summary and comparison of established techniques [21].

Table 2.1 : Summary and comparison of established CNT synthesis methods.

Method	Arc discharge	Laser ablation	CVD
Yield rate	>75%	>75%	>75%
SWCNT or MWCNT	Both	Both	Both
Operating Temperature	> 3000^{o}C	> 3000^{o}C	< 1200^{o}C
Operating Pressure	50-7600 Torr generally under vacuum	200-700 Torr generally under vacuum	760-7600 Torr
Advantage	Simple, inexpensive, high-quality nanotubes	Relatively high purity	Simple, low temperature, high purity, large-scale production, aligned growth
Disadvantage	Purification required, tangled nanotubes	Method limited to the lab scale, purification required	Synthesized CNTs are usually MWCNTs

Arc discharge

The principle of the arc-discharge technique is the generation of an electric arc between two closely spaced graphite electrodes (<1 mm apart) under an inert atmosphere of helium or argon, and usually under reduced pressures of between 50 and 700 mbar. A direct current (between 50 and 120 A) carried by a driving potential of ~30 V creates a high-temperature plasma (>3000 °C) between the two electrodes [25]. The chamber also contains evaporated carbon molecules and some amount of metal catalyst particles (such as cobalt, nickel, and iron). In the proses of arcing, about half of the evaporated carbon solidifies on the cathode (negative electrode) tip, which is called cylindrical hard deposit or cigar-like structure. The remaining carbon

deposited on the periphery and condenses into ‘chamber soot’nearby the walls of the chamber and ‘cathode soot’ on the cathode. The inner core, cathode soot and chamber soot, which are dark and soft, yield either single-walled or multi- walled carbon nanotubes and nested polyhedral graphene particles. In the arc discharge synthesis of MWCNTs could be done without use of catalyst precursors but synthesis of SWCNTs utilizes different catalyst precursors and, for expansion in arc discharge, utilizes a complex anode, which is made as a composition of graphite and a metal [21]. Since the arc discharge technique uses higher temperatures, the expansion of CNTs occurs with fewer structural defects in comparison with other methods [21].

Laser ablation

In the laser ablation method, a high power laser source is used to generate high temperatures and a quartz tube containing a block of pure graphite is heated inside a furnace at 1200 ^{o}C in an Ar atmosphere. The vaporized carbon rapidly cools in a carrier gas stream, and forms CNTs. For generation of SWCNTs, with laser technique adding of metal particles as catalysts to the graphite targets is necessary.

The diameter of the nanotubes depends upon the laser power. When the laser pulse power is increased, the diameter of the tubes becomes thinner. This method has a potential for production of SWCNTs with high purity and high quality. The principles and mechanisms of laser ablation method are similar to the arc-discharge technique, but in this method, a laser, which hit a pure graphite pellet holding catalyst materials, provides the needed energy. One another difference of this method is, CNTs with a defined chirality can be synthesized by laser ablation [21, 25].

Unfortunately, the laser technique is not economically advantageous because the process involves high-purity graphite rods, high laser powers are required, and the amount of nanotubes that can be synthesized per day is not viable [18].

Chemical vapor deposition (CVD)

CVD is essentially a thermal decomposition of a hydrocarbon vapor in the presence of a metal catalyst. In this process, high temperature catalyst material decomposes the hydrocarbon while the hydrocarbon vapor passing through a tubular reactor typicallay 15-60 min. First step is decomposition of hydrocarbon vapor into carbon and hydrogen species, when comes in contact with the “hot” metal nanoparticles.

Hydrogen species flies away and carbon species gets dissolved into the metal. At the second step, dissolved carbon precipitates out and crystallizes in the form of a cylindrical network, when the carbon, in the metal catalyst, reaches the carbon-solubility limit at the same temperature. The cylindrical network is energetically stable since there are not dangling bonds. Hydrocarbon decomposition (being an exothermic process) releases some heat to the metal's exposed zone, while carbon crystallization (being an endothermic process) absorbs some heat from the metal's precipitation zone. This precise thermal gradient inside the metal particle keeps the process on [26].

There are two general cases for CVD process; tip growth, and base growth (Figure 2.5). At the tip growth model, since the catalyst-substrate interaction is weak, hydrocarbon decomposes on the top surface of the metal, carbon diffuses down through the metal and CNT precipitates out across the metal bottom, pushing the whole metal particle off the substrate. To the time, the metal is fully covered with excess carbon, CNT continues to grow and the growth is stopped when the catalytic activity of metal ceases. In the base growth model, the catalyst-substrate interaction is strong, so CNT precipitation fails to push the metal particle up. Initial hydrocarbon decomposition and carbon diffusion take place similar to that in the tip growth case and precipitation is compelled to emerge out from the metal apex. First carbon crystallizes out as a hemispherical dome and then extends up in the form of seamless graphitic cylinder [26].

The diameter of the CNTs is closely related to the diameter of the metal nanoparticles. Small metal catalysts yield CNTs with a small diameter and larger diameter CNTs are grown on large metal nanoparticles (Figure 2.6) [27]. The size of catalyst particles also states the CNTs wall conditions. For example, SWCNT forms when the particle size is a few nm, and MWCNT forms when the particle size is a few tens nm [26].

CVD technique further enables CNTs to be synthesized for a wide range of end-use applications and in a controlled orientation, for instance, field emission devices and patterned CNTs on substrates, which cannot be fabricated using the arc-discharge or laser ablation techniques [25].

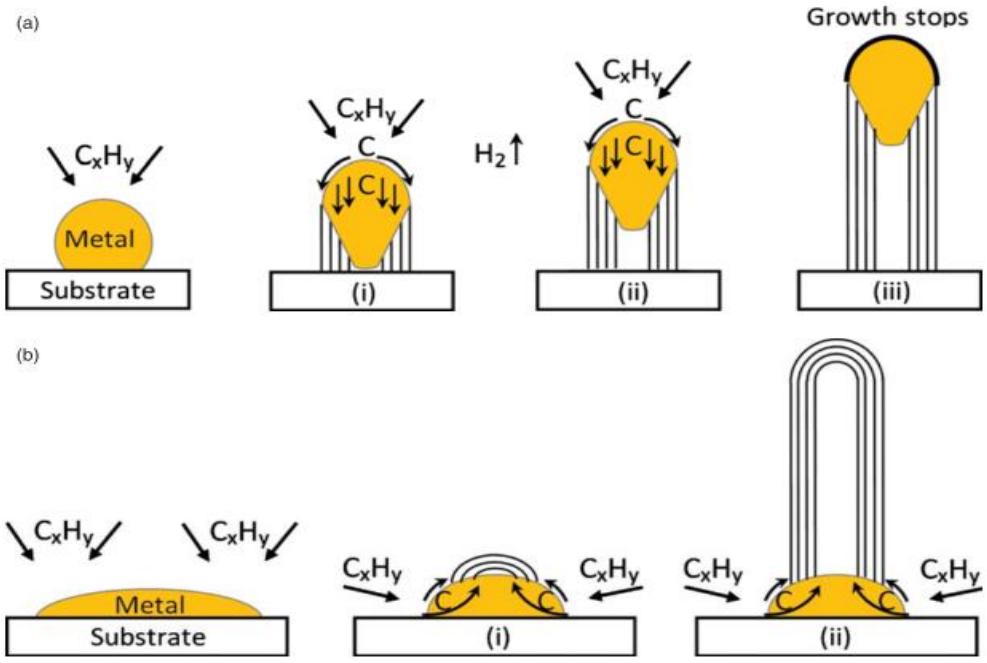

Figure 2.5 : (a) Tip growth model, (b) Base growth model [26].

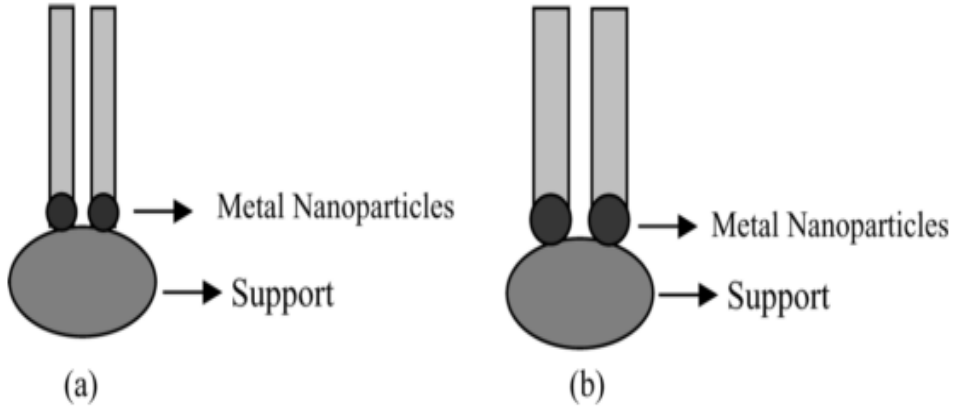

Figure 2.6 : (a) Small metal nanoparticles yield small nanotube diameters; (b) large metal nanoparticles yield larger nanotube diameters [27].

2.2.4 Mechanical and electrical properties

The properties of CNTs are extremely affected by several parameters such as diameter, chirality and degree of graphitization. CNTs have a high aspect ratio, high tensile strength, low mass density, high heat conductivity, large surface area, and accomplished electronic behavior [27].

Mechanical properties

CNTs are often referred to as one-dimensional "quantum wires" due to the quantum confinement effect on the carbon nanotube circumference. Since C–C bonds in the honeycomb lattice of CNTs structures are one of the strongest bonds in nature, it give

reason to explore the mechanical properties of CNTs. In addition, when the graphene sheet is rolled to form an SWCNT, the axial component of the σ bonding between carbon atoms increases significantly. This is the main reason why CNTs are stiffer than diamond and have the highest Young's modulus and tensile strength. Young's modulus is independent of tube chirality, but depends on tube diameter [27].

Since the mechanical properties of CNTs are assumed very high according to their structures, many experimental studies were performed to determine numerical results for these properties to compare with other materials. By assuming CNT as a structural member, such as bar, beam, and shell model, the elastic properties of CNT can be obtained from experimental observations [28]. For instance, Treacy et al. [29] were the first to report fitting Young's modulus of MWCNT to experimental data. Their work was based on analysis of thermal vibration of MWCNT, modeled as a continuous beam. For a total of 11 MWCNT's Young's modulus values were reported as ranging from 0.4 to 4.15 TPa with a mean of 1.8 TPa. A cantilevered beam model has been used in the experiment by Wong et al. [30] in which individual MWCNT were bent using an atomic force microscope (AFM) tip (Figure 2.7). By fitting the measured static response to the analytical solution for a cantilevered beam, a Young's modulus of 1.28 ± 0.59 TPa was obtained. SWCNTs with diameter between 1 and 2 nm are found to have a Young's modulus of about 1 TPa [31]. However, it is shown experimentally that the Young's modulus of CNTs decreases from 1 TPa to 100 GPa when the diameter of an SWCNT bundle increases from 3 nm to 20 nm [32]. The Young's modulus of MWCNTs is generally higher than that of SWCNTs due to different nanotube diameters contained coaxially in the MWCNTs and due to van der Waals forces acting between the tubes. In addition, CNTs can be twisted and sustain large strains (40%) in tension before fracture, whereas most materials fail with a strain of 1% or less due to propagation of dislocations and defects [27].

Another amazing property of CNTs is high tensile strength. Since carbon nanotubes have the sp2 bonds which orbitals are close to nucleus and the bonds are short, between the individual carbon atoms, they have a higher tensile strength than steel and Kevlar [21].

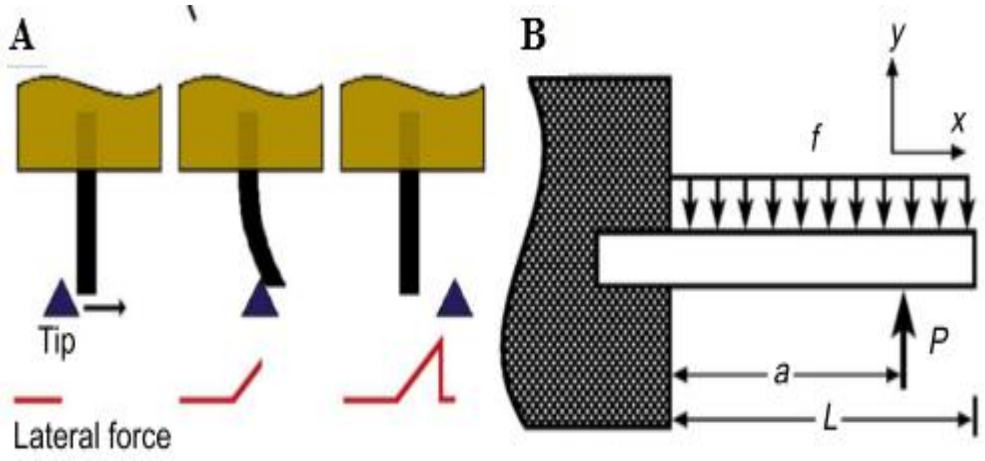

Figure 2.7 : (A) Schematic of beam bending with AFM tip. (B) Schematic of a pinned beam with a free end [30].

Electrical properties

Electrical response of CNTs substantially depends on degree of crystallinity and geometric differences such as defects, chilarity, and diameter. Since bundle like particles do not give exact value for electrical conductivity because of agglomerated CNTs, the best way to determine the conductivity of MWCNTs and SWCNTs is direct 4-probe (or 2 probe) measurements on crystalline individual tubes [18]. Due to their low resistance and very few defects along their structures, CNTs have higher electrical conductivity than copper. The electrical resistivity of CNTs was found to be as low as 10^{-6} Ω.m and often can be altered by modifying the structure of the nanotube lattice [27].

2.3 Polymer Nanocomposites

Polymer nanocomposites (PNCs) are two phase systems consisting of polymers loaded with reinforcing fillers [33]. Enhanced mechanical, electrical and thermal properties of CNTs lead to use of them as fillers in polymeric systems. In general, nanomaterials provide reinforcing efficiency because of their high aspect ratios. The properties of a nanocomposite are greatly influenced by the size scale of its component phases and the degree of mixing between the two phases. In PNCs dispersion of the nanoparticle and adhesion at the particle–matrix interface play crucial roles in determining the mechanical properties of the nanocomposite. With proper dispersion, the nanomaterial will offer improved mechanical properties such as interlaminar shear strength, delamination resistance, fatigue and corrosion

resistance over that of conventional composites, in fact, a poorly dispersed nanomaterial may decrease the mechanical properties as seen in many research articles [34, 35].

As-produced CNTs are held together in bundles or entanglements by van der Waals forces (Figure 2.8). Difficulty of entangled CNT dispersion during processing and poor interfacial interaction between CNTs and polymer matrix limits the application of CNTs as reinforcement of the polymer systems. Size of the CNTs plays an important role in dispersion condition, because CNTs have small diameter in nanometer scale with high aspect ratio, which creates large surface area. In addition, large surface areas of fillers provide large interphase area between the filler and matrix for good bonding, which also cause agglomeration of CNTs as a bundle. That is why, using CNTs as nanofillers at high weight fractions can cause a decrease in mechanical properties of nanocomposites [35].

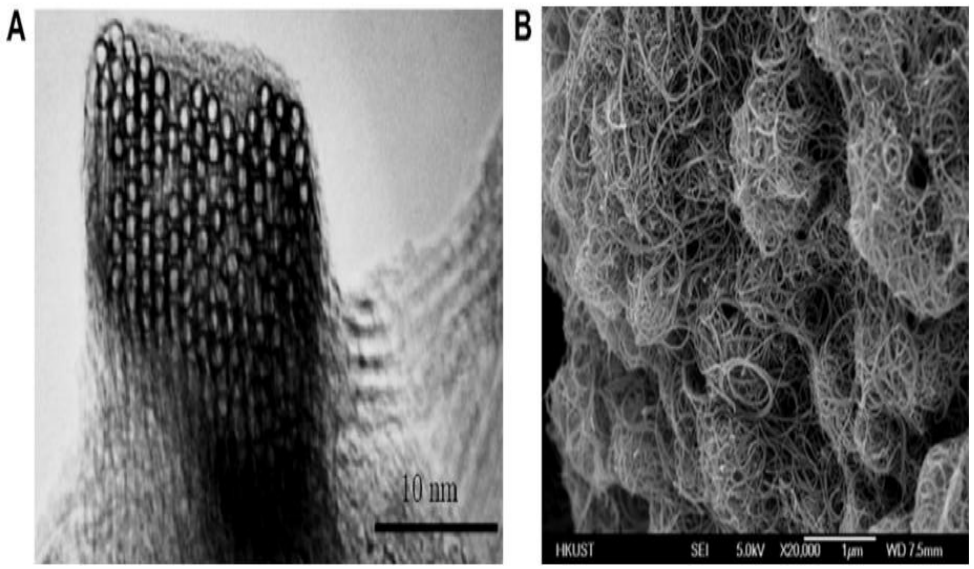

Figure 2.8 : Electronic microscope images of different CNTs: (A) TEM image of SWCNT bundle, (B) SEM image of entangled MWCNT agglomerates [35].

To improve dispersion state, some techniques were (such as ultrasonication, calendering, ball milling, shear mixing and extrusion) developed for CNT dispersion in polymer matrix (Figure 2.9). Proper dispersion technique is selected according to polymer matrix and CNT type and weight fraction. For example, ultrasonication is an effective method to disperse in liquids having a low viscosity and extrusion is a popular technique to disperse into solid polymers like thermoplastics. In addition to

dispersion techniques, chemical or physical functionalization of CNTs can be performed to modify surface properties of CNTs for sufficient bonding between CNT and matrix [35].

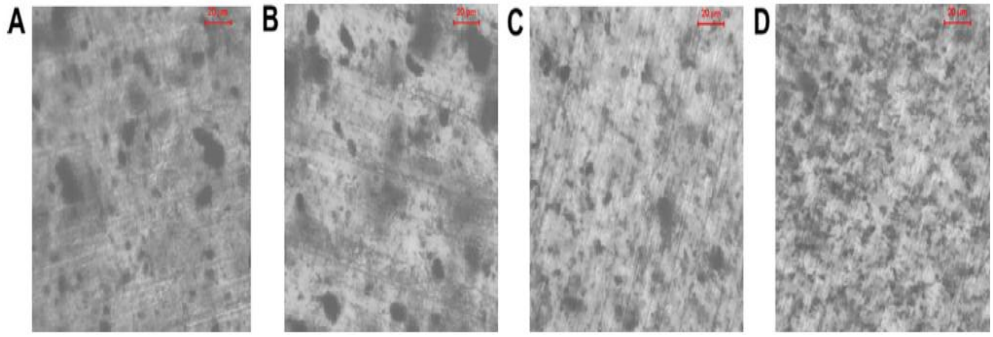

Figure 2.9 : Dispersion of CNTs in nanocomposites fabricated using different techniques (A) sonication in water bath, (B) shear mixing, (C) probe sonicator, (D) calendering [35].

The conventional filler content in polymer composites is in the range of 10-70 wt%, however, the properties of the composites can be largely modified even at an extremely low content of nano filler which is also the main aim to achieve enhanced properties in low CNT loadings from researchers. For instance, Li et al. [36], fabricated PNCs with various weight fractions of nanofillers (0.05, 0.1, 0.25, 0.5 and 1 wt%) using different combinations of dispersion techniques (Table 2.2). According to results of PNCs, electrical conductivity can be enhanced several orders of magnitude with less than 0.5 wt.% of CNTs addition (Figure 2.10).

Table 2.2 : Processing methods used to disperse CNTs [36]

Dispersion Condition	Dispersion Method
A	Shear mixing for 30 minutes at 3000 rpm
B	CNTs dispersed by ultrasonication for 1 hour in acetone Ultrasonication for 2 hours at 60^{o}C with epoxy
C	UV/O_3 treatment of CNT for 1 hour and ultrasonication for 2 hours in acetone Shear mixing for 30 minutes at 3000 rpm with epoxy
D	Ball milling for 2 hours, ultrasonication in toluene for 1 h, UV/O_3 treatment for 2 hours, silane treatment Ultrasonication for 2 hours at 60^{o}C with epoxy

In addition, mechanical properties also improve with well dispersed low fraction of CNTs that have sufficiently large aspect ratio. Qian et al. [37] obtained 35% and 25% increase in elastic modulus and tensile strength, respectively with polystyrene

nanocomposite reinforced with 1.0 wt% CNTs. To discuss the effect of geometric orientation of CNTs in polymer matrix Thostenson et al. [38], made an experimental study with polystyrene composite films containing random and oriented CNTs with 5 wt%. They achieved 10% increment for storage modulus of the polystyrene composite films containing randomly oriented CNTs even the increment is 49% for films that reinforced with oriented CNTs (Figure 2.11).

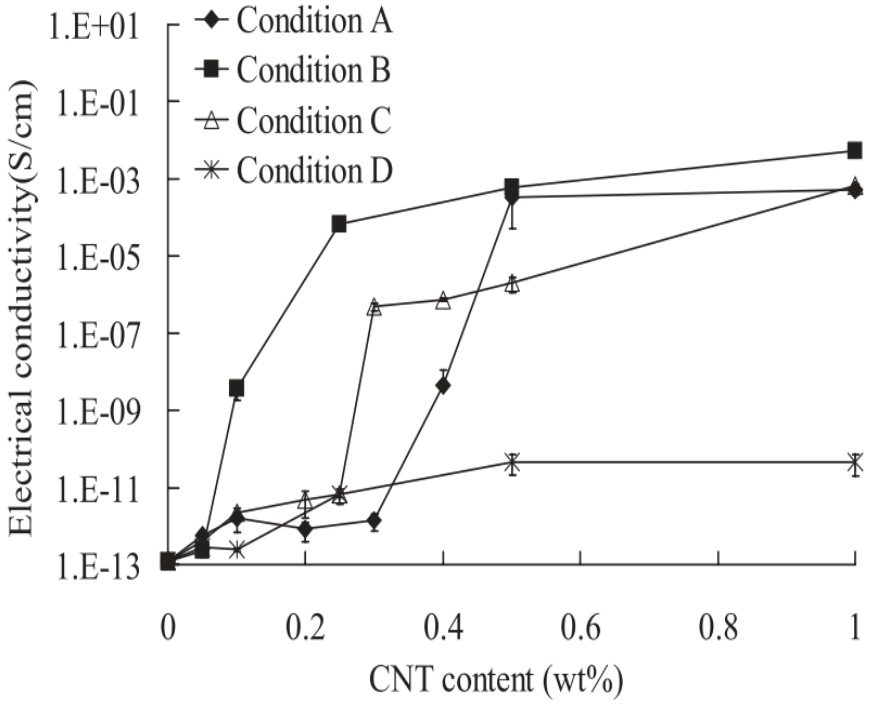

Figure 2.10 : Electrical conductivities of PNCs as a function of CNT content [36].

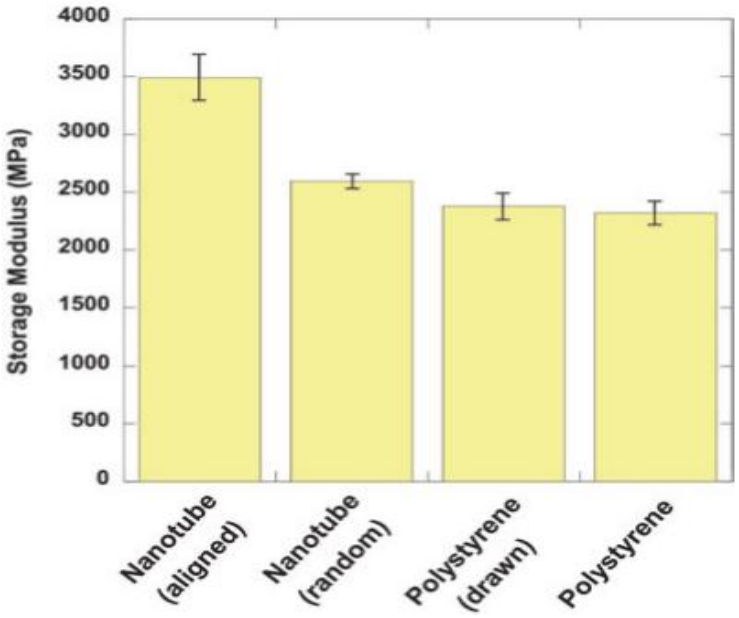

Figure 2.11 : Average storage modulus results [38].

As well as the improvements of mechanical and electrical properties, nanoparticle reinforcement also affect the crystallization and glass transition temperature (T_g) of the polymer. According to nanoparticle and polymer type and the interaction between them, T_g can both increase and decrease [39].

Eventually, advanced dispersion and alignment of CNTs in polymer matrices prominently improve mechanical and electrical properties of PNCs. As a result of this progress, PNCs are used for various applications.

2.4 Carbon Fiber Reinforced Polymer (CFRP) Composites

CFRP composites are increasingly being used as materials for structural applications in aerospace and automotive fields, because of their excellent mechanical properties like high specific stiffness and strength. Although; the in-plane mechanical properties are remarkable with specified configurations of fiber architectures achieved by various fiber orientations, the interlaminar properties are relatively weak and lead to failure of structures due to delamination or other damage modes [40]. Delamination failure is the most significant damage mode in CFRP composites and fiber properties have considerably less influence on delamination resistance in polymer epoxy composites [41]. Several common methods such as using 3D-textiles, stitching, and z pinning are used to strengthen the interface of composite structures. Since these existing solutions precipitate reduction of in-plane mechanical properties due to lamina and laminate damage and in-plane fiber volume loss, an alternative method for increasing interlaminar properties is adding nanoscale fibers such as CNTs into the system [42].

On the other hand, fiber reinforced composites have low damage tolerance, so the growth of damage is difficult to control and predict. At that point, the serious interest in the use of composite materials has led to the necessity of the development of innovative ways to monitor the status of the composite structures in service time. Various approaches have been used for monitoring the status of the structure. Using strain gages, piezoelectric and piezoresistive sensors or fiber optic sensors are the oldest methods for monitoring [43-45]. From this point of view, CNT embedded sensors can be an interesting solution due to its particular properties like high electric conductivity and light weightness [46-48].

2.5 Nano-Enhanced Composites

By means of being light, efficient and energy saving structures, CFRP composites gain more and more in importance day after day. However, because of the incremental demand of industry, conventional CFRP composites are advanced at last decades by adding an ingredient with superior mechanical, electrical and thermal properties. At this point, as a result of their extraordinary intrinsic properties (electrical conductivity, thermal conductivity, wear resistance, service temperature, flame retardancy and surface finish) and wide range of potential applications, CNTs attract huge attention. A nanoscale CNT reinforcement is utilized alongside traditional microscale reinforcing fibres for development of nano-enhanced (or hierarchical, or hybrid, or nanostructured, or multiscale) composites [1]. Supplementing of CNTs into conventional fiber reinforced polymer composites has been achieved predominantly through four different ways (Figure 2.12);

a) Dispersing CNTs entirely throughout the composite matrix [1, 49],

b) Growing (fuzzy) CNTs on fiber [50],

c) Interleaving bucky papers made from CNTs at certain laminar interfaces [51],

d) Stitching CNTs directly onto primary reinforcing fiber [52].

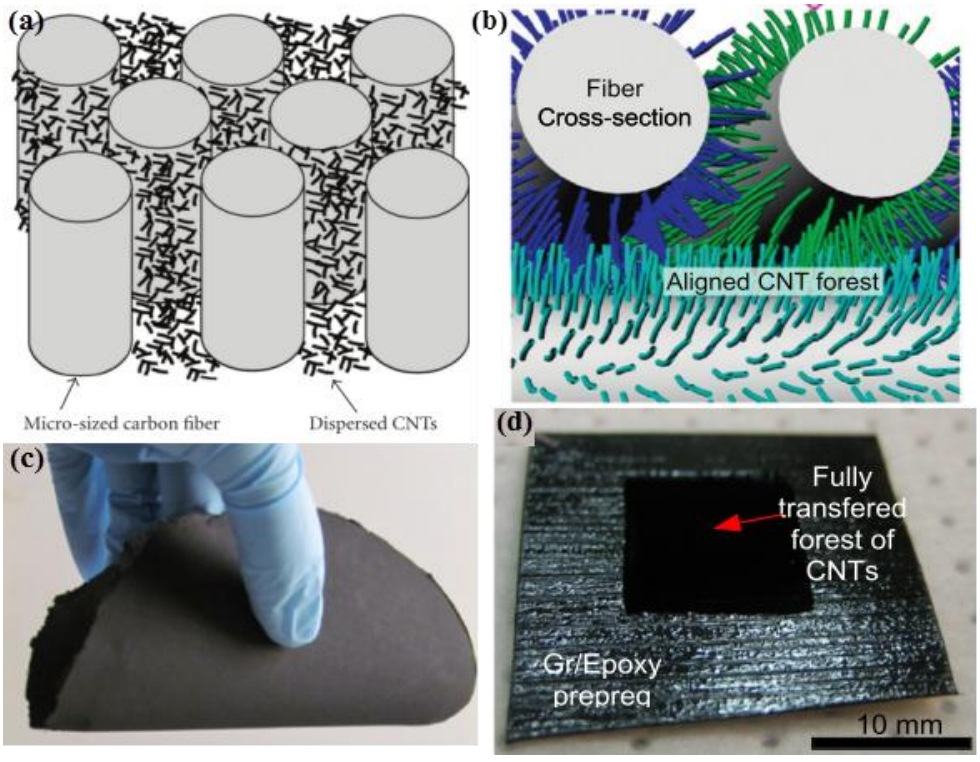

Figure 2.12 : Supplementing methods for CNTs (a) dispersing [49], (b) fuzzy fiber [50], (c) bucky paper [51], (d) stitching [52].

In nano-enhanced composites, adding CNTs up to 2 wt% into the matrix are not affect the in-plane properties substantially, on the other hand, matrix dominated properties, like interlaminar shear strength and fracture toughness, are improved by about 8-30% and 100% respectively [1].

To improve the efficiency, functionalized CNTs are also used for good dispersion and good bonding between CNT and matrix. Inam et al. [49] used amino-functionalized double wall CNTs in carbon fiber reinforced composites were prepared by a resin infusion method. By adding small amounts of CNTs (0.025, 0.05, and 0.1 wt%) to epoxy resin higher flexural strength, flexural modulus, and absorbed impact energy were obtained. The mechanical properties show a decrease above 0.05 wt% CNT, mainly because of inhomogeneous CNT dispersion or wetting and bonding problems. However, with 0.05 wt% CNT concentration they achieved a 35% improvement in flexural modulus, a 5% increment in flexural strength, a 6% improvement in absorbed impact energy, and 23% decrease in the mode I interlaminar toughness.

The improvement of commercial composites with CNTs is prevented by difficulties in dispersing CNTs in matrix at high weight fractions while obtaining uniform and strong interactions with the polymer matrix. Therefore, instead of dispersing CNTs into the matrix, stitching aligned CNTs (A-CNTs) on fiber surface (named as nano-engineered composite structures) helps to improve properties of composites due to controlled morphology and orientation (Figure 2.13). For instance, by using CNT stitched modified interface Garcia et al. [52] achieved 1.5-2.5 times increment in mode-I and 3 times increment in mode-II fracture toughness.

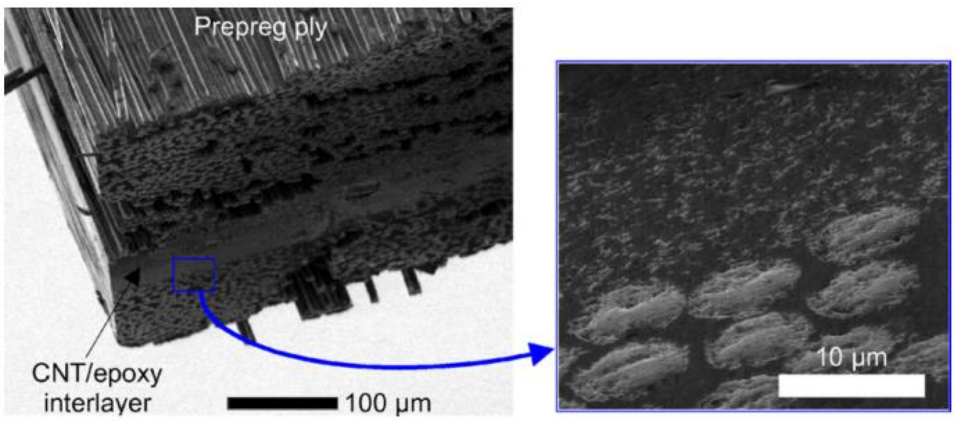

Figure 2.13 : SEM image of a 2-ply aligned CNT interlayer hybrid composite [52].

In addition, bucky papers made from CNTs are also used to fabricate nano-enhanced composites. As an example, Khan and Kim [51], obtained 31% increment in ILSS and 104% increment for mode-II interlaminar fracture toughness by adding randomly oriented carbon nanofiber (CNF)-bucky paper interleaves into carbon fiber reinforced composites. The ILSS of CFRP composites were measured by short beam shear (SBS) test. Figure 2.14 shows scanning electron microscopy (SEM) images of the fracture surfaces of the specimens. According to images, the matrix in the neat CFRP composites was seperated from the fiber and the matrix material had significant plastic deformations between the seperated fibers. However, bucky paper interleave was intact after fracture and indicating strong interfacial adhesion. As a result, bucky paper acted as reinforcement to the matrix and promoted matrix shear properties by offering resistance to matrix cracking.

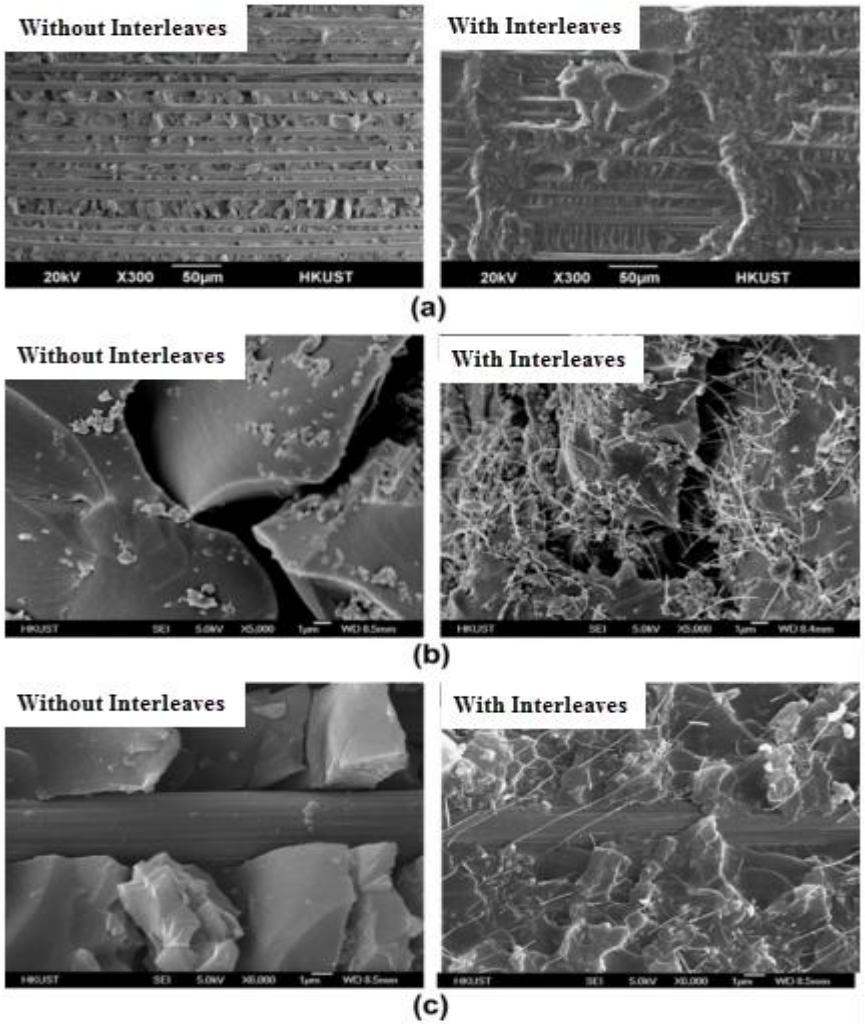

Figure 2.14 : SEM images of the fracture surface of SBS test specimens (a) global view at a low magnification, (b) matrix cracking behavior, (c) fiber/matrix interfacial region [51].

As well as enhancement in mechanical properties, CNTs also provide improvement for electrical conductivity by means of their ability to form conducting network. Since the fiber polymer composites have a electrical anisotropy, the conductivity in the fiber direction is nearly an order of magnitude higher than that in the transverse direction, using CNTs with controlled through thickness orientation, may lead to increase of the electrical conductivity in the transverse direction [1].

In addition, Qiu et al. [53], also used CNTs to enhance out-of-plane properties of polymer composites. Fabrication of nano-engineered composites performed with vacuum assisted resin transfer molding (VARTM). The MWCNTs dispersed resin was infused through glass fiber fabrics in the thickness direction (Figure 2.15). With using 1 wt% loading of MWCNTs, 11 order of magnitude higher electrical conductivity was obtained for nano-enhanced composites. However, with using functionalized MWCNTs, only 2 order of magnitude increment was achieved for electrical conductivity.

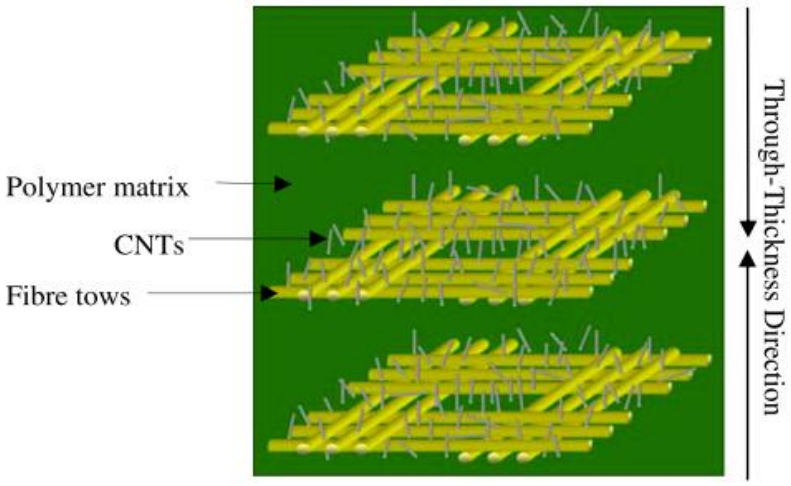

Figure 2.15 : Lay-up of fabric impregnated with MWCNT/resin fluid [53].

2.5.1 CNT-enhanced interface through electrospinning

Interlaminar resistance to failure in laminated composite materials has been an active research field for a long time because of the delamination problem of common composite structures. Introducing effective sub-phases and reinforcement without significant weight penalty to improve the mechanical properties of interlaminar regions is an ongoing subject in literature [54]. After it was discovered, extensive attention has been paid to nanofibers and nanoparticles as the superior reinforcements of engineering composites [1, 55]. The polymer composites

reinforced with nanotubes and nanofibers in matrices are expected to possess superior mechanical properties, however, because of an inadequate dispersion and alignment problems the improvements of mechanical properties are lower than what have been expected. In addition, obtaining a continuous interface is also important to provide well stress transfer between composite layers. To eliminate these problems, incorporation of nanoreinforced mats between composite layers is a widely studied method [56, 57].

Fabrication of CNT embedded nano-reinforced mats is achieved by electrospinning. With optimized electrospinning parameters, such as

- Applied voltage,
- Solution flow rate
- Tip to ground distance

a homogenious electrospun mat can be fabricated.

As an example, Bilge et al. [54] fabricated polystyrene-co-glycidly methacrylate P(St-co-GMA)/MWCNT electrospun mats on carbon/fiber epoxy prepregs through electrospinning. With an additional weight of electrospun mats as low as 0.2% of the prepreg ply weight they obtained 17% increase in flexural strength, and 70% increase in mode II strain energy release rate.

In addition, Chen et al. [56] also analysed the effects of electrospun carbon nanofiber mats on interlaminar properties. With only an additional 5% weight, 86% improvement in interlaminar shear strength had been achieved. They also studied for effects of elecrospun nanofiber mats on electrical conductivities. By means of nanofiber enhancement, the out-of plane conductivity increased 150% and the in-plane conductivity increased 20%. After they showed the effects of electrospun mats on properties of composite structures, they carried out a parametric study to determine the most effective electrospun mat collecting time. Electrospun collecting time was studied for 5, 10, 20 and 30 min (Figure 2.16). According to results of mechanical tests (Figure 2.17), best mechanical properties were achieved with 10 min collecting time and further increase of the collection time did not improve the properties of composite. These results can be attributed to the presence of beads or beaded nanofibers, which could function as the structural defects [57].

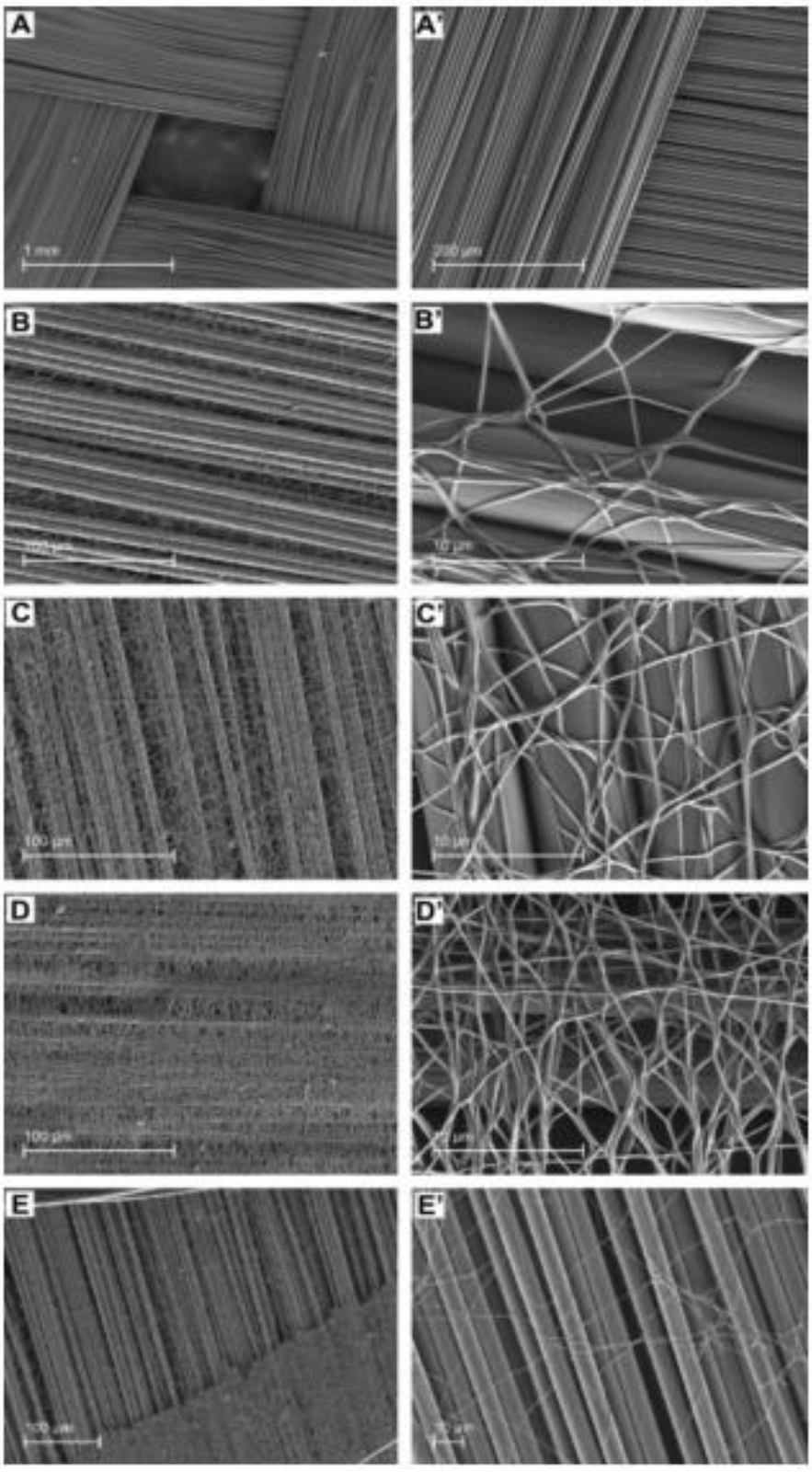

Figure 2.16 : SEM images of carbon fiber fabric and ECN mats. Collecting times were set at (A) 0 min, (B) 5 min, (C) 10 min, (D) 20 min, (E) 30 min, A', B', C', D', E', are the SEM images with higher magnification [57].

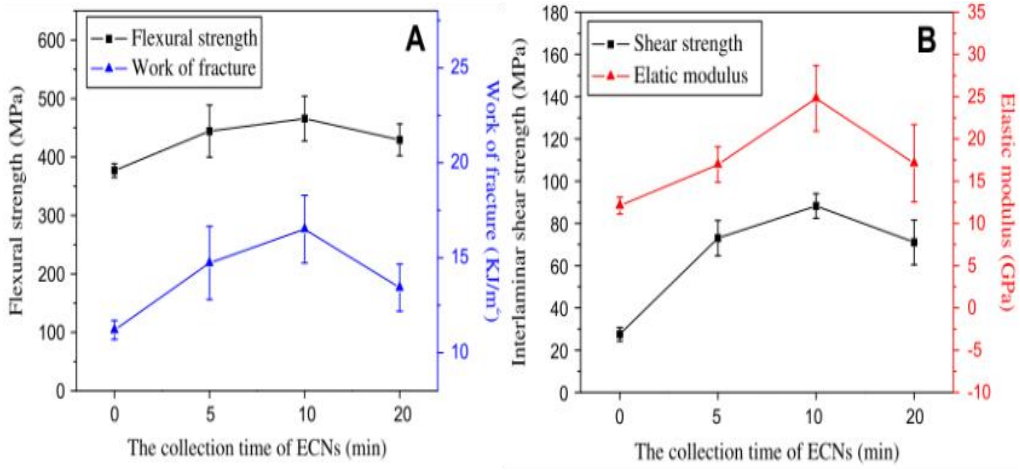

Figure 2.17 : Mechanical properties (A: flexural strength and work of fracture and B: interlaminar shear strength and elastic modulus) of epoxy composites reinforced with carbon fiber fabrics or ECN mats [57].

2.5.2 An overview on CNT nanocomposites for SHM applications in advanced composite structures

Composite materials are being increasingly used because of their excellent mechanical properties like high specific stiffness and strength. However, since the mechanical performance of composite materials may be severely altered when damage occurs, the serious interest in the use of composite materials has led to the necessity of the development of innovative ways to monitor the status of the composite structures in service time [46, 47].

SHM has been studied for many decades and different approaches have been used for these systems. Using strain gages, piezoelectric or piezoresistive, sensors are the oldest methods for SHM. Also using fiber optic sensors for aerospace applications is an ongoing study for SHM, which have not been commercialized as expected yet [43-45]. From this point of view, CNT can be an interesting solution due to its particular properties like high electrical conductivity, piezoresistivity and lightweight. Since the carbon fiber reinforced composites have a lower electrical conductivity compared to metals, the solution to abnormal operations like lightning strike, electromagnetic interference (EMI) shielding is to cover the composite structure with a metal paint or foil that adds significant weight and process parameters to the related component. As an alternative solution, CNT-epoxy smart systems will be used instead of metal covering to achieve same electrical conductivity without any weight penalty.

CNTs are theoretically 100 times stronger than steel and having a higher electrical conductivity than copper wire. Due to their sensitivity, CNTs can be used as strain sensors or damage sensors for advanced applications. Electrical conductivity of composites consisting of conducting fillers and insulating matrices is explained by percolation theory. The critical filler content, where the composite undergoes an insulator to conductor transition, is referred as the percolation threshold. At that point, the measured electrical conductivity of the composite sharply jumps up several orders magnitude due to the formation of continuous electron paths or conducting networks (Figure 2.18) [35].

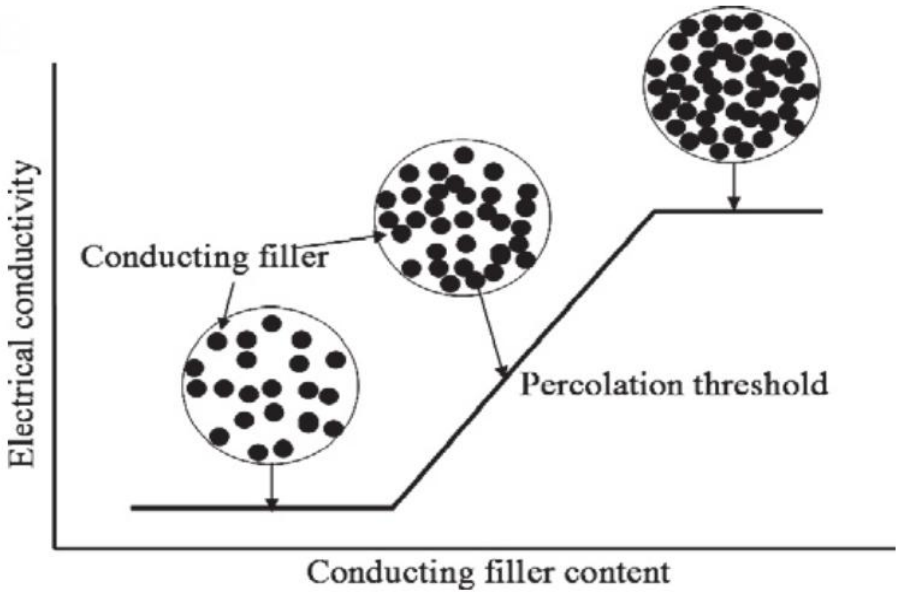

Figure 2.18 : Schematic of percolation phenomenon and conducting network in conducting composites [35].

Bauhofer and Kovacs [58] carried out a review study to discuss the effect of experimental parameters on the percolation threshold of CNT-polymer nanocomposite. Almost 120 publications about electrical percolation threshold of CNT polymer nanocomposites were reported. According to these publications, the parameters, affect the percolation tresholds are listed as;

- CNT type
- CNT synthesis method
- CNT treatment and dimensions
- Polymer type
- Dispersion method

There are two types of percolation threshold, one of them is statistical percolation threshold that defines the situation where the randomly distributed filler particles form percolating paths and other is a kinetic percolation threshold, where the particles are free to move and there by can form a conducting network. Since the theoretical analyses ignore the particle movement, most of the predictions depend on statistical percolation threshold.

According to study of Kovacs et al. [59] statistical percolation threshold was achieved with nearly 0.1 wt% filler concentration. Three different sample preparation methods were studied as slow stirring (50 rpm), medium stirring (100 rpm), and fast stirring (2000 rpm). As a result, Figure 2.19 shows that, when the filler concentration approached the statistical percolation threshold, stirring conditions did not affect the conductivity.

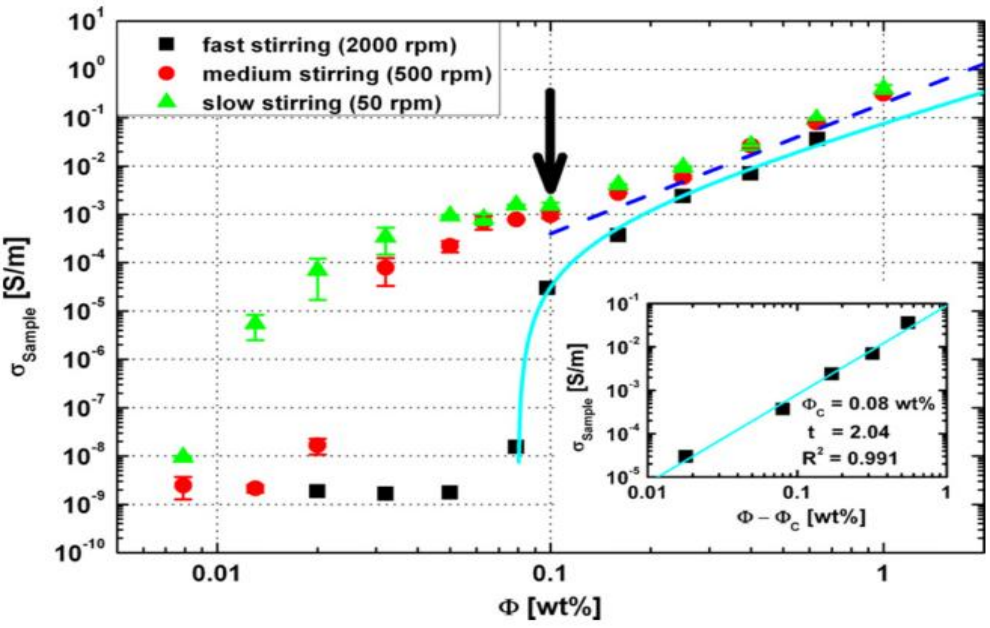

Figure 2.19 : Comparative log-log plot of the nanocomposite conductivity as a function of nanotube weight fraction for the three different sample preparation methods [59].

One another important parameter for percolation threshold is CNT dimensions. Since longer CNT fibers would entangle more and detangle less with mechanical strain in contrast with shorter CNT fibers [60], the aspect ratio of the CNT affect the percolation threshold in a positive manner and the statistical percolation threshold decrease with increasing aspect ratio. According to statistical percolation threshold, nano fillers are not free to move; therefore, nano fillers have to be long enough to form a conductive path [61, 62].

CNT orientation is also a significant parameter for most of applications. In electrical properties, Du et al. [63] and Behnam et al. [64] showed that, maximum conductivities achieved with slightly aligned, rather than perfectly aligned CNTs. In perfectly aligned CNT systems, each nanotube forms very few junctions with its neighbors, since it lies almost parallel to them. Depending on the decrease in the number of the junctions and the conduction paths, the resistivity increases at the perfectly aligned CNTs. On the other hand, since the randomly aligned CNTs have higher ability to form many junctions, resistivity decreases on the randomly aligned CNTs.

According to study of Gojny et al. [65], filler content of CNT is variable, which depends on functionalization, to exceed percolation treshold. Since the non-functionalized CNTs have tendency to re-agglomerate, they may not form a conductive network. Depends on results, filler content of non-functionalized CNTs has been lower than 0.1 wt%. On the other hand, functionalization causes structural changes and also, aspect ratio of CNTs decrease because of functionalisation processes. As a result, it was determined that the filler content of amino functionalised CNTs, have to be between 0.1 and 0.3 wt% (Figure 2.20).

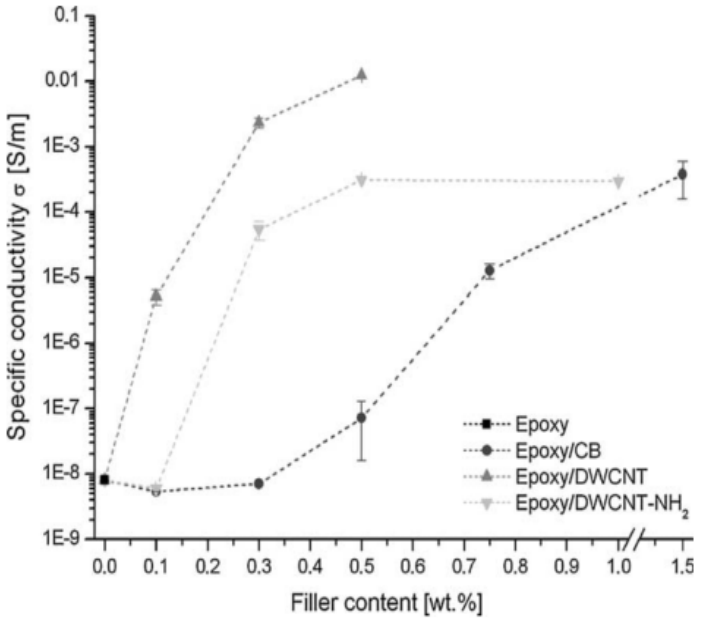

Figure 2.20 : Electrical conductivity of the nano-particle reinforced epoxy resin [65].

Depending on their remarkable electrical properties, CNT-polymer nanocomposites are used in sensing applications like gas sensors or strain sensors. The high electrical conductivity of CNTs allow the capability of monitoring mechanical stresses during

loading by increased resistance, sensing the damage to or around CNTs [66, 67]. For instance, de Villoria et al. [68] fabricated nano-enhanced composites by using fuzzy fibers (CNTs were grown on the surface of alumina fibers) with 2% volume fraction of CNT. They used thermography to detect the damage inspection and damage progression with local, low-power resistive heating (Joule effect) technique. With this method in situ damage detection for both internal and surface damage were achieved. According to Figure 2.21, with a low-power application (1 W), a large temperature increase (14.5 ^{0}C) was observed on an open-hole composite plate. In addition, damaged areas in pure CNT films grown on silicon substrates were investigated by resolution of the technique (Figure 2.21 (b)).

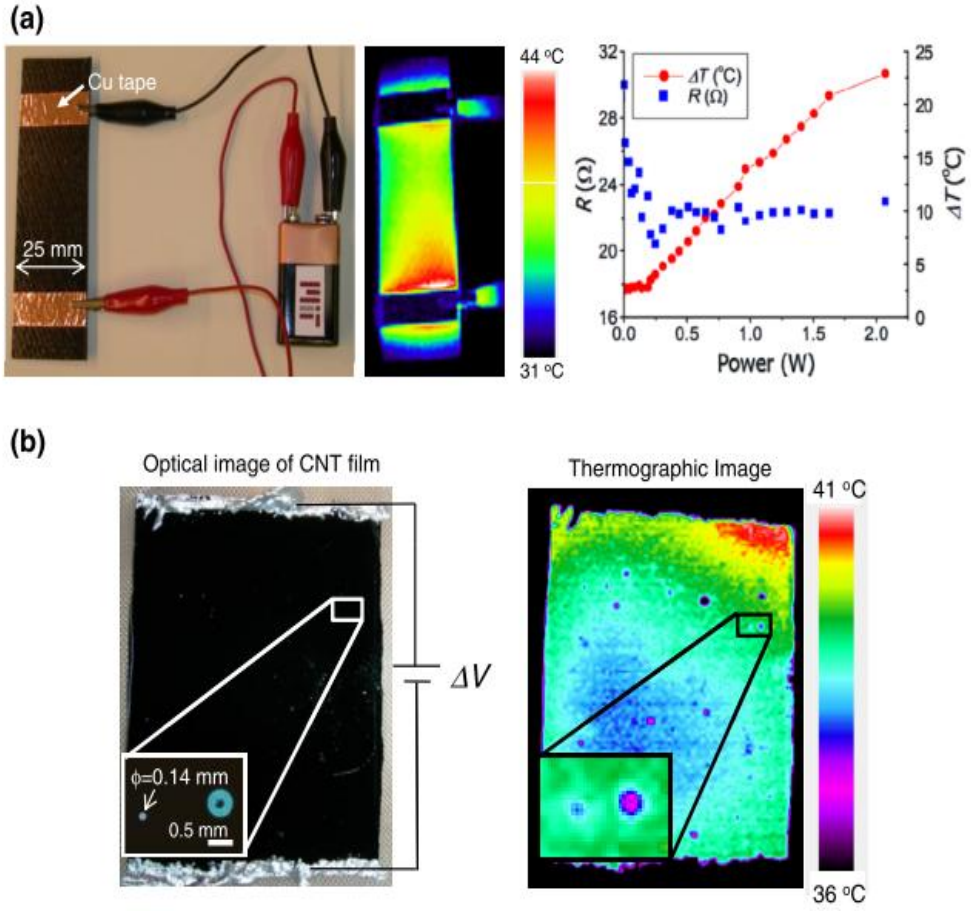

Figure 2.21 : Power and resolution characteristics of the NET-NDE technique: (a) optical image, thermograph, and power resistance/temperature plot of a composite specimen heated via a 9 V battery, (b) optical image and thermograph of vertically aligned CNTs with detective regions [68].

CNT dispersion method is also used for strain sensor applications. As an example, Grammatikos et al. [69] fabricated CFRP composites with 0.5 wt% CNT embedded matrix. They applied increasing cycling loading protocol for both base CFRP and

CNT embedded CFRP, to determine electrical resistance response to applied mechanical load. According to electrical resistance measurements, electrical resistance shows a decisive increase response to increasing cycling loading. While the base CFRP does not show a definite residual electrical resistance, the residual electrical resistance, obtained with CNT embedded CFRP, illustrate the internal damage and structural degradation of the composite (Figure 2.22).

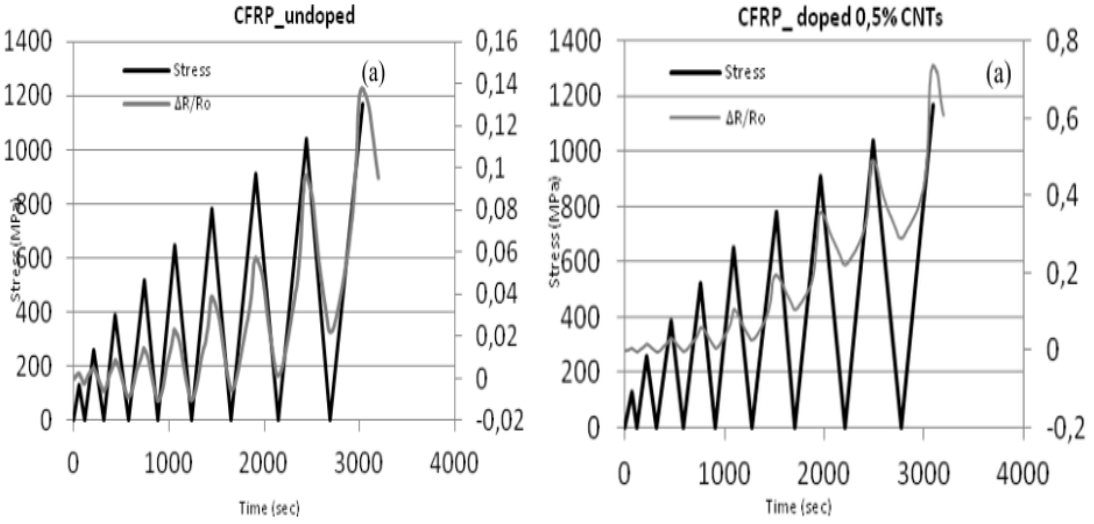

Figure 2.22 : Loading-unloading testing: stress / $\Delta R/R_o$ vs. time graph for undoped and doped CFRP [69].

In addition, CNT fibers are also used for damage sensing in composite structures. Alexopoulos et al. [47] fabricated MWCNT fibers with a coagulation process. They placed the CNT fiber between first and second layer of glass fiber reinforced polymer (GFRP) composites (Figure 2.23). Both tension tests and three point bending tests were performed to determine electrical resistance response of CNT fiber. According to these test results, applied mechanical stress and electrical resistance response of CNT fiber were correlated for different tensile loading. While incrementally tensile loading-unloading steps, residual electrical resistance were observed this could be attributed to possible damage of the CNT fiber.

Instead of adding CNT fillers into the composite structures, applying onto the surface of composite parts is also another approach for strain sensor applications. For example, Chiacchiarelli et al. [48], studied optimized graphene-epoxy application as a strain sensor in a carbon fiber reinforced composite subjected to bending loads. They used 2 wt% graphene nanoplate (GNP) concentration into the reactive mixture.

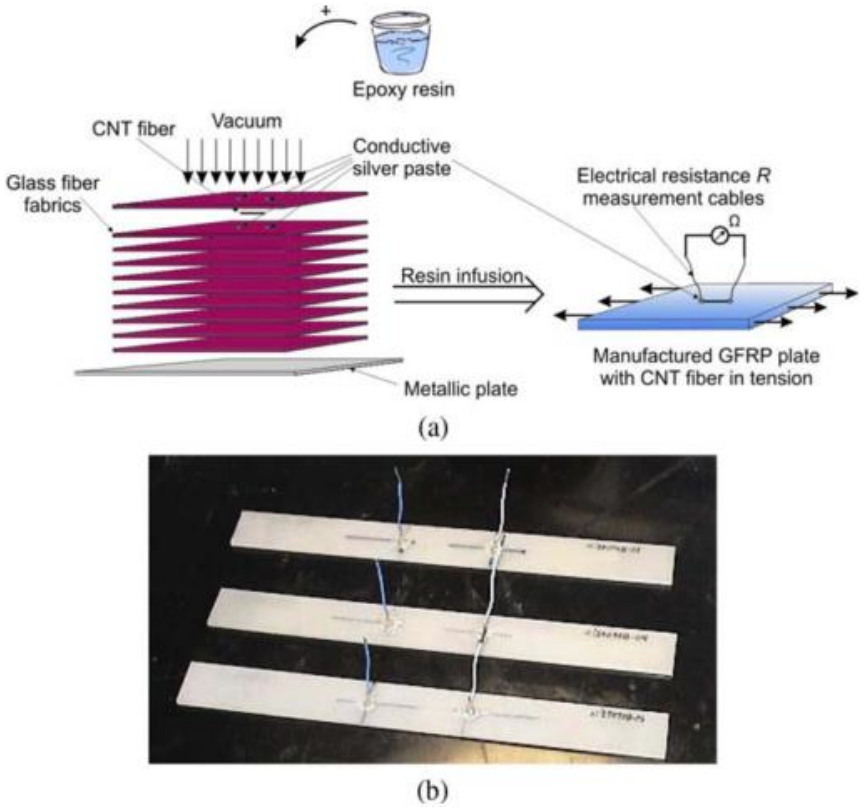

Figure 2.23 : (a) Manufactured GFRP plate with embedded CNT fiber, (b) manufactured specimens with embedded CNT fiber and connection cables [47].

This reactive mixture was then used to create a coating onto the carbon fiber epoxy composite specimens. To evaluate the relationship between the stress applied to the tested material and the piezoresistivty measured by the sensor, three point bending tests were applied and electrical resistance of the conductive coating was measured by Keithley electrometer simultaneously. In Figure 2.24, both maximum flexural stress and piezoresistivity was plotted as a function of deformation. Within its elastic zone (Zone I) the stress increased linearly, at the same time, piezoresistivity also increased continuously as a function of deformation. For higher deformation, the specimen started to fail and correspondingly piezoresistivity showed an important increase.

One another study for the surface application of nanocomposite as a strain sensor was performed by Pinto et al. [70]. In their study, they used 1 wt% MWCNTs to form an electrically conductive film. The CNT film was applied to both sides of the samples by spray deposition to employ as a sensor in GFRP samples (Figure 2.25).

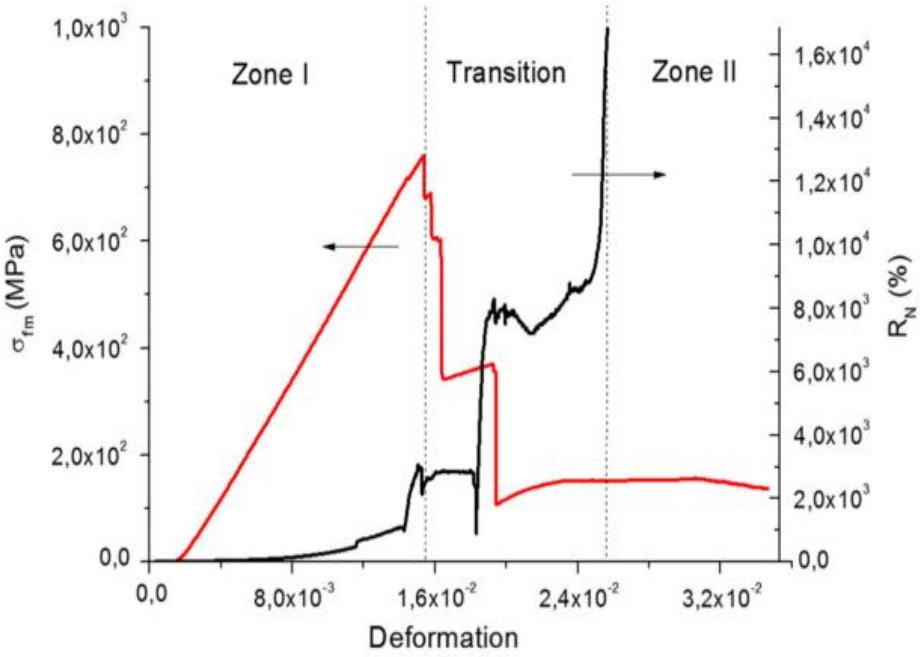

Figure 2.24 : Flextural stress and piezoresistivity as a function of deformation [48].

Figure 2.25 : Spray deposition of CNT film onto glass fibers [70].

They performed four point bending test and also measured the electrical resistance of CNT film simultaneously. They used two digital multimeters (DMM), each of allocated for sensing on one of the sample sides. While flexural loading the regions above and below the neutral axis of the sample dominated by tensile and compressive strains. According to their test results (Figure 2.26), surface resistance increased linearly within strain on tension side. However, on compression side, resistance showed an initial decrease and there is a transition point from decreasing

to increasing resistance changes. This transition point was commented as, at high strain levels the film could be prone to damage and causing this transition in resistance changes.

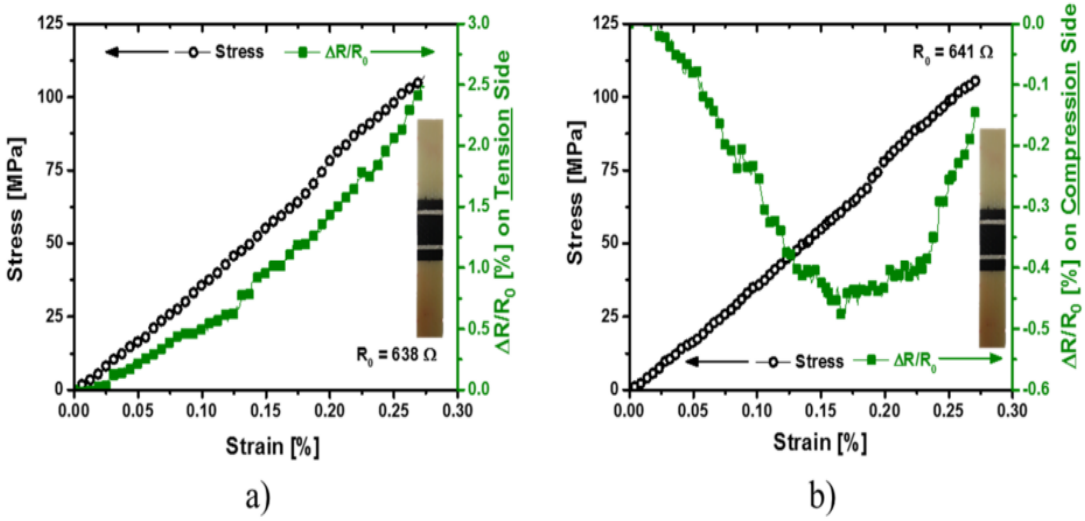

Figure 2.26 : Flexural loading using a CNT film as a sensor, in a GFRP sample (a) under tension, (b) under compression [70].

Besides several approaches for using nanomaterials such as CNTs and graphene for SHM in various ways, this study will focus on using CNTs as a smart paint onto the CFRPs for damage detection. This approach will help to remove concerns of having joule heating due to dispersion of CNTs inside the epoxy and as well as adding a protective layer of CNT polymer nanocomposite onto the CFRP which may help to achieve also enhanced environemntal protection which is not a focus of this thesis however will be evaluated for further studies.

3. SYNTHESIS AND CHARACTERIZATION OF ALIGNED CNTs

In this section, CNTs, which will be used to fabricate the polymer nanocomposite for smart paint and nano-enhanced composite structures, synthesis and characterization will be described. In the first part, customized thermal CVD method, used to synthesize vertically aligned CNTs (VA-CNTs) will be clarified. At the second part, morphological characterization of the synthesized CNTs will be performed to determine properties of CNTs.

3.1 Synthesis of CNTs by Thermal Chemical Vapor Deposition (th-CVD)

In this study, th-CVD method was used to synthesis CNTs, since it has offered opportunities for large-scale synthesis by allowing an ability to control the morphology and orientation of CNTs. CVD is a simple and low cost process, in which CNTs grow at low temperature and ambient atmosphere pressure, with usually moderated quality. Since it has high melting temperature and does not interact with gases at high temperature, <100> silicon (Si) wafer was used as substrate material. Also for base growth, Si wafer provides strong physical bond between substrate and catalyst. Si wafer substrate was coated at two steps:

1) ~ 300 nm SiO_2 coating was applied by Oxford Instrument Plasma Lab System 100 plasma enhanced CVD (PE-CVD),
2) Alumina oxide with a thickness of ~10 nm and a catalyst layer of Ferrous (Fe) with a thickness of ~ 2 nm were deposited on SiO2 at 4-6.10^{-6} torr by using Torr International Inc. electron beam evaporation technique (E-beam) (Figure 3.1).

SiO_2 was used as a support material and alumina was coated 10nm length on SiO_2 wafer to create porous interface between the substrate and catalyst. Selected catalyst element must have high carbon (C) solubility and high C diffusion rate at high temperature. The most popular catalyst elements are Fe, Co and Ni. In this study, Fe was selected as catalyst and was coated 2 nm thickness on alumina support. Catalyst

coating thickness plays significant role in CVD process. CNTs diameters depend on this thickness and with the increasing thickness CNTs diameters increase and it ends after a while.

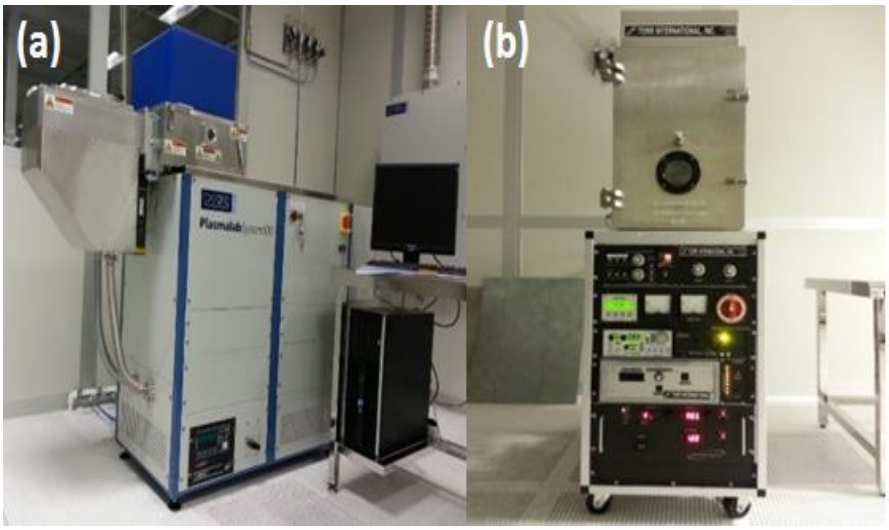

Figure 3.1 : (a) Oxford Instrument Plasma Lab System 100 plasma enhanced CVD (PE-CVD), (b) Torr International Inc. electron beam evaporation technique (E-beam)

As shown in Figure 3.2 the CVD process was performed at Linberg/Blue M tube furnace using 2-inch quartz tube. To control of gas flow rate, time and furnace temperature, software were customized by A. F. Ergenc. By this software and control system, the furnace can easily be automated for control over parameters and can be created a protocol for production.

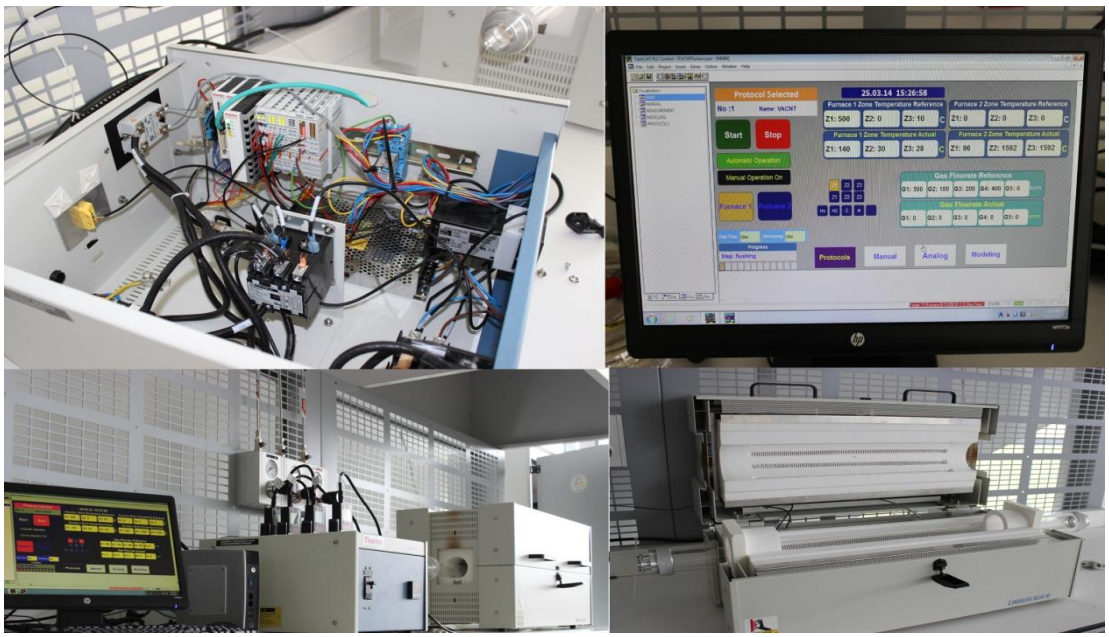

Figure 3.2 : CVD system.

CNT growth in the CVD system shows differences according to system and the growth recipe. The basics of the CNTs growth recipe can be given as:

1) Purging (He,Ar... etc.): the purpose of this step is to remove all the ambient gases like O_2 from the quartz tube.
2) Nucleation : Second step is heating the tube for activation of catalyst materials. While heating the tube, He and H_2 gases are flew throughout the tube channel.
3) Growth : When the tube come to stable temperature, besides H_2 and He, ethylene (C_2H_4) gas is also added as a hydrocarbon source.
4) Easy delamination: After growth procedure is done, in order to remove (easily and without any deformation) the CNTs, only H_2 gas is sent for a minute.
5) Cooling : In the last step just He gas is flew for high purity until about room temperature.

The optimization parameters for these steps are amount of gases, time and temperature. As a result of a parametric study optimized recipe was determined as given in Table 3.1. Even tough, the synthesis procedure and protocol is used for VA-CNT growth the system can be used within a quartz boat for the randomly oriented CNT synthesis as well. The reason for grwoing VA-CNTs is to achieve high quality and purity CNTs within the existing system, which is crucial for electrical conductivity and mechanical reinforcement.

Table 3.1 : Optimized A-CNTs growth recipe

Step	Gases	Flow rate (sccm)	Time (min.)	Temperature (°C)
1	He	2000	5	23
2	He, H_2	1600,1000	15	750
3	He, H_2, C_2H_4	1000,600,400	13	750
4	H_2	1000	1	750
5	He	1000		<100

3.2 Characterization of CNTs

CNTs can be characterized by several methods such as SEM, transmission electron microscopy (TEM), Raman spectroscopy and thermal gravimetric analysis (TGA), to determine their morphological, thermal properties.

SEM characterization was used to determine orientation and length of CNTs. The SEM images for this study were taken in the ITU Nano laboratory with QAUNTA FEG 250. As shown in Figure 3.3 (a), a VA-CNT forest has been obtained. From Figure 3.3 (b), it can be seen that, CNT forest has a porous structure and CNTs interact with each other. The total volume fraction of the CNTs on subsrate is ~1% and the rest is air. The growth procedure is a base growth, so the FE catalyst remained on the subsrate surface as seen from Figure 3.3 (c).

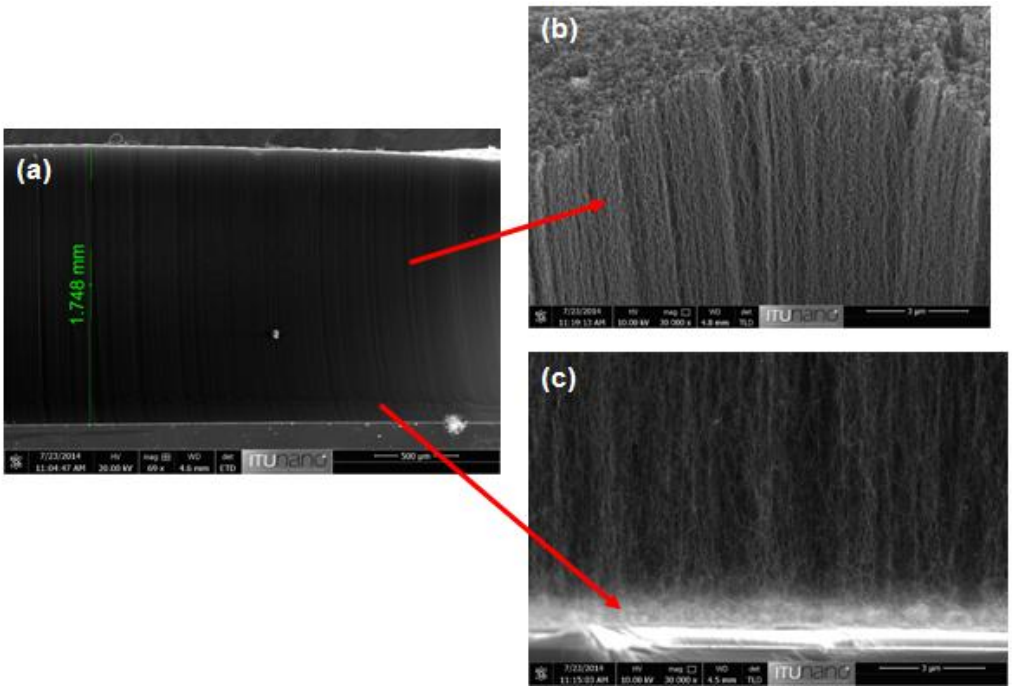

Figure 3.3 : SEM images of A-CNTs synthesized by CVD method showing the top and bottom sections of aligned arrays.

CNT types are determined according to TEM images. The wall number and outer and inner diameter of CNTs can be obtained. Figure 3.4 shows a MWCNT with 5 walls and outer diameter is about 10nm.

The quality of VA-CNTs is studied by both RAMAN Spectroscopy and TGA. In Raman spectroscopy, there are two peaks, named as G-band (graphite) and D-band (defect). According to carbon form of the structure, positions of peaks and intensity of bands are changed. It is desired that the G peak intensity must be higher than D peak intensity for CNTs. For SWCNTs and MWCNTs, G/D ratio measured by RAMAN spectroscopy can be a CNT quality indicator; G/D ratio is the ratio of intensity at G-band and at D-band [22, 71]. Figure 3.5 shows the RAMAN spectroscopy result of VA-CNTs for ~2nm Fe catalyst particles (G/D=1.39).

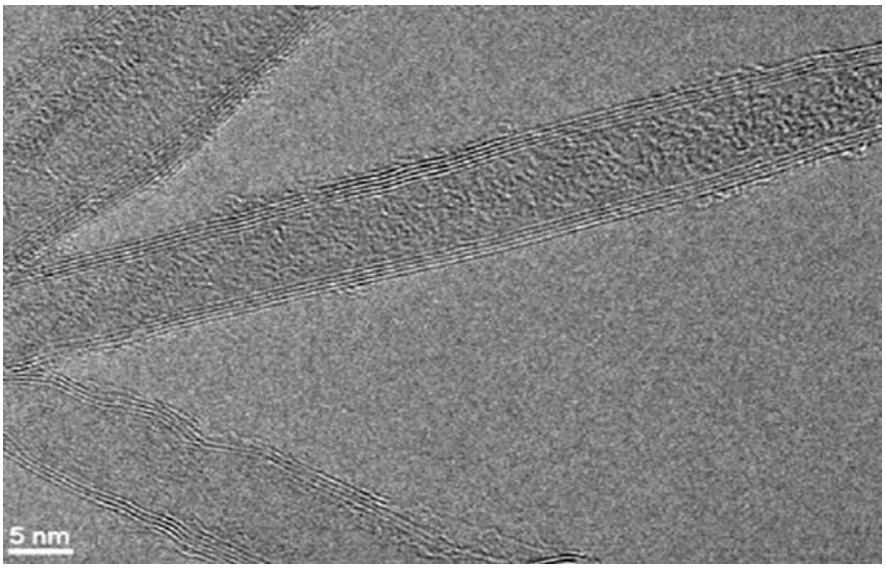

Figure 3.4 : TEM images of A-MWCNT.

TGA is a kind of quantitatively characterization methods to identify resistivity of oxidation [22]. In this method, weight loss of the material at depending on the temperature at desired atmospheric conditions is measured. Thermal analyses were carried out from room temperature to 900^{o}C using TA instruments brand SDT Q600 model DSC-TGA. Samples are heated in a platinum pan at 10°C/min. in air. Figure 3.6 shows that ten percentage of thermal degradation (T_d 10%) is found ~600°C. Patel et al. found that the offset value of A-CNT oxidation synthesized by chemical vapour infiltration technique was equal to 565°C [72].

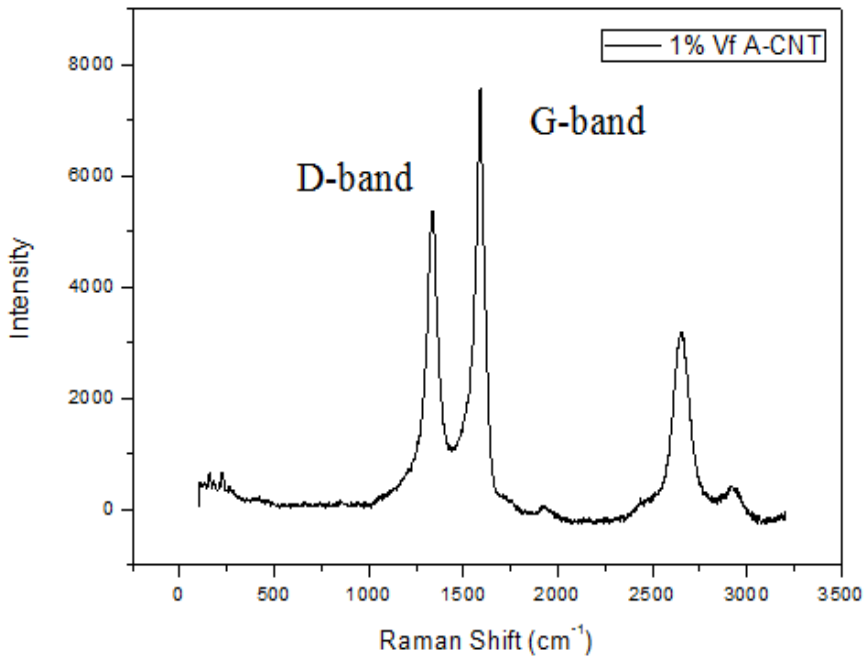

Figure 3.5 : Raman spectroscopy result (G/D=1.39).

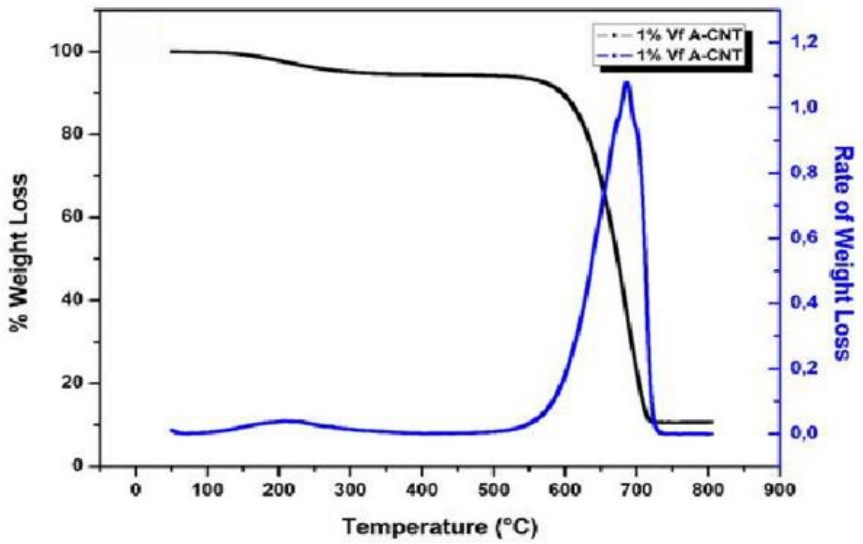

Figure 3.6 : TGA results ($T_{d\ (10\%)}$=600°C).

3.3 Parametric Study for CNT Growth Time

In CNT growth procedure, CNT growth time directly affect the length of synthesized CNTs. Since the CNT aspect ratio and purity are crucial parameters for electrical conductivity, a parametric study were performed to determine optimum growth time of CNTs synthesized for this studies.

For same growth procedure, only the growth time was changed. 15 sec., 30 sec., 45 sec., 1 min., 2 min., 5 min., 10 min., and 13 min. growth times were used and each type of CNTs were characterized with SEM and Raman spectroscopy for their length and purity. According to results as shown in Table 3.2, the maximum CNT length was obtained at 10 min growth time; however the G/D ratio was low when compared with other results. To optimize both CNT length and purity, 13 min growth time was selected on this study.

Table 3.2 : CNTs length and G/D ratio according to growth time

Growth Time	CNT length (μm)	G/D ratio
15 sec	12	2.53
30 sec	62	1.25
45 sec	79	1.35
1 min	79.4	1.77
2 min	178	1.16
5 min	469	1.94
10 min	839	1.00
13 min	623	1.88

4. DEVELOPMENT OF CNT SMART PAINT AS STRAIN SENSOR FOR SHM

Structural health monitoring systems can prevent catastrophic failure of safety–critical structures, which cannot be allowed to fail. CNT-based polymer nanocomposites (CNT-PNCs) are multifunctional materials that, in addition to their basic functions of physical and mechanical properties enhancement, allow the sensing and monitoring of strain or damage by the measurement of the material electrical resistance. The principle behind this is that the deformation of CNT-PNCs or the damage initiation and evolution in the nanocomposites can lead to changes in their electrical resistance. These electrical resistance changes provide the possibility of real-time health monitoring, which improves the safety of structures. In this chapter, fabrication of CNT smart paint (A multiwalled CNT and epoxy polymer nanocomposite paint) coated CFRP composites and tension and flexural testing were defined.

4.1 Fabrication of CNT Smart Paint and Application onto the CFRP Composite

In this part of the study, materials and methods that used to fabricate CNT smart paint coated CFRP composites were detailed.

4.1.1 Materials

The materials used for the fabrication of the CFRP composites are high strength, bidirectional 5H Satin carbon fiber with 375 g/m^2 weight and 0.38 mm thickness from Hexcel and Epikote resin MGS L160/hardener with Epikote curing agent MGS H160. For CNT smart paint fabrication same epoxy system is used with CNTs that are growth in laboratory of ITU-ARC and provided commercially from Sigma-Aldrich with 6-9 nm outer diameter, 5 μm length and 95 % carbon content (Figure 4.1).

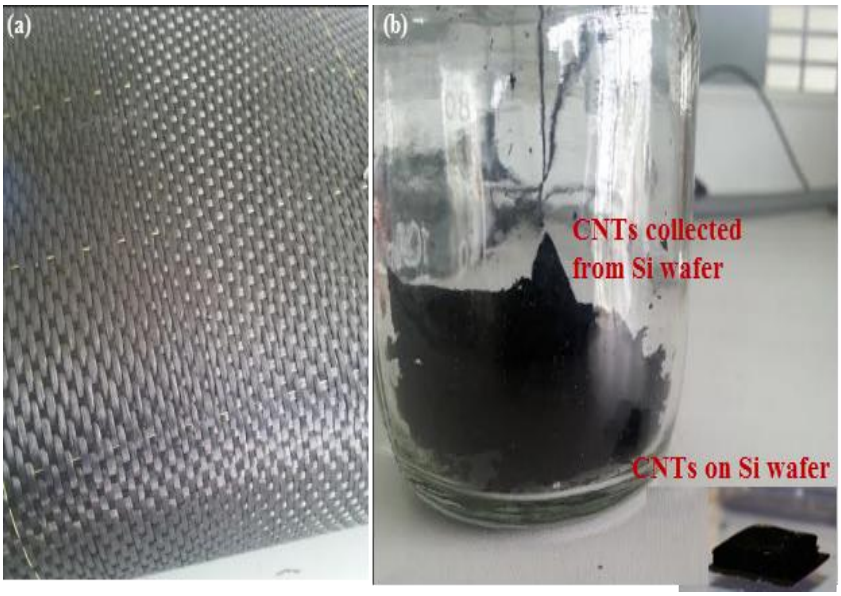

Figure 4.1 : (a) Carbon fiber, (b) CNTs.

4.1.2 Fabrication and characterization of CNT smart paint

To fabricate CNT smart paint with commercial CNTs, these CNTs were directly added into the epoxy system with various weight fractions (0.25, 0.5 and 1 wt%). Since the length of commercial CNTs is really small (5 μm) only shear mixing was applied for dispersion.

To synthesis CNTs at laboratory, some parameters were taken into consideration. For example, as mentioned at Chapter 2.4, CNT aspect ratio is an important parameter for high electrical conductivity and according to previous studies, CNTs should have high aspect ratio to form a conductive network. When SEM images and Raman results at Chapter 3 was examined, 13 min. growth time was selected to growth CNTs with high length and purity. In addition, functionalisation was not performed since, as mentioned Chapter 2.4, electrical conductivity of the functionalised CNTs was lower than pure CNTs. As a result, synthesized CNTs were directly added into epoxy system with different weight fractions. For dispersion of CNTs, two dispersion conditions were performed.

- Shear mixing: only shear mixing by hand was applied
- Homogenization and shear mixing: first, homogenization at 5000 rpm for 10 minutes were applied for Epikote resin and CNTs, after curing agent was added, hand shear mixing was applied as a second step (Figure 4.2).

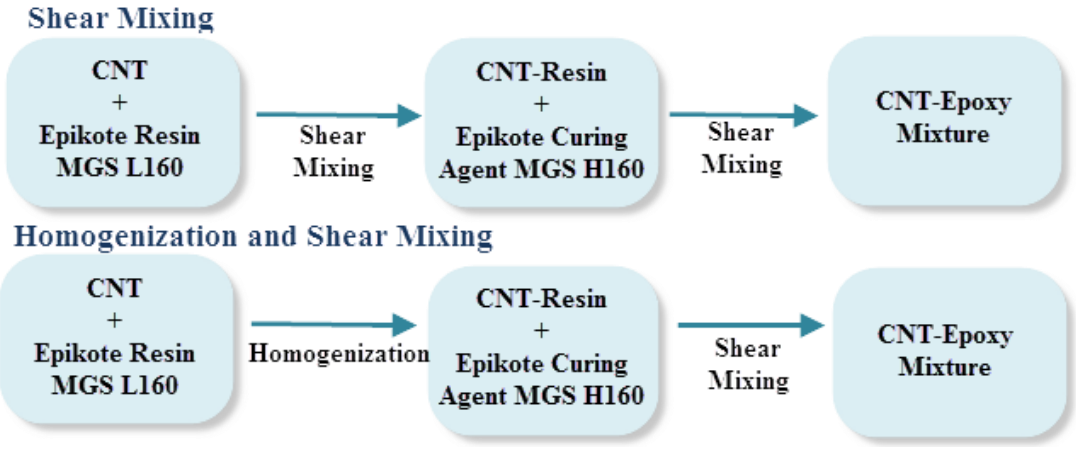

Figure 4.2 : Dispersion steps for CNT into epoxy resin system.

Electrical characterization of CNT-PNCs was made with 2-probe electrical conductivity measurements. To prepare conductivity measurement samples, the CNT epoxy mixtures were cured in silicon molds as CNT-PNCs. After curing, surface of CNT-PNCs were sanded and polished to obtain a smooth surface for measurements. Two parallel electrodes were deposited on relevant sample surfaces and voltage (10 Volt) was applied (Figure 4.3). The current across the sample was measured and resistance of sample was obtained. Conductivity of sample was calculated according to equation (4.1), where L (m) is the span between two electrode point, A (m^2) is the cross sectional area of sample and R (Ω) is the resistance.

$$\sigma = \frac{L}{RA} \tag{4.1}$$

Figure 4.3 : Electrical conductivity measurement setup of CNT-PNCs.

Conductivity measurements were taken from three places of CNT-PNC surface (Figure 4.4). Conductivity results of CNT-PNC samples were given at Table 4.1.

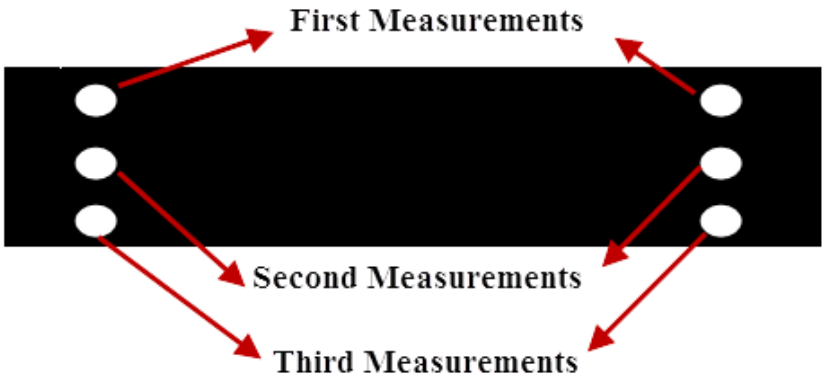

Figure 4.4 : Conductivity measurement places on CNT-PNC surface.

Table 4.1 : Conductivity results of CNT-PNC samples.

Samples	Dispersion Method	First Measurement [S/m]	Second Measurement [S/m]	Third Measurement [S/m]
0.1 wt% CNT	Shear	2.3 E-3	2.0 E-3	2.6 E-3
0.25 wt% CNT-1	Shear	1.9 E-1	1.2 E-1	4.7 E-1
0.25 wt% CNT-2	Shear	3.4 E-3	1.8 E-3	0.5 E-3
0.25 wt% CNT-3	Shear	1.0 E-1	0.13 E-1	0.3 E-1
0.5 wt% CNT	Shear	5 E-1	1.7 E-1	1.7 E-1
0.25 wt% CNT-1	Hom.+Shear	0.6 E-1	0.7 E-1	0.3 E-1
0.25 wt% CNT-2	Hom.+Shear	0.9 E-1	1.0 E-1	0.6 E-1
0.25 wt% CNT-3	Hom.+Shear	1.1 E-1	1.2 E-1	1.2 E-1
0.5 wt% CNT-1	Hom.+Shear	1.8 E-1	2.2 E-1	1.8 E-1
0.5 wt% CNT-1	Hom.+Shear	2.3 E-1	3.1 E-1	2.1 E-1
0.5 wt% CNT-1	Hom.+Shear	1.7 E-1	1.5 E-1	2.6 E-1
0.25 wt% Sigma	Shear	2.5 E-7	6.4 E-7	1.18 E-6
0.5 wt% Sigma-1	Shear	2.9 E-6	1.8 E-6	6.4 E-7
0.5 wt% Sigma-2	Shear	2.9 E-7	5.2 E-7	9.5 E-7
0.5 wt% Sigma-3	Shear	7.6 E-7	1.2 E-6	1.7 E-6
1 wt% Sigma-1	Shear	3.8 E-5	5.2 E-6	2.8 E-5
1 wt% Sigma-2	Shear	3.2 E-5	4.1 E-7	6.7 E-6
1 wt% Sigma-3	Shear	4.2 E-6	2.4 E-7	5.4 E-5

Conductivity of CNT-PNCs is directly related to CNT weight fraction, CNT type and dispersion method. When the weight fraction of CNT was increased from 0.1 to 0.25 wt% the electrical conductivity increased two order of magnitude. However, there is not a linear correlation between electrical conductivity and CNT weight fraction because of CNT agglemaration at higher contents (Figure 4.5). The samples prepared with combined homogenization and shear-mixing method, have similar electrical

conductivities rather than other samples, which were prepared with, shear mixing method. However, when the average electrical conductivity results were compared for shear mixed and homogenized and shear mixed samples, there were not a distinctive differences between these two dispersion methods. Sigma CNT embedded PNCs (S-CNT-PNCs) have nearly five order of magnitude lower electrical conductivity then growth CNT-PNCs even if the CNTs weight fraction is higher.

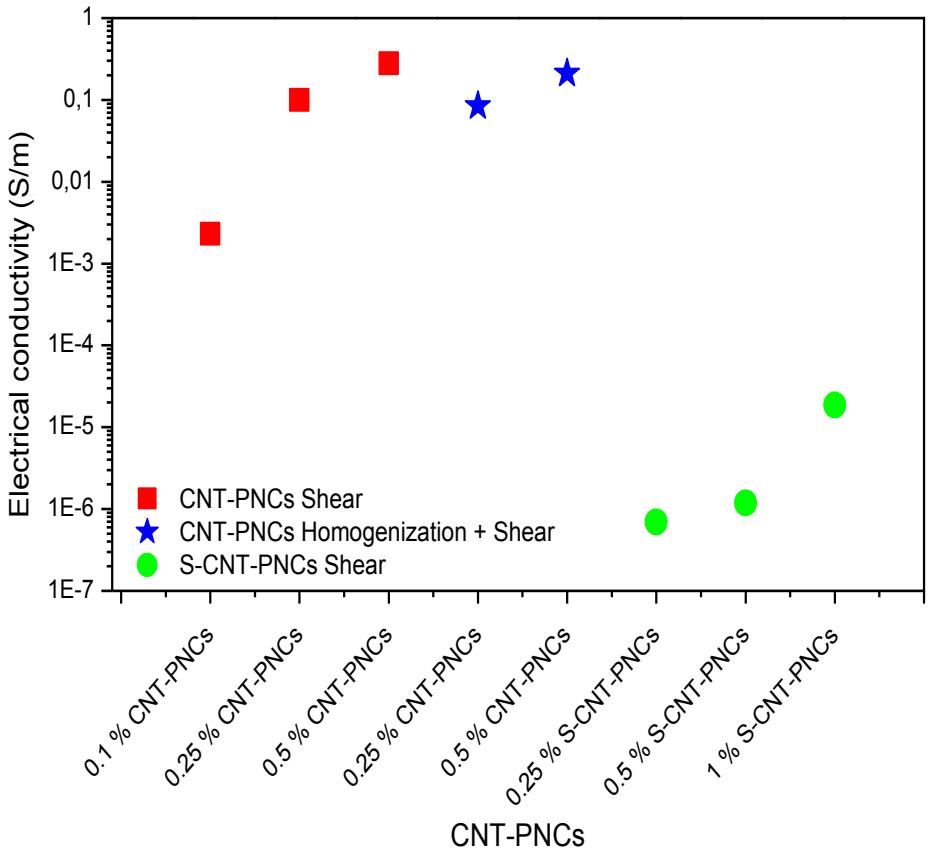

Figure 4.5 : Electrical Conductivity of CNT-PNCs.

The measured conductivity of CNT-PNCs was also compared with the conductivity of other CNT-PNCs in the literature. As seen from Figure 4.6, the CNT-PNCs, that were prepared with growth CNTs, were measured to have better conductivity than most of the other examples and electrical conductivity is beyond the percolation threshold even at low CNTs loading [58]. However, S-CNT-PNCs below the percolation threshold; the small length (5µm) of Sigma CNTs would cause this result. On the other hand, conductivity of VA-CNT-PNCs is about two orders of magnitude higher than our randomly oriented CNT-PNCs [73]. This diversity would be attributed to alignment and distribution quality of CNTs in polymer. Aligned and long CNTs make an effective contribution to the conduction property of PNCs.

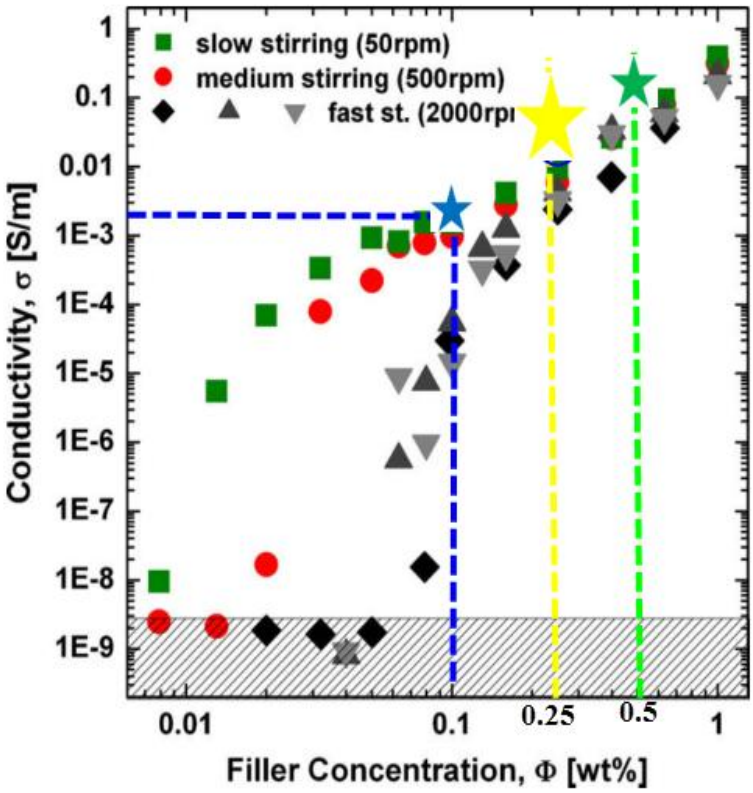

Figure 4.6 : Comparison of electrical conductivities of CNT-PNCs [58].

Morphological characterizations of CNT-PNCs were performed with SEM. The prepared samples were broken from one end and SEM images were taken from this fracture surfaces. As seen from Figure 4.7, a well CNT dispersion was obtained in polymer system within the shear mixing and homogenizator approaches.

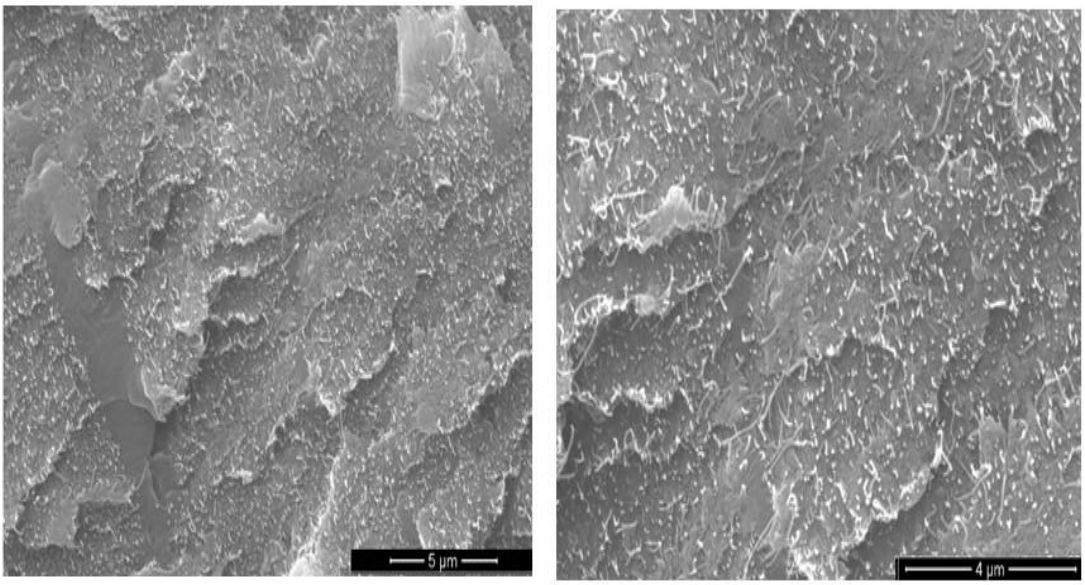

Figure 4.7 : SEM images of CNT polymer nanocomposite (0.5 wt% CNT).

4.1.3 Fabrication of CFRP composite

For the fabrication of CFRP composites, 5 plies carbon fiber fabrics were cut at required dimensions (300 x 300 mm). Each layer was laid on a metal flat plate repeatedly. Vacuum infusion method was used to fabricate composite plates (Figure 4.8). The steps of vacuum infusion method were:

1) A release agent was applied to the surface of metal plate,
2) Carbon fiber layers were placed,
3) Peel-ply and infusion mesh was laid out on fiber layers,
4) Spiral hoses were placed to opposite sides of the metal plate,
5) Metal plate was covered with appropriate bagging material,
6) The air, inside the vacuum bag was vacuumed,
7) Epoxy resin was infused into the system,
8) Resin infusion was finished when the all fabrics were wetted.

The plate was cured for 24 h at room temperature. After fabrication of this plate, tension test specimens (250 x 25 mm) and flexural test specimens (80 x 12 mm) were cut from plate.

GFRP tabs (40 x 25 mm) were prepared for tension test specimens to attach end of the specimens for preventing crushing while testing. Thin copper plates were also attached on GFRP tabs to prevent sliding of specimens from tensile test machine under high loads.

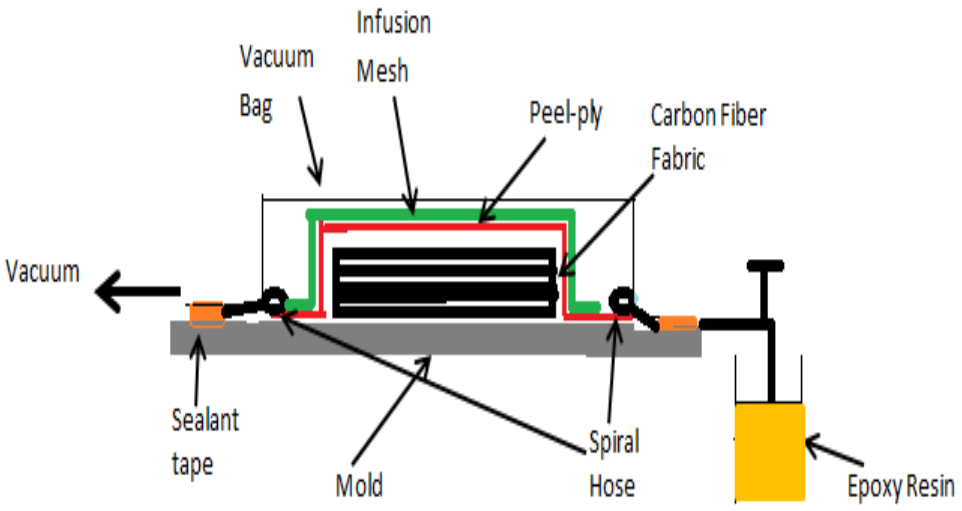

Figure 4.8 : Vacuum infusion method.

4.1.4 Application of CNT smart paint onto the CFRP composite

In this part of the study, same CNT-epoxy resin mixtures that were used to fabricate CNT-PNCs, were also applied onto the surface of CFRP composites as a strain sensor to make a correlation between electrical conductivity and strain sensing capabilities of PNCs. CNT-epoxy resin mixtures were applied as a smart paint with specified dimensions (50 x 10 mm) with the help of 0.5 mm thickness metal mask (Figure 4.9). Firstly, aluminum electrodes were placed on CFRP composite and then CNT smart paint was applied on them. The CNT smart paint was cured for 24 h at room temperature. Figure 4.10. shows the smart paint coated tension test specimen.

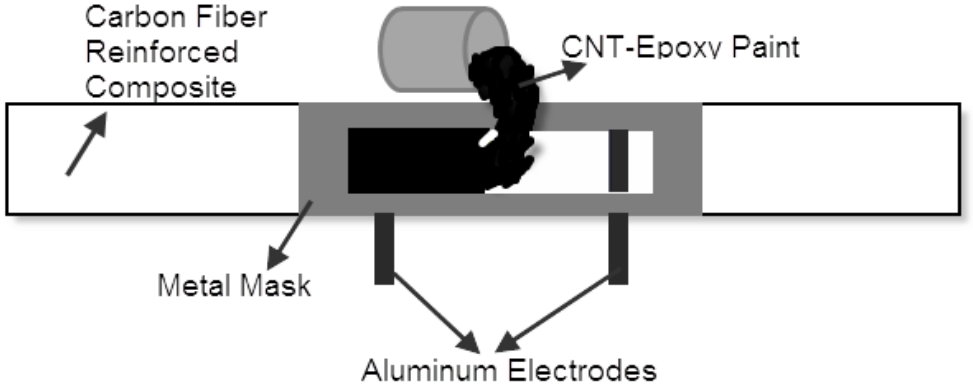

Figure 4.9 : CNT smart paint application on CFRP composite with specified dimensions.

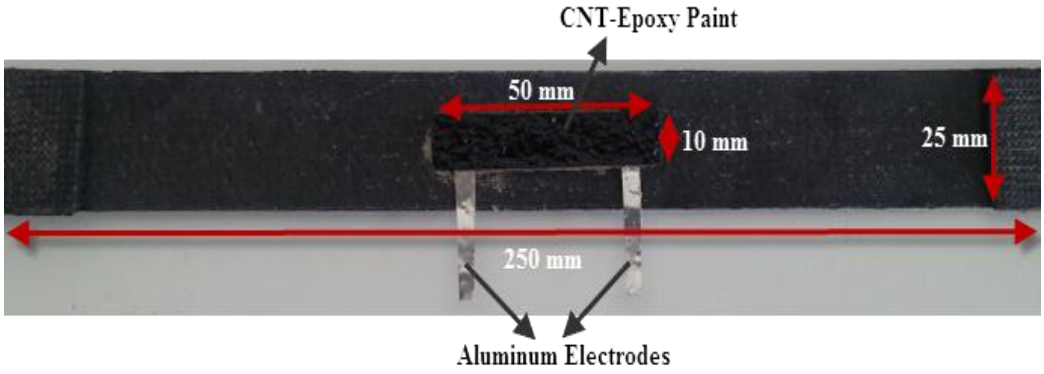

Figure 4.10 : CNT smart paint coated tension test specimen.

4.2 In-Situ Structural Health Monitoring of CFRP Composites Unter Tensile and Flextural Loading

Tension and three point bending tests were performed with MTS tension test machine at Composite Laboratory of Faculty of Aeronautics and Astronautics. Dimensions of tension test specimen and test conditions were determined according

to ASTM D3039 Test Method for Tensile Properties of Polymer Matrix Composite Materials Standard. For three point bending test ASTM D790 Test Methods for Flexural Properties of Unreinforced and Reinforced Plastics and Electrical Insulating Materials Standard were used. While mechanical tests were being performed, electrical resistance of the smart paint was recorded simultaneously with a Keithley source meter model 2400 (Figure 4.11). The instrument electrodes were attached to the aluminum conductive strips. A constant voltage of 10 V was applied and current was measured to determine electrical resistance of CNT smart paint.

Figure 4.11 : Test system for in situ diagnostics at tensile testing.

For tension tests, two different loading conditions were performed:

- Elastic mode: Loading speed was 2 kN/min. Loading was applied upto 16 kN and unloading was applied from 16 kN to 0 kN in one minute. The maximum loading condition for this mode was determined according to result of base specimens that were tested to state elastic region of the specimens. In this test an extensometer was also used to follow strain conditions besides the CNT coating (Figure 4.12).
- Plastic mode: Loading speed was 4 kN/min. Loading was performed until the specimens were fractured.

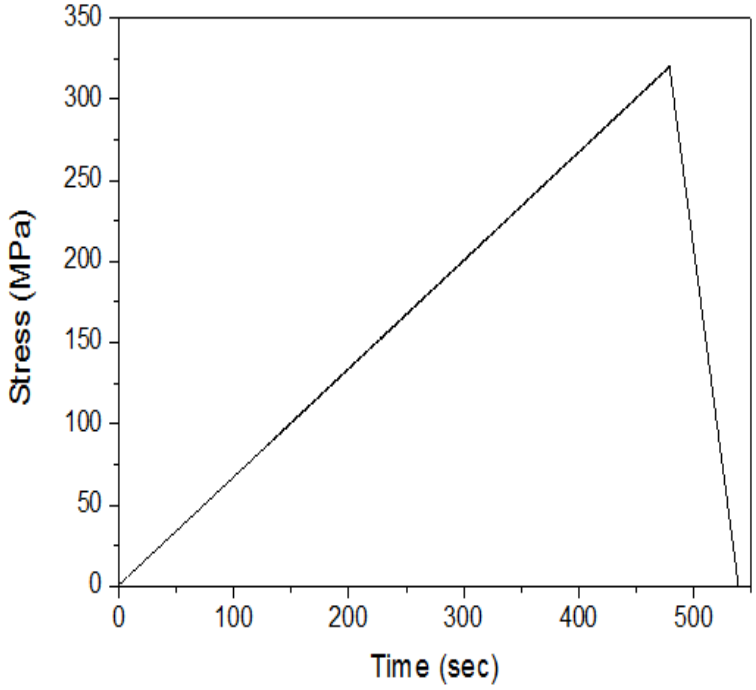

Figure 4.12 : Elastic deformation loading.

Elastic mode tests were performed for three CNT smart paints that include 0.1, 0.25, 0.5 wt% CNTs. Base specimens without smart paint were also tested as a reference materials. For both base and CNT smart paint coated CFRP composites, three testing specimens were analyzed.

Resistance change of the CNTs smart paint was calculated with equation (4.2), according to the definition of Alamusi et al. [46].

$$RC = \frac{R_i - R_0}{R_0} \tag{4.2}$$

In this equation R_i is the measured resistance during the tests and R_0 is the initial resistance of material. R_0 were measured just before the mechanical loading were started. During the resistance measurement, one data was taken for each second.

The results of the elastic mode tests were given at Figure 4.13. Stress and strain results of test specimens were plotted upto maximum loading point (16 kN). Maximum stress was nearly 320 MPa and maximum strain was nearly 0.55 % for all specimens. As seen from the result of base specimen (Figure 4.13(a)), resistance did not show a remarkable change for stress increament. When base and 0.1 wt% CNT specimens were compaired CNT smart paint showed an important effect on resistance change (Figure 4.13(b)). The resistance change increased upto 120 % for

0.1 wt% CNT smart paint. However, 0.1 wt% CNT smart paint displayed huge variances for resistance change at high stress conditions. In addition, for strain conditions lower than 0.1 %, the resistance did not change effectively. Resistance of the 0.25 wt% CNT smart paint increased continuously as a function of deformation (Figure 4.13(c)). The maximum resistance change reached to 120 %. Also, variance of resistance change was relatively small when compared with 0.1 wt% CNT smart paint. Resistance of the 0.5 wt% CNT smart paint was displayed a continuous increase as a function of deformatin and also it did not show notable variances when compared with other CNT smart paints (Figure 4.13(d)). However, the percentage increament of resistance change (60%) was nearly half of the 0.25 wt% CNT smart paint. The reason of relativeley small resistance change would be the amount of CNTs. When CNTs are thoroughly dispersed in polymeric materials, electrically connected networks of CNTs are formed which provide continuous conductive pathways for the transmission of electrical current. A nanotube network has two sources of electrical resistance, the first one is the intrinsic resistance along the nanotube itself and the second one is contact resistance at a nanotube junction. The second resistance is mainly caused by tunneling-type contacts between the CNTs, that is, when the thickness of the inter-nanotube matrix region is sufficiently small, the electrons can cross this region by electrical tunneling effect. It should be noted that the tunneling-type contact resistance plays a dominant role in the electrical transport properties of nanocomposites. The resistance increament is a result of degradation of conductive network because of the deformation of the surface. Since the amount of CNTs in the 0.5 wt% CNT smart paint was twice of the amount of CNTs in the 0.25 wt% CNT smart paint, the degradation of conductive network is relatively small at 0.5 wt% CNT smart paint. As a result of this, the resistance change was not as high as the 0.25 wt% CNT smart paint. When all results for elastic mode were evaluated, the outcome was obtained that, 0.25 and 0.5 wt% CNT smart paints were more effective as a strain sensor to follow the elastic deformation within the tension test and applied loading conditions.

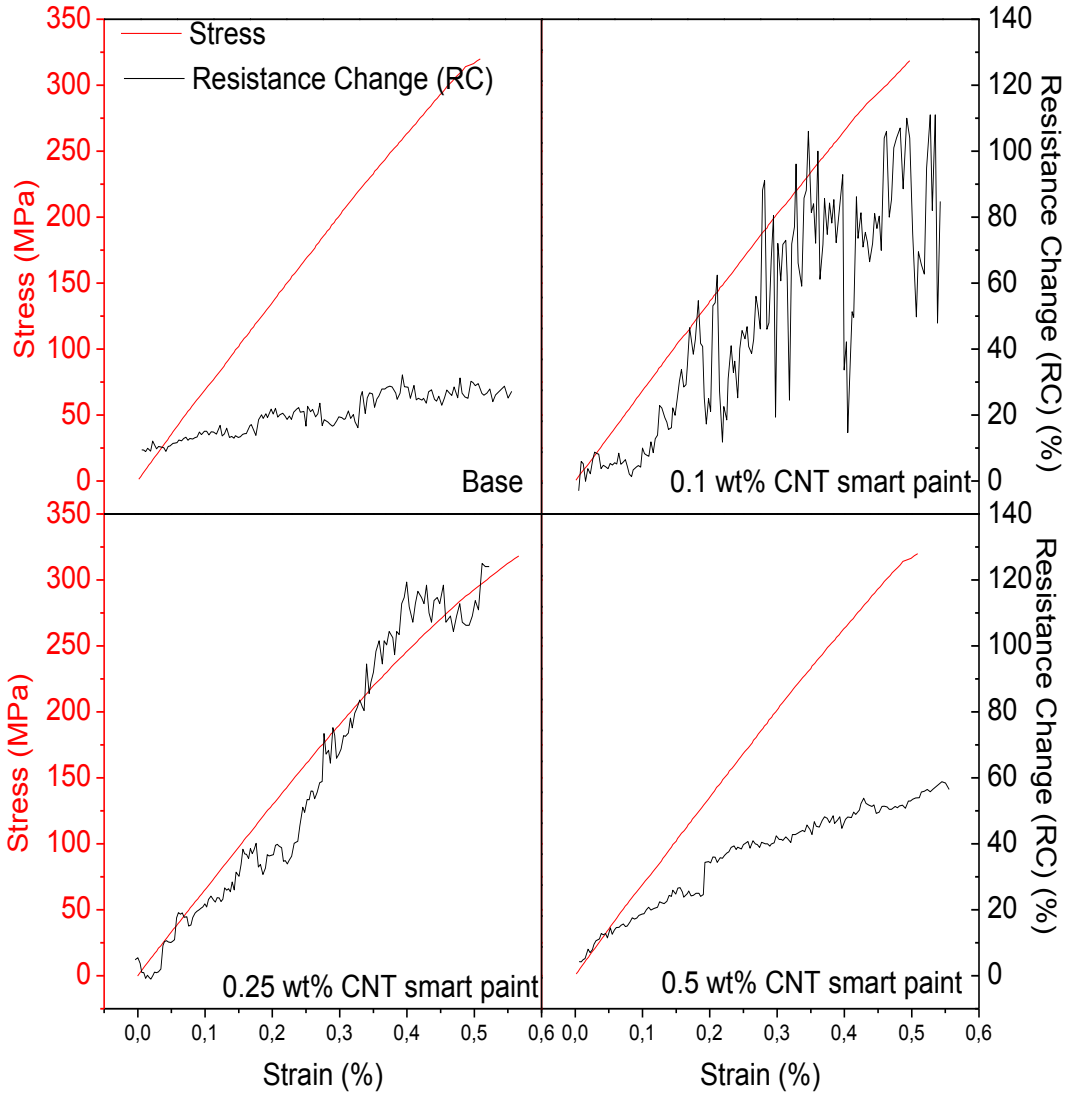

Figure 4.13 : Stress / Resistance Change vs. Strain results (a) base specimen, (b) 0.1 wt% CNT specimen, (c) 0.25 wt% CNT specimen, (d) 0.5 wt% specimen.

Depending on the results of elastic mode tests, the plastic mode tests were performed for 0.25 and 0.5 wt% CNT smart paints to determine the effectiveness of these CNT smart paint under high strain conditions. For both specimens maximum stress and maximum strain were approximately 650 MPa and 1.8 % respectively (Figure 4.14). Both CNT smart paint type showed an incremental trend as a function of strain. The sudden increase of resistance would be the result of inner plies rupture that could not be followed from stress-strain graphics.

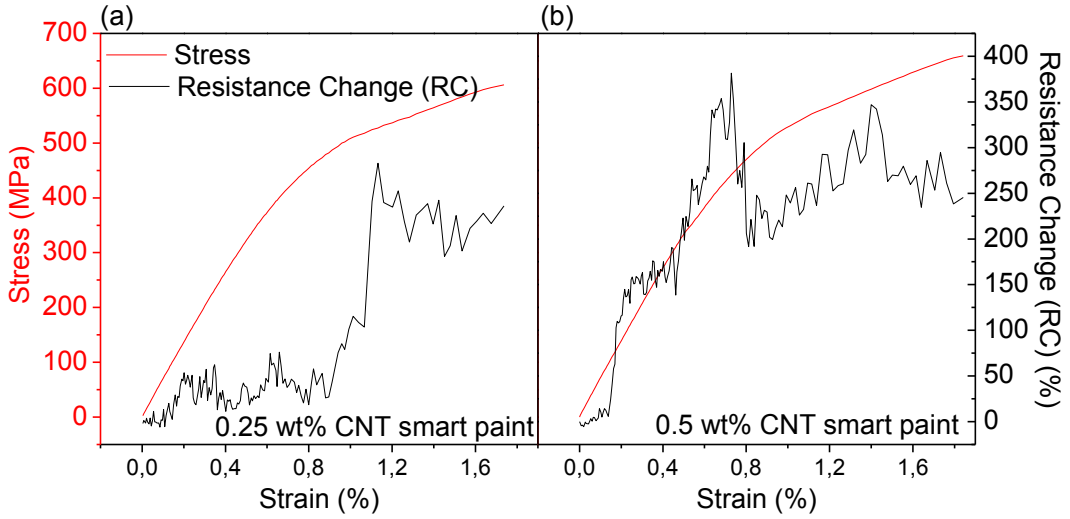

Figure 4.14 : Stress / Resistance Change vs. Strain results for plastic deformation (a) 0.25 wt% CNT specimen, (b) 0.5 wt% CNT specimen.

For flextural tests, CNT smart paint samples were prepared with the CNT-epoxy mixtures that homogenization and shear mixing applied. CNT smart paints were prepared with 0.25 and 0.5 wt% CNT loadings. CNT smart paint was applied with the dimensions, 50 mm length, 10 mm width and 0.5 mm thickness. The smart paint application procedure was same with the tension test specimens. While flextural tests were being performed, electrical resistance of CNT smart paint was measured simultaneously. Flextural tests were performed with 66 mm support span length and the velocity of cross head was 3 mm/min for all tested specimens. Plastic deformations were occured at all specimens. The stress and resistance change versus strain results of flextural tests were given in Figure 4.15.

According to stress strain results, both specimens showed same failure mode. The resistance change for 0.25 wt% CNT smart paint specimen was nearly 100% and it was increase up to 250% for 0.5 wt% CNT smart paint specimen. In contrast to elastic mode tension test results, 0.5 wt% CNT smart paint showed higher resistance change for both plastic mode tension tests and flextural tests. Plastic deformation would be the explanation for this result. At the beginning of the tests 0.5 wt% CNT smart paint had higher electrical conductivity and that is why the resistance of specimen was lower. However when the smart paint was totally fractured the current only passed from CFRP composites where the electrical resistance was very high. As a result, the resistance change from beginning to end of the tests was higher for 0.5 wt% CNT smart paint specimens. From that point of view, to eliminate the CFRP

composite from the system, non-conductive acrylic paint was applied between CFRP composite and CNT smart paint (Figure 4.16). Aluminium strips were placed on acrylic paint and CNT smart paint was applied on them. For this application, 0.25 wt% CNT smart paint specimens were prepared and flextural test with same conditions of previous tests were performed.

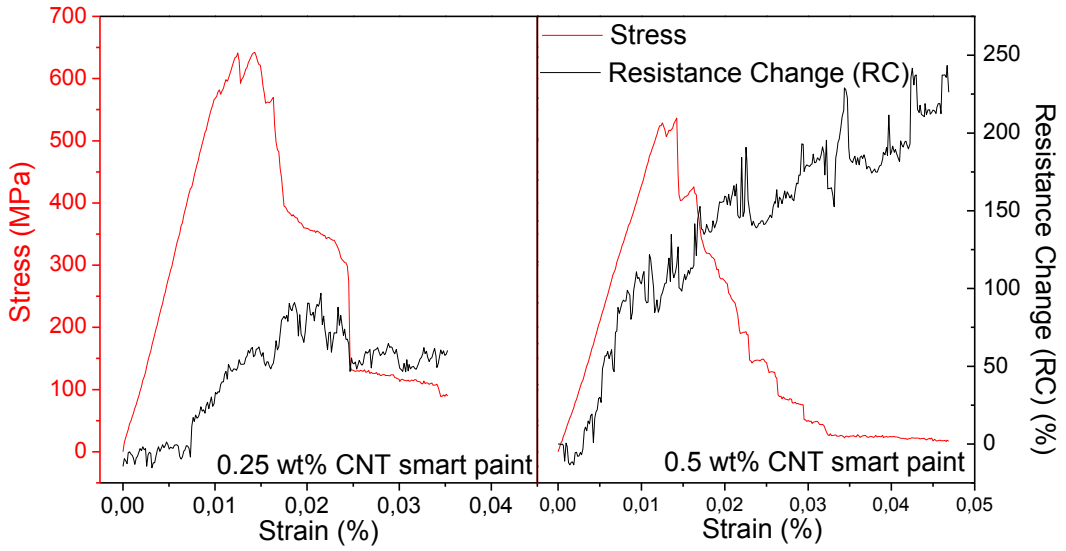

Figure 4.15 : Stress / Resistance Change vs. Strain results for flextural tests for 0.25 wt% CNT smart paint specimen and 0.5 wt% CNT smart paint specimen.

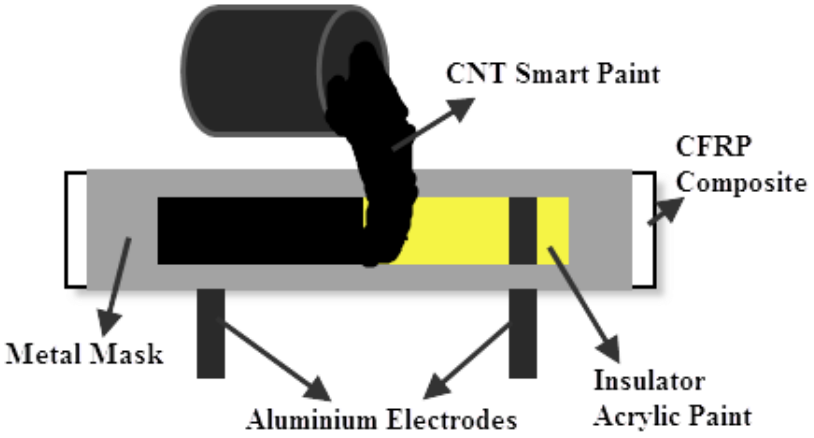

Figure 4. 16 : Insulator acrylic paint application between CFRP composite and CNT smart paint

As seen from Figure 4.17, when the CFRP composite eliminated from SHM system, resistance change showed a sudden and huge increament after fracture of specimen. The resistance change increased up to 50% for elastic deformation part and at the plastic deformation part of resistance change showed sudden increaments depending on ply failure of composite specimen. Resistance change showed a proper compliance with damage of composite structure. In a conclusion, acrylic paint application totally eliminated the CFRP composite from SHM system and the

measured resistance change was only the result of CNT smart paint. Since the main purpose of this study was the evaluation of CNT smart paint damage sensing capability, acrylic paint application between composite and CNT smart paint was more reasonable to obtain accurate results.

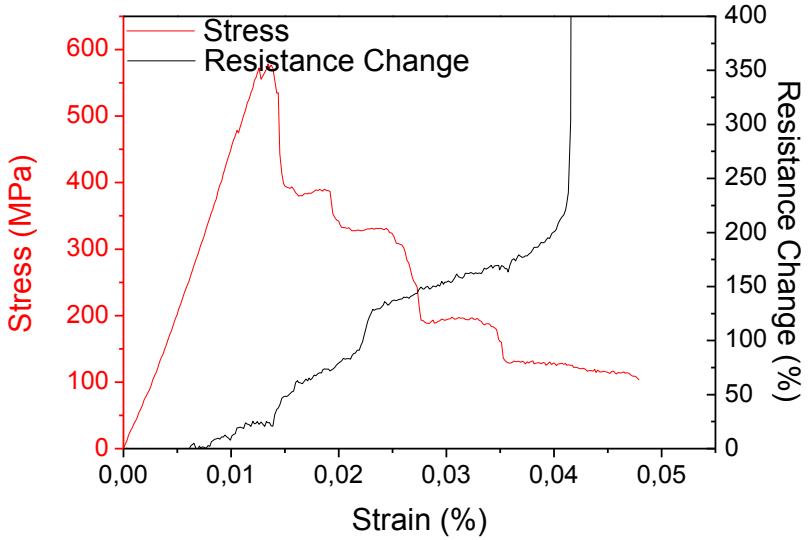

Figure 4.17 : Stress / Resistance Change vs. Strain result for flextural test of 0.25 wt% CNT smart paint specimen with acrylic paint.

5. FABRICATION AND TESTING OF INTERLAMINAR PROPERTIES OF ELECTROSPUN CARBON NANOFIBER (ECN) COATED CARBON FIBER PREPREG COMPOSITES (CFp-RC)

In this part of the study, effects of CNTs on the interlaminar properties of CFp-RC were investigated. Since the nano-enhanced composites shows different failure modes when compared with advanced composites, a specific investigation have to be performed to determine effect of CNTs on the mechanical properties of structures before the SHM systems improved for these structures.

The cylindrical hollow structure composites are widely used in aerospace and automobile industry as engine shafts. Torsional forces act on these shafts cause inter-laminar fracture and its occurrence considerably deteriorates the mechanical properties of the shafts in service. To enhance the mechanical properties of inter-laminar surface ECNs mats were used in this study. PVB nanofibers were electrospun directly onto the carbon fiber prepregs to obtain well adhesion between ECNs and carbon fiber prepregs. Cylindrical hollow structure tubes were fabricated with different layer properties and torsion tests were performed to discuss mechanical improvement of inter-laminar surface with reinforcement of ECNs mats.

Hand-laid-up fabrication of cylindrical composites had some difficulties such as proper wrapping of layers without any gap was not possible if there was not a machine for this work, also all specimens have to be wrapped with same toughness. Since the fabrication parameters could not be specified to eliminate effects of them on mechanical properties, the results of torsional tests were not be evaluated as required to determine effectiveness of ECN mats. So, flat specimens with same ECN mats for Mode-I Mode-II mixture fracture toughness test were also fabricated.

5.1 Fabrication of ECN Mats

For this study, electrospinning was performed at ITU Textile and Apparel Laboratory of Excellence and ECNs mats coated CFp-RC were fabricated at ITU ARC laboratory. Torsion tests were achieved at ODTU-RUZGEM laboratory.

5.1.1 Materials

The materials used for the fabrication of the CFp-RC cylinders with embedded ECNs mats were carbon fiber prepreg with VTP H310 resin system, kindly supplied by SPM Composite Advanced Materials Technologies Company, polyvinyl butyral (PVB), commercial MWCNTs with 6-9 nm outer diameter, 5-µm length and 95 % carbon content, were supplied by Sigma Aldrich.

5.1.2 Custom-made ECN mats fabrication by electrospinning

CNTs were growth with same applications that were mentionad at Chapter-3. 13-minute growth time was applied and 0.5 wt% CNT were used for preparation of polymer solution. However, because these CNTs have higher length/diameter ratio than commercial products, proper dispersion into the solution could not be obtained and Commercial CNTs were also used to test the effect of different CNT types. To prepare polymer solutions first polymer PVB were added in methanol at 10 wt% and then magnetically stirred for 24 hour to ensure a good dispersion. For growth CNT polymer solution, adequate dispersion were not be obtained by magnetical stirring. So tip sonicator for 5 minutes with 5 cycle was also applied for this suspension and an additional 24 hours magnetical stirring was performed after tip sonication. Electrospinning method was used to fabricate ECNs mats on carbon fiber prepreg (Figure 5.1). Applied voltage, solution flow rate and tip to ground distance were provided according to CNT types as given in Table 5.1.

The polymer solutions were electrospun directly onto carbon fiber prepreg layers. Although a specific effort was expended on growth CNT polymer solutions, a continuous electrospinning could not be achieved due to agglomerations of CNTs and large CNT chunks were observed in ECNs mats. Thus, Sigma commercial-CNTs were selected for rest of this study.

To discuss the effect of CNTs, three different weight percentages of Sigma-CNTs (0.5, 1 and 2 wt% respect to polymer amount) were used. The CNTs corporated polymer solutions were electrospun directly onto carbon fiber prepreg layers. Consequently, a thin layer of CNTs reinforced nanofibers was collected on the prepreg surface to form the interlayer. As seen from SEM image (Figure 5.2), the epoxy resin impregrated the nanofibers on the surface and only the nanofibers

between 0^0 and 90^0 carbon fibers were remained. According to high-resolution image, the obtained fiber diameter of the electrospun nanofiber was nearly 0.35 µm.

Figure 5.1 : Electrospinning set-up for carbon fiber prepreg composite.

Table 5. 1 : Required electrospinning production parameters

	Voltage (kV)	Flow Rate (mL/h)	Tip-to-ground Distance (cm)
Growth CNT-Solution	24	1.6	15
Commercial CNT-Solution	15	0.5	15

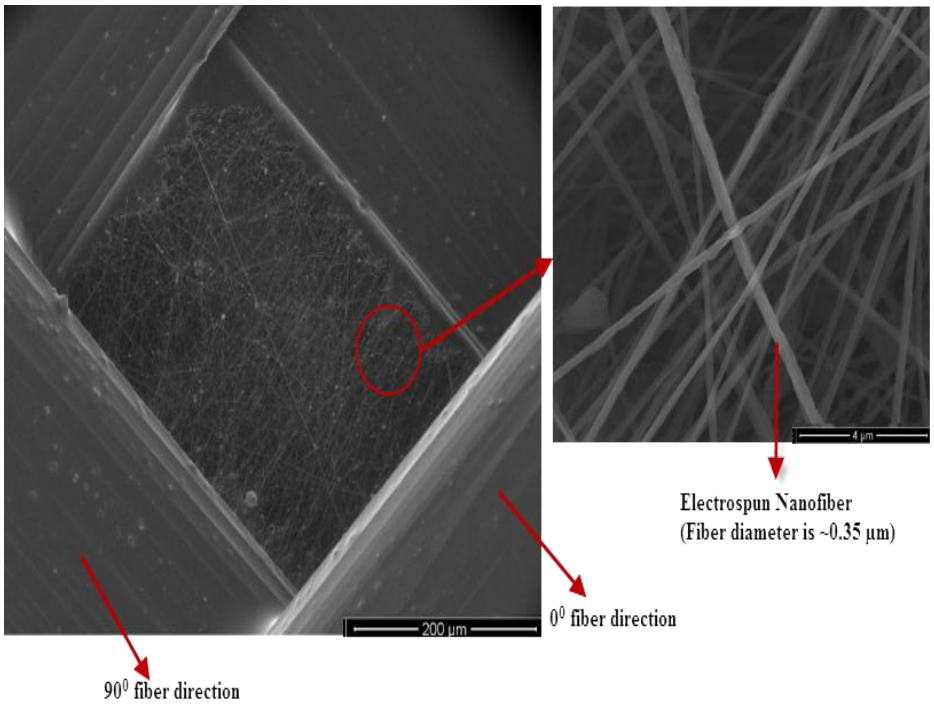

Figure 5.2 : SEM image of ECN mats.

5.2 Fabrication of ECN Mats Coated CFp-RC

The specimen fabrication of the CFp-RC cylinder with embedded ECNs mats includes three types of specimens, such as;

- Base specimens,
- Middle interphase specimens,
- Separate interphase specimens.

Base specimens without ECNs mats were fabricated as reference materials. For middle interphase specimens the ECNs mats applied to middle four surfaces. For separate interphase specimens ECNs mats applied to separate four surfaces (Figure 5.3). During electrospinning application, the surfaces that did not electrospun were closed with a paper to prevent unwanted distribution of ECNs mats. A continuous carbon fiber prepreg were used to fabricate cylindrical composites. Plies were wrapped to cylindrical mold continuously upto 10 plies of carbon fiber prepreg were achieved. The weight fraction of ECNs mats for four surfaces was nearly 4 wt% for all electrospun CRp-RC specimens. To calculate this fraction, weight of the carbon fiber prepregs that were dimensioned specifically for fabrication of 10 ply cylindrical composite, were weighed before and after electrospinning. The difference between them was taken as the weight of ECNs mats and weight fraction was calculated according to masses of four plies, which were coated by ECNs mats.

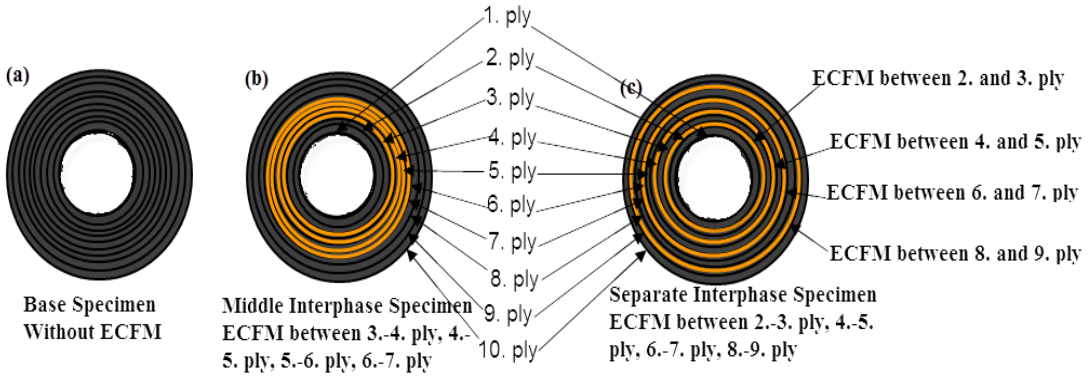

Figure 5.3 : Cross section af (a) base specimen, (b) middle interphase specimen, (c) seperate specimen.

As first trial, cylindrical composite fabrication iron sticks were used as a cylindrical mold. A slippery seperator paper was used between mold and carbon fiber prepreg to provide an easy seperation after curing. Peel-ply was wrapped on carbon fiber prepreg and vacuum bagging was applied. Finally, the specimens were cured at 150

^{0}C for 2 hours under vacuum. Since, an outer mold was not used at first fabrications; the specimens were not exactly cylindrical because of vacuum effect and loose wrapping of layers, because of hand-made fabrication. In addition, although a seperator paper was used there were still some difficulties to to split up the composite from mold. Later, Teflon molds were selected and 6 mm diameter teflon strip was used as an inner mold. In addition, a hollow Teflon hose with 12 mm inner diameter was used as an outer mold to prevent deformation of cylindrical shape of composites (Figure 5.4(a)). A liquid release agent was used on the surface of inner mold and also on the inner surface of outer mold. After curing performed, the specimens were splitted up from mold and 3 cm aluminium pieces were placed at each end of the specimens to prevent damage of specimens because of gripping of torsion machine (Figure 5.4(b)).

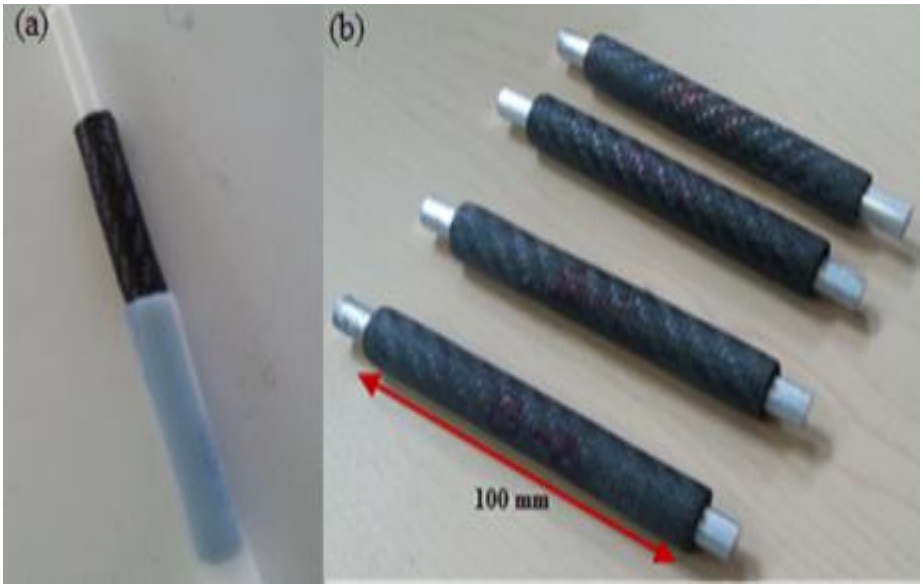

Figure 5.4 : (a) Cylindrical mold, (b) cylindrical hollow structure composite specimens.

5.3 Interlaminar Properties of ECN Mats Coated CFp-RC

To determine the interlaminar properties of cylindrical hollow structure composites and examine the effect of ECNs mats on the shear strength of composites torsional tests were performed by MTS Axial and Torsional Test Machine for composite specimens (Figure 5.5).

A standard torque speed 5^o/min was applied to each specimen from one end where the the other end was fixed (Figure 5.6). Axial loading was hold at constant zero

force. All specimens were rotated 75°. Torsional force versus strain data were recorded continuously to calculate the maximum shear strength of composites according to Equation (5.1) where T_{max} is the maximum torque applied to the cylinder [N.m], R_o is the outer radius and R_i is the inner radius.

$$S_{12} = \frac{T_{max} R_o}{\frac{1}{2}\pi(R_o^4 - R_i^4)} \tag{5.1}$$

Figure 5.5 : Torsional test of cylindrical hollow structure composite.

Figure 5. 6 : Loading conditions for specimens.

At the first set, base specimens and middle and seperate specimens with 0.5 wt% CNT-ECNs mats were fabricated and tested (Figure 5.7). For base condition seven specimens were prepared as first set of specimens and three specimens were tested for middle and seperate interphase conditions. The maximum average torsional torque that carried by base, middle interphase and seperate interphase specimens were 23.3, 20.7 21.8 N.m respectively. Specimens did not break off up to 75° torsion

angles. As seen from Figure 5.8, base specimen was carried higher shear stress for same strain conditions when compared with middle interphase and seperate interphase. In addition, the distribution of ECNs mats did not show a distinctive difference for load carrying capacities of middle interphase and seperate interphase specimens.

Figure 5.7 : Torsion test specimens: base, middle and seperate with 0.5 wt% CNT-ECNs mats.

Torsion tests for 0.5 wt% CNT-ECNs mats were repated to eliminate curing fluctuations and 1 wt% and 2wt% CNT-ECNs mats coated specimens were also fabricated to determine the effect of CNT amounts. Torsinal test results of second set of trials were given in Figure 5.9 seperately. When the middle and seperate type composite structures were compaired for all weight percentage in itself, these two type did not show a remarkable differences for 1 and 2 wt% CNT-ECNs mats structures. For 0.5 wt% CNT-ECNs mats, seperate type specimens showed a higher resistance to torsional deformation. The torsional rotation begins from outer surface and goes on through inner side. Since the first ECNs mats on seperate type were closer to outer surface, it act as an obstacle for crack propagation through inner side and after the first crack of the structure, the stress was nearly constant by means of ECNs mats. The better results for 0.5 wt% CNTs seperate specimens would be the outcome of good dispersion of CNTs. Figure 5.10 also supported this conclusion. 0.5 wt% CNT-ENCs mats seperate specimens displayed higher strength than all other specimens. 1 wt% CNT-ECNs mats specimens also durable than base specimens, since the ECNs mats provided resistance to failure after ply cracks. The worse results of 2 wt% CNT-ENCs mats might be attributed to CNTs agglomeration and decreased curing degree that causes decrease on mechanical properties of structures.

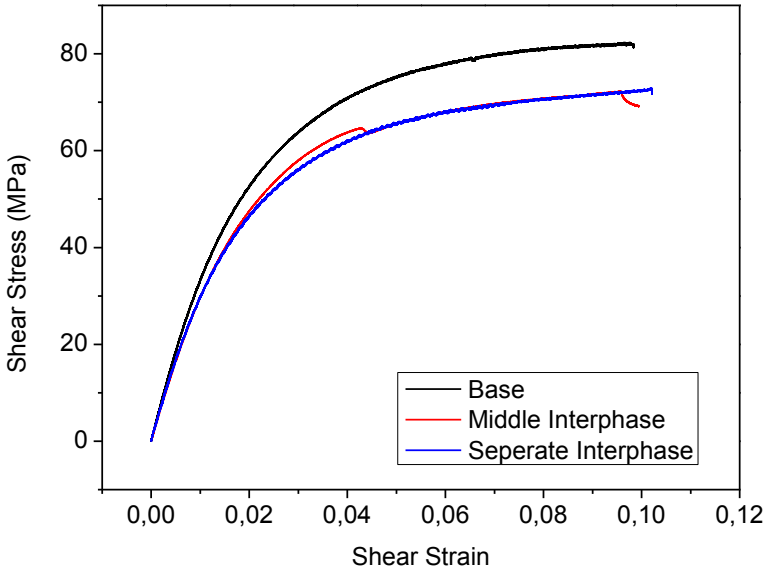

Figure 5.8 : First set results for base, 0.5 wt% CNT-ECNs mats middle interphase and seperate interphase specimens.

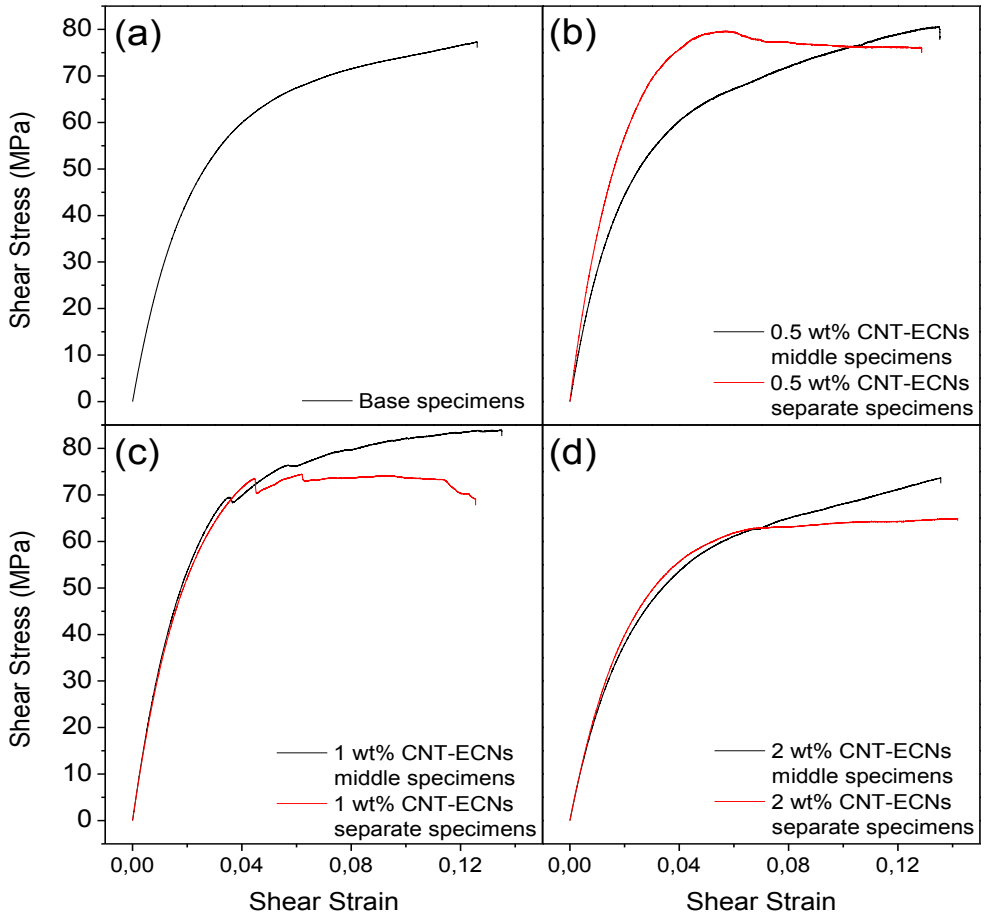

Figure 5.9 : Torsional test results (a) base specimens, (b) 0.5 wt% CNT-ECNs mats specimens, (c) 1 wt% CNT-ECNs mats specimens, (d) 2 wt% CNT-ECNs mats specimens.

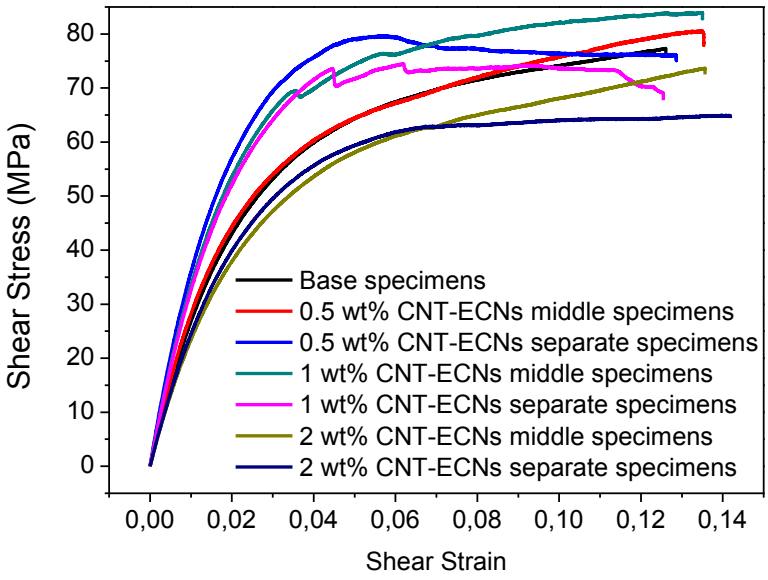

Figure 5.10 : Comparison for all type of cylindrical hollow composite structures.

Optic microscope images taken from cross sections of base and 0.5 wt% CNT-ECNs mats seperate specimens were seen in (Figure 5.11). There were some small gaps between layers but there was not any crack or delamination at inner layers of cylindrical composites.

Figure 5.11 : Optic microscope images of cross section of (a) base specimen, (b) 0.5 wt% CNTs reinforced seperate specimen after torsion tests.

Hand-made cylindrical composites were difficult to fabricate and because of the fabrication parameters' effects on mechanical properties, the results of torsion tests were not be evaluated as expected. To completely determine the contribution of ECNs mats on mechanical properties of structures and investigate the CNT weight fraction effects, Mode-I, Mode-II mixture fracture test specimens were also fabricated with same ECNs mats. Test specimens were prepared according to dimensions that specified at ASTM-D6671 (Figure 5.12).

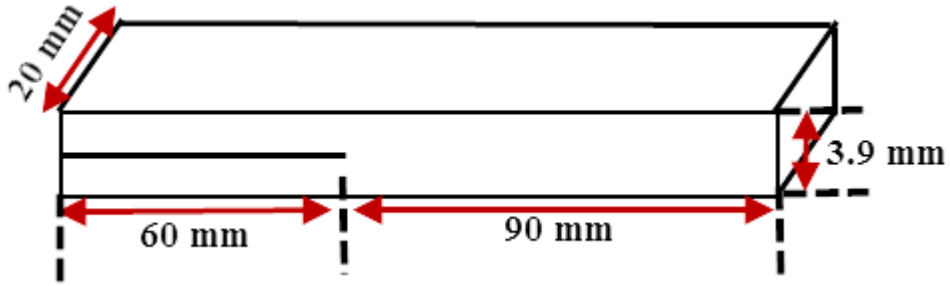

Figure 5.12 : Mode-I Mode-II mixture fracture test specimen dimensions.

For fabrication of test specimens, 16 plies of carbon fiber prepreg were used to obtaine the specified thickness; in addition, the laminates must containe an even number of plies to place the delamination at the middle surface of the lamiantes. Both base and ECNs mats coated specimens were fabricated. Only one layer of ECN mats were used for each specimens and ECNs mats coated carbon fiber prepreg was placed to the middle surface of laminates. ECNs mats were applied upto the crack initiation points and a release film were placed after the ECNs mats to obtaine delamination at the middle surface. Laminates were cured at 150 ^{0}C for 2 hours under 800-psi vacuum. Test specimens were cut from laminates with specified dimensions. Hinges were placed to the delamination ends of the specimens. Before bonding, both hinge surface and composite surface were sanded and cleaned with acetone to provide perfect bonding between composite surface and hinge. A strong-quick cure epoxy was used as an adhesive. After the test specimens were prepared control lines with 0.5 mm intervals were drawn to the one side of specimens from crack initiation point to end of the specimens to follow crack propagation (Figure 5.13). The Mode-I Mode-II mixture tests were tried to make at ITU Textile laboratory, a base specimen were tested by trial and error (Figure 5.14) however, test machine is new and no one knows about the mode-I mode-II mixture test procedure. That is why, we are still trying to learn about test procedure to perform these test in a

correct way. After the mode-I mode-II mixture tests will be performed, effect of ECNs mats on crack propagation will be investigated and according to these results, torsion test with optimized ECNs mats applications will be repeated to determine ECNs mats contribution to the shear strength of cylindrical structures.

Figure 5.13 : Mode-I Mode II mixture tests specimens.

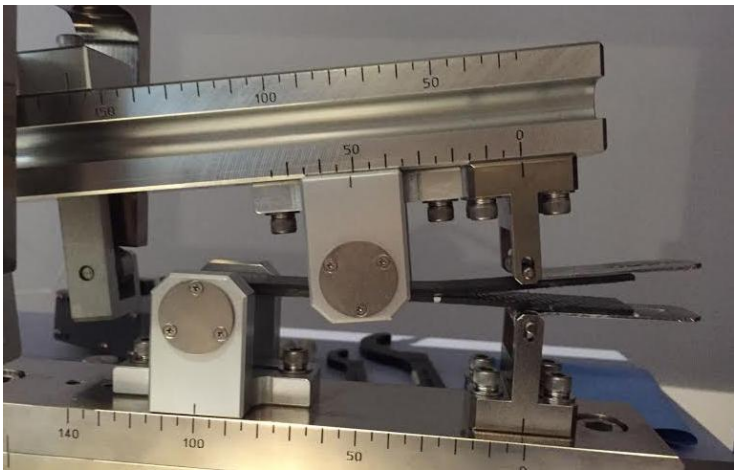

Figure 5.14 : First application of Mode-I Mode-II mixture test.

6. CONCLUSION AND FUTURE WORKS

In this thesis, both mechanical and electrical effectiveness of CNTs were evaluated. The superior mechanical, electrical and thermal properties of CNTs are wellknown subjects for a while. However, these properties show differences upto application areas. The important parameters to obtain expected results from the applications are:

- CNT synthesis type,
- CNT dimensions, such as aspect ratio,
- Functionalization (subject to application),
- CNT quantity in the system,
- Dispersion technique or application type such as bucky paper and fuzzy fiber.

To optimize the all these properties comprehensive experimental studies have to be performed. In this work, two different application areas were stuied and all parameters were tried to be optimized. For investigation of CNT smart paint effectiveness on strain sensing;

- Percolation threshold is obtained with low filler contents through proper CNT dimensions and dispersion,
- Response of the CNT smart paint application depends on the loading conditions and higher filler content shows higher resistance change for plastic deformation conditions,
- To obtaine a proper CNT smart paint application and determine effectiveness of CNT smart paint as a strain sensor it have to be isolated from other materials.

For the second part of this thesis, to determine the effectiveness of ECNs mats, torsion tests were performed for cylindrical structures. According to results;

- Increasing CNT weight fraction affected the curing degree of epoxy and decreased the mechanical properties of structures,

- Place of ECNs mats affected the shear stress of structures and separate ECNs mats which are closer to outer surface of structure shows higher shear strength for 0.5 wt% CNT-ECNs mats.

The future steps of this study are,

- Performation of CNT smart paint SHM tests with optimized application for different loading conditions such as, cycling loading, tension tests and flextural tests,
- Determination of effectiveness of ECNs mats for Mode-I Mode-II loading conditions and optimizing application of ECNs mats for cylindrical structures,
- Investigation of applicability of CNT smart paint SHM method on nano-enhanced and complex shaped structures.

REFERENCES

1. Qian, H., et al., *Carbon nanotube-based hierarchical composites: a review.* Journal of Materials Chemistry, 2010. **20**(23): p. 4751-4762.
2. Baur, J. and E. Silverman, *Challenges and opportunities in multifunctional nanocomposite structures for aerospace applications.* Mrs Bulletin, 2007. **32**(4): p. 328-334.
3. Kessler, S.S. and S.M. Spearing. *Design of a piezoelectric-based structural health monitoring system for damage detection in composite materials*. in *Smart Structures and Materials 2002 Conference*. 2002. San Diego, Ca.
4. Preeti Pisupati, S.K.D., Ravi Kumar, *Structural Health Monitoring Enabling Technology for Paradigm Shift in Next Generation Aircraft Design and Maintenance*. 2009.
5. Choi, H., et al., *Structural Health Monitoring System based on Strain Gauge Enabled Wireless Sensor Nodes.* Inss 2008: Proceedings of the Fifth International Conference on Networked Sensing Systems, 2008: p. 211-214.
6. Silva-Munoz, R.A. and R.A. Lopez-Anido, *Structural health monitoring of marine composite structural joints using embedded fiber Bragg grating strain sensors.* Composite Structures, 2009. **89**(2): p. 224-234.
7. Zhao, X., et al., *Ultrasonic Lamb wave tomography in structural health monitoring.* Smart Materials & Structures, 2011. **20**(10).
8. Coleman, J.N., et al., *Small but strong: A review of the mechanical properties of carbon nanotube-polymer composites.* Carbon, 2006. **44**(9): p. 1624-1652.
9. Nessim, G.D., *Properties, synthesis, and growth mechanisms of carbon nanotubes with special focus on thermal chemical vapor deposition.* Nanoscale, 2010. **2**(8): p. 1306-1323.
10. Chung, D.D.L., *Carbon materials for structural self-sensing, electromagnetic shielding and thermal interfacing.* Carbon, 2012. **50**(9): p. 3342-3353.
11. Iijima, S., *HELICAL MICROTUBULES OF GRAPHITIC CARBON.* Nature, 1991. **354**(6348): p. 56-58.
12. Endo, M., *The Growth Mechanism of Vapor-Grown Carbon Fibers*. 1975, University of Orleans: Orleans, France.
13. De Volder, M.F.L., et al., *Carbon Nanotubes: Present and Future Commercial Applications.* Science, 2013. **339**(6119): p. 535-539.
14. Endo, M., et al., *Development and application of carbon nanotubes.* Japanese Journal of Applied Physics Part 1-Regular Papers Brief Communications & Review Papers, 2006. **45**(6A): p. 4883-4892.
15. Popov, V.N., *Carbon nanotubes: properties and application.* Materials Science & Engineering R-Reports, 2004. **43**(3): p. 61-102.
16. Terrones, M., *Carbon nanotubes: synthesis and properties, electronic devices and other emerging applications.* International Materials Reviews, 2004. **49**(6): p. 325-377.
17. Sinnott, S.B. and R. Andrews, *Carbon nanotubes: Synthesis, properties, and applications.* Critical Reviews in Solid State and Materials Sciences, 2001. **26**(3): p. 145-249.

18. Terrones, M., *Science and technology of the twenty-first century: Synthesis, properties and applications of carbon nanotubes.* Annual Review of Materials Research, 2003. **33**: p. 419-501.
19. Thostenson, E.T., Z.F. Ren, and T.W. Chou, *Advances in the science and technology of carbon nanotubes and their composites: a review.* Composites Science and Technology, 2001. **61**(13): p. 1899-1912.
20. Belin, T. and F. Epron, *Characterization methods of carbon nanotubes: a review.* Materials Science and Engineering B-Solid State Materials for Advanced Technology, 2005. **119**(2): p. 105-118.
21. Eatemadi, A., et al., *Carbon nanotubes: properties, synthesis, purification, and medical applications.* Nanoscale Research Letters, 2014. **9**.
22. Lehman, J.H., et al., *Evaluating the characteristics of multiwall carbon nanotubes.* Carbon, 2011. **49**(8): p. 2581-2602.
23. Iijima, S. and T. Ichihashi, *SINGLE-SHELL CARBON NANOTUBES OF 1-NM DIAMETER.* Nature, 1993. **363**(6430): p. 603-605.
24. Joseyacaman, M., et al., *CATALYTIC GROWTH OF CARBON MICROTUBULES WITH FULLERENE STRUCTURE (APPLIED PHYSICS LETTER, VOL 62, PG 202, 1993).* Applied Physics Letters, 1993. **62**(6): p. 657-659.
25. See, C.H. and A.T. Harris, *A review of carbon nanotube synthesis via fluidized-bed chemical vapor deposition.* Industrial & Engineering Chemistry Research, 2007. **46**(4): p. 997-1012.
26. Kumar, M. and Y. Ando, *Chemical Vapor Deposition of Carbon Nanotubes: A Review on Growth Mechanism and Mass Production.* Journal of Nanoscience and Nanotechnology, 2010. **10**(6): p. 3739-3758.
27. Enkeleda Dervishi, Z.L., Yang Xu, Viney Saini, Alexandru R. Biris, Dan Lupu, Alexandru S. Biris, *Carbon Nanotubes: Synthesis, Properties, and Applications. Particulate Science and Technology.* Particulate Science and Technology, 2009. **27**(0272-6351): p. 107-125.
28. Ruoff, R.S., D. Qian, and W.K. Liu, *Mechanical properties of carbon nanotubes: theoretical predictions and experimental measurements.* Comptes Rendus Physique, 2003. **4**(9): p. 993-1008.
29. Treacy, M.M.J., T.W. Ebbesen, and J.M. Gibson, *Exceptionally high Young's modulus observed for individual carbon nanotubes.* Nature, 1996. **381**(6584): p. 678-680.
30. Wong, E.W., P.E. Sheehan, and C.M. Lieber, *Nanobeam mechanics: Elasticity, strength, and toughness of nanorods and nanotubes.* Science, 1997. **277**(5334): p. 1971-1975.
31. Dresselhaus, M.S., Dresselhaus, G., Avouris, P., *Carbon Nanotubes: Synthesis, Structures, Properties and Applications*. 2001, Springer.
32. Delaney, P., et al., *Broken symmetry and pseudogaps in ropes of carbon nanotubes.* Nature, 1998. **391**(6666): p. 466-468.
33. Schaefer, D.W. and R.S. Justice, *How nano are nanocomposites?* Macromolecules, 2007. **40**(24): p. 8501-8517.
34. Hussain, F., et al., *Review article: Polymer-matrix nanocomposites, processing, manufacturing, and application: An overview.* Journal of Composite Materials, 2006. **40**(17): p. 1511-1575.
35. Ma, P.-C., et al., *Dispersion and functionalization of carbon nanotubes for polymer-based nanocomposites: A review.* Composites Part a-Applied Science and Manufacturing, 2010. **41**(10): p. 1345-1367.

36. Li, J., et al., *Correlations between percolation threshold, dispersion state, and aspect ratio of carbon nanotubes.* Advanced Functional Materials, 2007. **17**(16): p. 3207-3215.
37. Qian, D., et al., *Load transfer and deformation mechanisms in carbon nanotube-polystyrene composites.* Applied Physics Letters, 2000. **76**(20): p. 2868-2870.
38. Thostenson, E.T. and T.W. Chou, *Aligned multi-walled carbon nanotube-reinforced composites: processing and mechanical characterization.* Journal of Physics D-Applied Physics, 2002. **35**(16): p. L77-L80.
39. Paul, D.R. and L.M. Robeson, *Polymer nanotechnology: Nanocomposites.* Polymer, 2008. **49**(15): p. 3187-3204.
40. Wicks, S.S., et al., *Multi-scale interlaminar fracture mechanisms in woven composite laminates reinforced with aligned carbon nanotubes.* Composites Science and Technology, 2014. **100**: p. 128-135.
41. White, K.L. and H.-J. Sue, *Delamination toughness of fiber-reinforced composites containing a carbon nanotube/polyamide-12 epoxy thin film interlayer.* Polymer, 2012. **53**(1): p. 37-42.
42. Wicks, S.S., R.G. de Villoria, and B.L. Wardle, *Interlaminar and intralaminar reinforcement of composite laminates with aligned carbon nanotubes.* Composites Science and Technology, 2010. **70**(1): p. 20-28.
43. Abry, J.C., et al., *In-situ monitoring of damage in CFRP laminates by means of AC and DC measurements.* Composites Science and Technology, 2001. **61**(6): p. 855-864.
44. Lau, K.T., *Structural health monitoring for smart composites using embedded FBG sensor technology.* Materials Science and Technology, 2014. **30**(13A): p. 1642-1654.
45. Torres Gorriz, B., et al., *Experimental and numerical analysis of a hybrid FBG long gauge sensor for structural health monitoring.* Measurement Science & Technology, 2014. **25**(12).
46. Alamusi, et al., *Piezoresistive Strain Sensors Made from Carbon Nanotubes Based Polymer Nanocomposites.* Sensors, 2011. **11**(11): p. 10691-10723.
47. Alexopoulos, N.D., et al., *Structural health monitoring of glass fiber reinforced composites using embedded carbon nanotube (CNT) fibers.* Composites Science and Technology, 2010. **70**(2): p. 260-271.
48. Chiacchiarelli, L.M., et al., *The role of irreversible and reversible phenomena in the piezoresistive behavior of graphene epoxy nanocomposites applied to structural health monitoring.* Composites Science and Technology, 2013. **80**: p. 73-79.
49. Inam, F., et al., *Multiscale Hybrid Micro-Nanocomposites Based on Carbon Nanotubes and Carbon Fibers.* Journal of Nanomaterials, 2010.
50. Yamamoto, N., R.G. de Villoria, and B.L. Wardle, *Electrical and thermal property enhancement of fiber-reinforced polymer laminate composites through controlled implementation of multi-walled carbon nanotubes.* Composites Science and Technology, 2012. **72**(16): p. 2009-2015.
51. Khan, S.U. and J.-K. Kim, *Improved interlaminar shear properties of multiscale carbon fiber composites with bucky paper interleaves made from carbon nanofibers.* Carbon, 2012. **50**(14): p. 5265-5277.
52. Garcia, E.J., B.L. Wardle, and A.J. Hart, *Joining prepreg composite interfaces with aligned carbon nanotubes.* Composites Part a-Applied Science and Manufacturing, 2008. **39**(6): p. 1065-1070.

53. Qiu, J., et al., *Carbon nanotube integrated multifunctional multiscale composites.* Nanotechnology, 2007. **18**(27).
54. K. Bilge, E.O.Y., E. Simsek, Y.Z. Menceloglu, M. Papila, *Structural composites hybridized with epoxy compatible polymer/MWCNT nanofibrous interlayers.* Composite Science and Technology, 2012. **72**: p. 1639-1645.
55. Gibson, R.F., *A review of recent research on mechanics of multifunctional composite materials and structures.* Composite Structures, 2010. **92**(12): p. 2793-2810.
56. Chen, Q., et al., *Hybrid multi-scale epoxy composite made of conventional carbon fiber fabrics with interlaminar regions containing electrospun carbon nanofiber mats.* Composites Part a-Applied Science and Manufacturing, 2011. **42**(12): p. 2036-2042.
57. Chen, Q., et al., *Fabrication and mechanical properties of hybrid multi-scale epoxy composites reinforced with conventional carbon fiber fabrics surface-attached with electrospun carbon nanofiber mats.* Composites Part B-Engineering, 2013. **44**(1): p. 1-7.
58. Bauhofer, W. and J.Z. Kovacs, *A review and analysis of electrical percolation in carbon nanotube polymer composites.* Composites Science and Technology, 2009. **69**(10): p. 1486-1498.
59. Kovacs, J.Z., et al., *Two percolation thresholds in carbon nanotube epoxy composites.* Composites Science and Technology, 2007. **67**(5): p. 922-928.
60. Kuronuma, Y., et al., *Electrical resistance-based strain sensing in carbon nanotube/polymer composites under tension: Analytical modeling and experiments.* Composites Science and Technology, 2012. **72**(14): p. 1678-1682.
61. Celzard, A., et al., *Critical concentration in percolating systems containing a high-aspect-ratio filler.* Physical Review B, 1996. **53**(10): p. 6209-6214.
62. Bai, J.B. and A. Allaoui, *Effect of the length and the aggregate size of MWNTs on the improvement efficiency of the mechanical and electrical properties of nanocomposites - experimental investigation.* Composites Part a-Applied Science and Manufacturing, 2003. **34**(8): p. 689-694.
63. Du, F.M., J.E. Fischer, and K.I. Winey, *Effect of nanotube alignment on percolation conductivity in carbon nanotube/polymer composites.* Physical Review B, 2005. **72**(12).
64. Behnam, A., J. Guo, and A. Ural, *Effects of nanotube alignment and measurement direction on percolation resistivity in single-walled carbon nanotube films.* Journal of Applied Physics, 2007. **102**(4).
65. Gojny, F.H., et al., *Influence of nano-modification on the mechanical and electrical properties of conventional fibre-reinforced composites.* Composites Part a-Applied Science and Manufacturing, 2005. **36**(11): p. 1525-1535.
66. Georgousis, G., et al., *Strain sensing in polymer/carbon nanotube composites by electrical resistance measurement.* Composites Part B-Engineering, 2015. **68**: p. 162-169.
67. Kang, I., et al., *A carbon nanotube strain sensor for structural health monitoring.* Smart Materials & Structures, 2006. **15**(3): p. 737-748.
68. de Villoria, R.G., et al., *Multi-physics damage sensing in nano-engineered structural composites.* Nanotechnology, 2011. **22**(18).
69. Grammatikos, S.A., G. Gkikas, and A. Paipetis, *Monitoring strain and damage in multi phase composite materials using electrical resistance*

methods. Smart Sensor Phenomena, Technology, Networks, and Systems 2011, 2011. **7982**.

70. Pinto, B., et al. *A comparative study of a self strain-monitoring carbon nanotube film and carbon fibers under flexural loading by electrical resistance changes*. in *11th International Conference on Damage Assessment of Structures (DAMAS)*. 2015. Ghent Univ, Ghent, BELGIUM.
71. DiLeo, R.A., B.J. Landi, and R.P. Raffaelle, *Purity assessment of multiwalled carbon nanotubes by Raman spectroscopy*. Journal of Applied Physics, 2007. **101**(6).
72. Patel, H., L.M. Manocha, and S. Manocha, *Synthesis and microstructure analysis of aligned carbon nanotube/pyrocarbon composites.* New Carbon Materials, 2014. **29**(5): p. 374-379.
73. Cebeci, H., et al., *Multifunctional properties of high volume fraction aligned carbon nanotube polymer composites with controlled morphology*. Composites Science and Technology, 2009. **69**(15-16): p. 2649-2656.

CURRICULUM VITAE

Name Surname: **Yağmur ATEŞCAN**

Place and Date of Birth: **Milas, 10/04/1990**

E-Mail: **atescan@itu.edu.tr**

EDUCATION:

B.Sc.: **Aerospace Engineering/ITU**

PUBLICATIONS, PRESENTATIONS AND PATENTS ON THE THESIS:

*** Ateşcan, Y.**, Cebeci, H., 2016. In-situ Structural Health Monitoring of Carbon Fiber Reinforced Composites with CNT Smart Paint. *57th AIAA/ASCE/AHS/ASC Structures, Structural Dynamics, and Materials Conference 2016*. January 4-8, 2016 San Diego, California, USA, oral presentation.

* **Ateşcan, Y.**, Jahangiri, S., Özden-Yenigün, E., Cebeci, H., 2015. Inter-laminar Properties of Electrospun Nanofiber Mats Coated Carbon Fiber Prepreg Composites. *12th International Conference on Textile Composites*, May 25-29, 2015 Raleigh, NC, USA, oral presentation.

* **Ateşcan, Y.**, Wardle, B. L., Odegard, G. M., Turkmen, H., Cebeci, H., 2015. A Multiscale Approach for Investigation of CNT Waviness Effect on PNCs. *International Conference on Advances in Composite Materials and Structures*, April 13-15, 2015 Istanbul, Turkey, oral presentation.

* **Ateşcan, Y.**, Cebeci, H., Hadden, C. M., Odegard, G. M., Wardle, B. L., 2015. Molecular Dynamics and Finite Element Investigation of Polymer Interphase Effects on Effective Stiffness of Wavy Aligned Carbon Nanotube Composites. *56th AIAA/ASCE/AHS/ASC Structures, Structural Dynamics, and Materials Conference*, January 5-9, 2015 Orlanda, FL, USA, oral presentation.

*** Ateşcan, Y.**, Gürkan, İ., Kavrar, D., Cebeci, H., 2013. Impact Resistance of Hierarchical Composites Reinforced with Carbon Nanotubes. *Nano-TR Student Conference 2013*, October 22, 2013 Istanbul, Turkey, poster presentation.